
The Role of Horizontal System Cells in Optomotor Responses in *Drosophila melanogaster*

Väinö Haikala



München 2013

The Role of Horizontal System Cells in Optomotor Responses in *Drosophila melanogaster*

Väinö Haikala

Dissertation
an der Fakultät für Biologie
der Ludwig–Maximilians–Universität
München

vorgelegt von
Väinö Haikala
aus Helsinki, Finnland

München, 19.11.2013

Hiermit erkläre ich, daß ich die vorliegende Dissertation selbständig und ohne unerlaubte Hilfe angefertigt habe. Sämtliche Experimente wurden von mir selbst durchgeführt, außer wenn explizit auf Dritte verwiesen wird. Ich habe weder anderweitig versucht, eine Dissertation oder Teile einer Dissertation einzureichen bzw. einer Prüfungskommission vorzulegen, noch eine Doktorprüfung durchzuführen.

München, den

Erstgutachter: Prof. Dr. Alexander Borst

Zweitgutachter: Prof. Dr. Rainer Uhl

Tag der mündlichen Prüfung: 17.03.2014

Contents

Summary	xi
1 Introduction	1
1.1 Optomotor Responses	2
1.2 Motion Computation	7
1.2.1 Direction Selective Neurons	7
1.2.2 Compound Eye	11
1.2.3 Elementary Motion Detectors	15
1.2.4 Dscam (Down Syndrome Cell Adhesion Molecule) and Neural Circuit Formation	22
1.3 Visual Network	25
1.4 Relationship Between Lobula Plate Tangential Cell Responses and Optomotor Responses	26
1.5 Genetic Approaches	28
1.6 Project Goals and Achievements	31
2 Methods	33
2.1 Setup	33
2.1.1 Visual Stimulation	33
2.1.2 Torquemeter	35
2.1.3 Wing Beat Analyzer	39
2.1.4 Head Movement Detector	42
2.1.5 Optogenetic Activation	44
2.2 Experimental Preparation	46
2.2.1 Fly Strains and Genetics	46

2.2.2	Fly Preparation	47
2.2.3	Data Analysis	47
2.3	Genetic Modification of HS-cell Responses	48
2.3.1	Switchable Optogenetic Depolarization of HS-cells using ChR2(C128S)	49
2.3.2	Over-Expressing Dscam1 in HS-cells Modify Cell Mor- phology and Responses	51
3	Results	54
3.1	Comparison of HS-cell Activity and Yaw Optomotor Responses .	54
3.2	Optogenetic Activation of HS-cells	57
3.2.1	Activation of HS-cells Elicits Head Yaw Movements in the Preferred Direction of the Cell	58
3.2.2	Activation of HS-cells Elicits Yaw Optomotor Responses in Tethered Flying <i>Drosophila</i>	60
3.3	Role of HS-cell Receptive Fields for Yaw Optomotor Behaviour .	63
3.3.1	Changes in HS-cell Receptive Fields Modify Turning Be- haviour in Tethered Flying Flies	64
3.3.2	Changes in HS-cell Receptive Fields Modify Head Yaw Movements	69
4	Discussion	77
4.1	Comparison of HS-cell Activity and Yaw Optomotor Responses .	78
4.2	Optogenetic Activation of HS-cells	81
4.3	Role of HS-cell Receptive Field Layout for Yaw Optomotor Be- haviour	87
4.3.1	Changes in HS-cell Receptive Fields Modify Turning Be- haviour in Tethered Flying Flies	88
4.3.2	Changes in HS-cell Receptive Fields Modify Head Yaw Movements	93
4.4	Conclusions	96
	Bibliography	97

Acknowledgements

109

Curriculum Vitae

111

List of Figures

1.1	Definition of forces and moments during flight and optic flow for lift and roll	3
1.2	Initial optomotor behaviour measurements in flying flies	5
1.3	Schematic of the visual ganglia	8
1.4	Comparison of VS-cell responses in blow and fruit flies	9
1.5	HS-cell characteristics in <i>Drosophila</i>	10
1.6	Dendritic structure and receptive fields for HS-cells	11
1.7	Structure of a single ommatidium	12
1.8	The phototransduction cascade	14
1.9	The elementary motion detector model and its properties	16
1.10	Medulla connectome constituting an elementary motion detector	20
1.11	Dscam1 apparently promotes self-avoidance and Dscam2 regulates tiling in the flies visual system	22
1.12	Lobula Plate Network	26
1.13	Summary diagram of presumed lobula plate tangential cell activation and inhibition in response to half-field visual motion	27
1.14	Gal4/UAS System	29
2.1	LED arena used for visual stimulation	34
2.2	Schematic of the torquemeter	36
2.3	Test to find an appropriate tether length for the torquemeter	37
2.4	Closeup of measured forces using the torquemeter	38
2.5	Design of the wing beat analyzer	40
2.6	Example traces recorded with the wing beat analyzer	41
2.7	Head movement analysis	43

2.8	Optogenetic activation setup	44
2.9	Electrophysiological recordings from lobula plate tangential cells expressing ChR2(C128S)	50
2.10	Overexpression of a single Dscam1 isoform in HS-cells reduces dendritic branching and enhances unoccupied territory in the lob- ula plate	52
2.11	Overexpression of a single Dscam1 isoform in HS-cells causes a gap in the frontal receptive field	53
3.1	Comparison of head yaw responses in fixed flies with yaw turning responses in tethered flying flies	56
3.2	Optogenetic activation of HS-cells elicits head yaw movement in the preferred direction of the cell in fixed flies	59
3.3	Optogenetic activation of HS-cells during tethered flight elicits yaw turning responses in the preferred direction of the cell	61
3.4	Effects of Dscam gain-of-function in tethered flying flies for a stimulus excluding the frontal region of the visual field	65
3.5	Effects of a Dscam gain-of-function in tethered flying flies with one eye painted black, using a stimulus including the frontal re- gion of the visual field	68
3.6	Comparison of the sum of HSN and HSE receptive fields for con- trol and D(GOF) flies	70
3.7	Stimulus used for head movement experiments with D(GOF) flies	71
3.8	Comparison of head yaw movements and responses of D(GOF) and control flies elicited by a whole-field square wave pattern . . .	72
3.9	Comparison of head yaw following movements of D(GOF) and control flies	74
3.10	Comparison of the response difference in head yaw movement of D(GOF) and control flies with the difference of the receptive fields of D(GOF) and control flies	75

Nomenclature

H1 Horizontal 1

HSE Horizontal System Equatorial

HSN Horizontal System Northern

HSS Horizontal System Southern

VS Vertical System

ChR2(C128S) Bi-stable Channelrhodopsin-2 Variant (C128S)

ATR All-Trans-Retinal

Dscam Down Syndrome Cell Adhesion Molecule

D(GOF) Dscam Gain-of-Function

RWB Right Wing Beat

LWB Left Wing Beat

PD Preferred Direction

ND Null Direction

Summary

When confronted with a large-field stimulus rotating around the vertical body axis, flies display a following behaviour of the head and steer in the direction of motion. As neural control elements for this so-called ‘optomotor response’, the large tangential horizontal cells (HS-cells) of the lobula plate have been the prime candidates for long. When HS-cells are surgically damaged or genetically removed, flies display reduced optomotor responses.

To provide a better understanding of the role of HS-cells in the control of optomotor behaviour three approaches were taken. First, experiments were designed to investigate which of the HS-cells could be participating in head yaw movements in fixed flies and yaw turning behaviour during tethered flight. Horizontal motion at different elevations was presented to the flies. Comparison of the optomotor responses with HS-cell receptive fields suggests that HSN and HSE participate in head yaw movements whereas all three HS-cells are used to control yaw turning behaviour during flight.

Second, to test whether HS-cells are sufficient to elicit yaw optomotor responses, a bi-stable Channelrhodopsin-2 variant ‘ChR2 (C128S)’ was expressed in HS-cells using the Gal4 / UAS-system. Combining a blue light stimulus with ChR2(C128S) allowed to activate HS-cells without presenting a visual stimulus to the eye of the fly. These experiments revealed that blue light was sufficient to evoke robust head yaw movement in fixed flies as well as turning behaviour in tethered flying flies, thus, mimicking front-

to-back visual stimulation on the stimulated side.

Third, the role of the receptive field layouts of HS-cells for optomotor responses was studied. Flies with a gain-of-function of a single Dscam1 isoform in all HS-cells (Dscam gain-of-function (D(GOF)) flies) were tested. Compared with HS-cells of control flies, HS-cells of D(GOF) flies show reduced sensitivity to horizontal motion in the frontal and enhanced sensitivity to motion in the lateral part of visual space. The optomotor response of tethered flying flies were analyzed. Compared with control flies, D(GOF) flies responded significantly weaker to visual stimuli extending over the entire azimuth extension of HS-cell receptive fields. Stimulating flies with additional motion in the rear part of visual space significantly reduced optomotor responses of control flies, whereas D(GOF) flies responded to both visual stimuli with about equal strength. Although D(GOF) HS-cells had dramatically reduced sensitivity to motion in the frontal part of visual space, D(GOF) flies responded robustly to motion in this region of visual space. D(GOF) and control flies also showed differences in head yaw movements. These behavioural differences did not correlate with the difference in the receptive fields of D(GOF) and control HS-cells.

The experiments indicate that HS-cells are sufficient to trigger yaw turns of the head and whole body. All three HS-cells control body turns during flight and head yaw turns are controlled by HSN- and HSE-cells. The layout of HS-cell receptive fields, however, does not correlate 1 : 1 with optomotor responses. During flight, flies rely additionally on cells sensitive in the frontal part of visual space. Furthermore, the layout of the HS-cell receptive fields is important for incorporating motion information in the rear part of visual space to the optomotor responses.



Chapter 1

Introduction

Flies can be annoying when buzzing around during siesta time and landing on one's nose. Although not always welcome, flies show remarkable abilities including escaping the approaching hand of an unlucky tired person in less than 200 ms (Card and Dickinson, 2008) or chasing a moving target with delays of approximately 30 ms (Collett and Land, 1975; Land, 1993). When comparing these time scales with human eye blinking, which on average takes between 200-300 ms (VanderWerf et al., 2003), it is clear that flies live in a world where decisions must be taken extremely fast and in which there is no time for long delays between neuronal activity and motor output. Because of their small sized brains, flies offer the opportunity to study these and other skills at the neuronal level.

For successful behaviour it is necessary that flies sense their environment and take decisions for appropriate maneuvers based on the gathered information. Neuronal circuits used for these tasks are called sensory-motor neuronal pathways. One highly important pathway is the visuo-motor pathway upon which flies rely on to perform diverse visually guided behaviours such as: “phototaxis”, approaching a light source (Schümpferli, 1973); “fixation”, flying or walking towards an object (Reichardt and Wenking, 1969; Wehner, 1972; Bahl et al., 2013); “visually elicited landing response”, preparing to land by expanding their legs when perceiving an expanding visual stimulus in the frontal field of view (Borst, 1986).

All these visually elicited responses play an important role in flies' everyday life. Without these visuo-motor pathways flies would not be able to navigate in a precise and fast way safely through an environment. For this, information about

the environment, external disturbances and self-motion need to be taken into account. Using various visual cues during locomotion, flies are able to stabilize their gaze (Hengstenberg, 1993), control their flight course (Götz, 1975; Kern and Egelhaaf, 2000; Mronz and Lehmann, 2008) and to avoid collisions (Tammero and Dickinson, 2002). It is clear that vision is essential for flies, but how is visual information computed and how are the correct decisions for all these maneuvers taken?

1.1 Optomotor Responses

Running through a corridor with your eyes closed is a difficult task. Approaching objects can not be detected and it is impossible to stay in the center of the corridor and avoid collisions with the walls. This is not different for flies and this is why vision plays such a crucial role during locomotion. During locomotion flies not only need to control generated forces (thrust, lift and side-slip) but also the necessary moments to produce rotations around their three body axis (yaw, pitch and roll; Figure 1.1A). This control has to be done in a closed loop, i.e. the reaction to the applied correcting forces must be detected and corrected by applying another force until the desired effect has been achieved.

When a fly moves through space, an image of the environment is projected onto the fly's retina. Using the shifting image points on the retina it is possible to compute visual motion. Since this visual motion, also called optic flow, depends on the speed and direction of the fly's self-motion and moving obstacles, analyzing it enables flies to deduce how the outside world is moving with respect to their body. If for example a fly flies straight up, the world projected onto its retina moves downwards on both of its eyes (Figure 1.1B). On the other hand, during a rotation around the fly's longitudinal axis, the world moves up on one and down on the other side (Figure 1.1C). For these two examples, to deduce which scenario occurred it is not enough to analyze the optic flow in a visual hemifield (local optic flow) since in certain regions both movements produce equal optic flow (Figure 1.1B and C, gray boxes). The previous example highlights why the entire optic flow needs to be analyzed when self-motion is to be deduced. Furthermore, optic flow analysis allows the animals to detect objects such as moving

Optic flow describes the movement of each point in visual space caused by the movement of the observer within the visual scene



targets and obstacles. Such objects cause local optic flow that differs in speed and / or direction when compared with the global optic flow. Note that for object detection the local optic flow plays an important role.

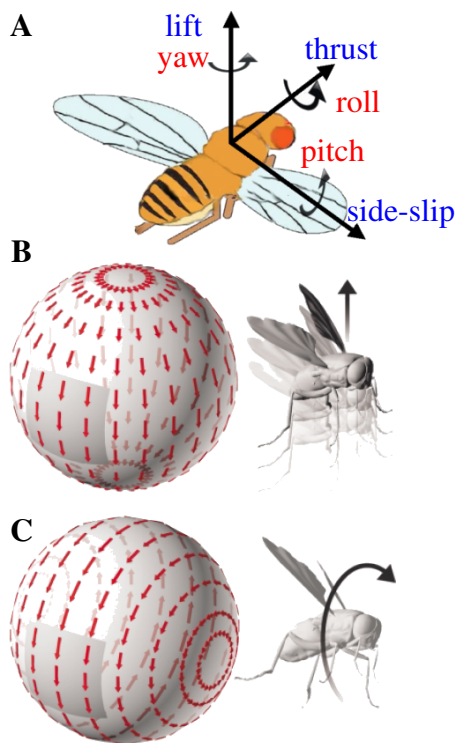


Figure 1.1: Definition of forces and moments during flight and optic flow for lift and roll. (A) Definition of all six degrees of freedom a fly has during flight. Depicted in red three torques (yaw, roll, and pitch) and in blue three forces (lift, thrust and side-slip) a fly can produce in order to navigate through space. (B) and (C) Optic flow experienced by a fly during lift and roll (Adapted from (Zbikowski, 2005)). During lift (B) the visual space projected onto both eyes moves downwards, whereas during roll (C) one eye perceives the world moving up and the other downwards. Gray boxes indicate areas in visual space in which both local optic fields cannot be differentiated.

Following the above idea, during straight flight the optic flow perceived by the fly on both hemispheres shows similar properties, i.e. the world detected by both eyes moves from the front to the back. If an external disturbance occurs, e.g. a gust of wind, and the fly is shifted during straight flight course towards one side, the projected image onto the eyes of the fly moves on both eyes against the self-motion. In order to correct its flight course, the fly has to correct against the self-motion which is equivalent to following the visual motion.

First attempts to understand fly vision using optomotor responses confirmed the feasibility of such a control strategy. During these experiments, flies were tethered and placed in the center of a textured drum rotating horizontally around the fly while simultaneously the yaw torque produced by the fly was measured (Figure 1.2A; (Fermi and Reichardt, 1963; McCann and MacGinitie, 1965)). Torque analysis showed that under these conditions flies exhibited a following reaction to the

Optomotor response describes the strength of the turning response elicited by visual sensory input

visual pattern motion (Figure 1.2B). In accordance with the assumption that optic flow triggers correcting turns in flying flies, the strength of these optomotor responses depended on the characteristics of the visual motion (direction and speed of rotation) and of the pattern (spatial wavelength and contrast). For example, when presenting a grating with a certain spatial wavelength (λ) rotating with different speeds (v) around the fly, the following reactions were strongest at a certain speed (v_o). When defining temporal frequency as λ/v , it could be observed that the optimum temporal frequency (λ/v_o) was constant for different spatial wavelengths, i.e. the larger the wavelength of the presented pattern the higher the speed was to elicit the strongest responses (Fermi and Reichardt, 1963; McCann and MacGinitie, 1965). Interestingly, to elicit such following movements the presentation of a moving pattern to only one eye was sufficient (Fermi and Reichardt, 1963). Further experiments established that these optomotor reactions were not only restricted to flying flies, but were also present during tethered walking (Götz and Wenking, 1973) with similar properties.

Later, using a torquemeter that can be used in any orientation, allowed to also record pitch and roll torque responses. Both responses turned out to have strikingly similar properties as reported for the yaw responses described above (Blondeau and Heisenberg, 1982). These experiments suggest that the described optomotor responses are controlled in a similar manner and serve to stabilize locomotion for rotations around all three body axis.

Since the early experiments a lot of interesting features about flight forces have been deduced observing tethered flight. Detailed analysis of wing kinematics of tethered flying flies suggests that to produce torque during flight, flies reduce their wing beat amplitude on the side they turn to while enlarging it on the opposite side (Götz, 1968; Götz et al., 1979). Equal to rowing a boat, the produced torque is not continuous but rather pulsating according to the wing beat frequency or equivalently to the rowing frequency in the analogy (Dickinson and Gotz, 1996a).

Using wing beat kinematics as readout revealed that flies not only follow visual motion but do it extremely fast. Astonishingly, these reactions have delays in the order of only about 20 ms and time-to-peak of about 100 ms (Theobald et al., 2010). This allows flies to react upon undesired movements swiftly and shows the feasibility that these optomotor reactions can indeed be used by a fly during flight

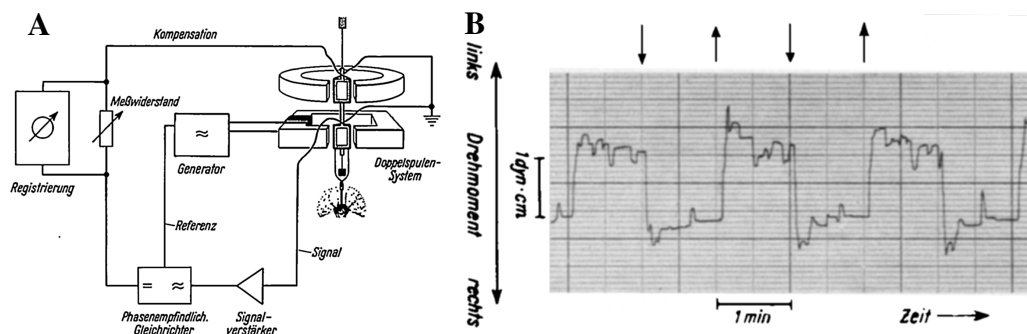


Figure 1.2: Initial optomotor behaviour measurements in flying flies.

(A) Schematic of a setup for measuring yaw torque responses in flying tethered flies. A tethered fly is glued to a piece of cardboard and fixed to the torquemeter consisting of two coils. The upper coil is placed in a constant and the lower one in an oscillating magnetic field. When the fly exerts torque, both coils turn and an alternating voltage, proportional to the angle of rotation, is induced in the lower coil. Depending on the direction of rotation the induced voltage is phase shifted in 180° . Using the properties (phase and amplitude) of the induced voltage a compensatory current is calculated and passed through the upper coil producing a torque in the opposite direction of the torque generated by the fly. (B) Sample trace of measured torque elicited by visual motion rotating clockwise (upward arrow) and counter-clockwise (downward arrow). The fly follows the direction of rotation (Adapted from (Fermi and Reichardt, 1963)).

maneuvers.

Flies are able to produce only one force pointing at approximately 24° with respect to their longitudinal body axis. To fly faster or to produce more lift, flies must change their body angle during flight, i.e. in order to hover flies need to position their body to approximately 60° with respect to the horizon (Götz, 1968). However, for the latter contradictory evidence exists which states that lift and thrust are not strongly coupled, at least in *Calliphora vicina* (Blondeau, 1981a).

Although tethered flying experiments provide valuable information on how flies react upon changes in visual motion, they fail to show all characteristics of flight maneuvers performed during free flight. For example, during free flight the blow fly flight can be divided into saccadic episodes and episodes between saccades (Hateren and Schilstra, 1999). During saccades, blow flies turn with angular speeds up to $4000^\circ / \text{s}$ whereas between saccades angular velocities are

Saccades are fast turns between straight flight course segments

greatly reduced. For *Drosophila*, during fixed tethered flight, saccades last up to 500 ms (Tammero and Dickinson, 2002) which is about 10 times longer than in free flight (Fry et al., 2003). In contrast, when permitting a tethered fly to actually turn fast, for example using a magnetic tether which allows the fly to rotate in place around 360°, it is possible to observe these fast saccades also in tethered flying *Drosophila* (Bender and Dickinson, 2006b). These differences in the saccadic behaviour are believed to be a product of the closed loop control of flight course correction. During free flight, flies must first generate torque to start rotating and soon after produce a counter torque, not observed in tethered flight, to stop turning (Fry et al., 2003). Increasing or decreasing haltere movement has an effect on this saccadic behaviour (Bender and Dickinson, 2006a). This hints towards visual information triggering turns and halteres controlling their termination. Thus, during free flight more than visual sensory input is needed and all sensory input needs to be fused together in an appropriate way.

Halteres are small dumb-bellshaped organs derived through evolutionary transformation of the hind wings

Even though angular velocities between saccades are smaller than during saccades, they are still large enough for spatial details to be blurred complicating the correct analysis of the optic flow patterns. The use of small sensor coils mounted on the thorax and head of freely flying blow flies demonstrated that flies not only turn their body but also turn their heads with respect to the thorax (Hateren and Schilstra, 1999). Since visual motion is perceived by the eyes, the relevant angular velocities are those of the head. These speeds are only approximately half of the angular velocities of the thorax and lie in the range of 0 to 100° / s which is low enough to reduce the visual blur due to rotations. Simultaneous measurements of head movement and turning behaviour in tethered flying flies have similar response characteristics to visual motion (Duistermars et al., 2012). This suggests that both behaviours are controlled using a common mechanism.

Tethered flight is not a natural situation for flies and it does not involve all the sensory integration done during free flight. Nevertheless, it has one great advantage over analyzing reactions of freely flying flies: It allows to observe behavioural reactions which are produced mostly by visual input. Since visual stimuli can be designed at will, tethered behaviour allows to study any visual paradigm with high precision. Contrary to tethered flight, during free flight no exact control over the visual stimuli can be achieved so far. Furthermore, the reactions are not only due



to visual input, thereby making the analysis much more complicated.

1.2 Motion Computation

To understand how the above described following responses are elicited in flies, it is necessary to understand how flies compute motion. For this, optomotor experiments are not the optimal way to proceed. During the experiment the visual motion must be sensed, computed and then the motor responses must be elicited. Since optomotor behaviour incorporates all these steps, the use of behaviour as a readout for motion computation does not reflect the real dynamics of the computed motion output signal. Thus, the best way to understand how flies compute motion is to directly record the responses of neurons participating in its computation.

1.2.1 Direction Selective Neurons

Soon after the first optomotor responses had been observed in tethered flying flies the first recordings of cells in the visual system of the fly were performed (Bishop and Keehn, 1967). Flies were immobilized using wax and extra-cellular micro electrodes were used to record cells in the visual system while presenting similar visual stimuli to the fly as shown in optomotor experiments. During these recordings cells were found which responded in a direction selective way to visual stimuli. In addition, the cellular responses exhibited the same characteristics as reported for optomotor measurements. This led to the conclusion:

“We feel that it may be concluded from the correlations between the firing patterns of the directional units and the behavioral optomotor response that the directional units are a link in the transfer of the information prerequisite to the optomotor response.” (Bishop and Keehn, 1967)

Today much more is known about the visual system than when Bishop and Keehn performed their recordings 50 years ago. The visual world is detected by the photoreceptors in the retina and beneath it, three successive neuropils form the visual ganglia. These are lamina, medulla and the lobula plate complex, which

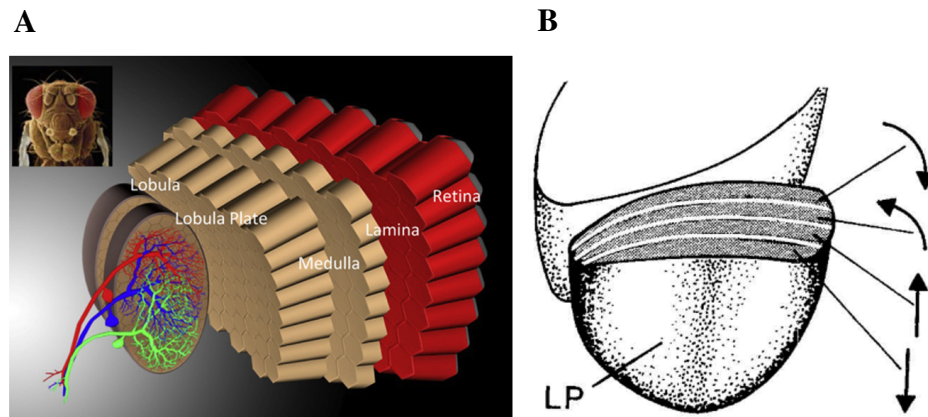


Figure 1.3: Schematic of the visual ganglia. (A) The visual ganglia consist of the retina, lamina, medulla and lobula plate complex (lobula and lobula plate). One representative group of cells in the lobula plate contains three cells sensitive to horizontal motion, HSN (red), HSE (blue) and HSS (green) (Adapted from (Borst and Euler, 2011)). (B) The lobula plate can be divided in four layers, each sensitive to motion in a different direction. Going from anterior to posterior the schematic displays the layers sensitive to front-to-back, back-to-front, upward and downward motion (Adapted from (Buchner et al., 1984)).

in turn consists of the lobula and lobula plate (Figure 1.3A; for a review refer to (Borst et al., 2010)). 50 direction-sensitive neurons with large dendrites have been identified in the blow fly's lobula plate and many of these lobula plate tangential cells (LPTCs) have also been found in *Drosophila*. When motion is presented in their preferred direction (PD), these cells depolarize. Motion in the opposite direction, also called the null direction (ND) of the cell, hyperpolarizes the cells. All these cells are not located randomly. Using deoxyglucose experiments, Buchner et al. concluded that the lobula plate can be divided into four layers. Going from anterior to posterior these layers are sensitive to front-to-back, back-to-front, upward and downward motion (Figure 1.3B; (Buchner et al., 1984)).

One representative group of cells sensitive to downward motion in the lobula plate is the group of Vertical System cells (VS-cells). In blow flies 10 VS-cells and in *Drosophila* 6 VS-cells have been identified. In both fly species, VS-cells depolarize for downward motion and hyperpolarize for upward motion (Figure 1.4A; (Haag and Borst, 2004; Joesch et al., 2008)). Similar to optomotor

LPTCs Lobula plate tangential cells

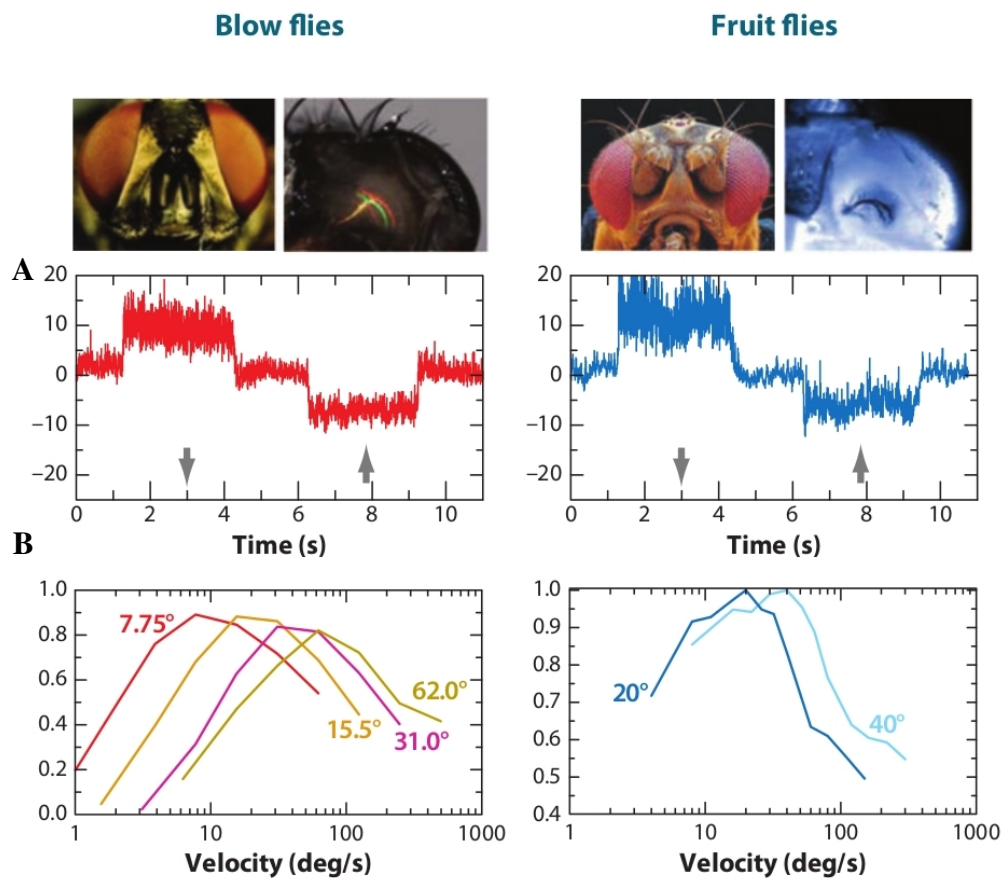


Figure 1.4: Comparison of VS-cell responses in blow (left column) and fruit flies (right column). (A) VS-cell responses to up- and downward motion (arrows indicate direction of presented motion). (B) Normalized response curves for a sine wave grating with different spatial wavelength moving at different constant velocities (Adapted from (Borst et al., 2010)).

responses, when presenting a sine wave grating moving at different speeds, the longer the spatial wavelength of the sine wave grating, the higher the pattern velocity at which the highest cell response occurs (Figure 1.4B).

Figure 1.3A depicts another group of lobula plate tangential cells which contains three cells of the Horizontal System (HS-cells, two shown in Figure 1.5A). All three cells depolarize in response to motion in the front-to-back direction and hyperpolarize for motion in the opposite direction (Figure 1.5C; (Schnell et al., 2010)). The strength of depolarization of each HS-cell depends on the

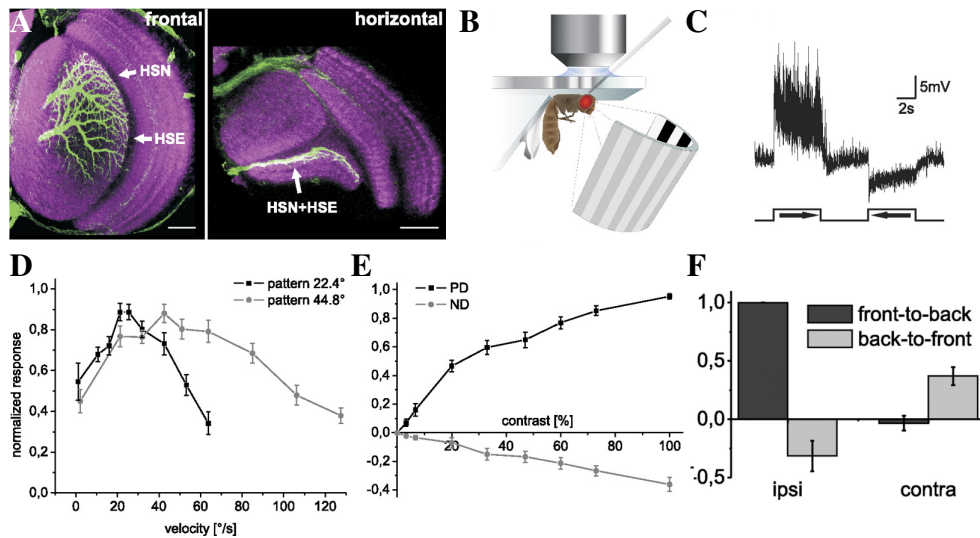


Figure 1.5: HS-cell characteristics in *Drosophila*. (A) Anatomy of HSN and HSE cells in *Drosophila* (Scale bar: 25 μm). (B) Scheme of the recording preparation for patch-clamp recordings in *Drosophila*. (C) Directional sensitive response of an HSN-cell. Motion in front-to-back direction (right pointing arrow) depolarizes the cell and motion in back-to-front direction (left pointing arrow) hyperpolarizes it. (D) Velocity dependency of HS-cells for a sine grating with two different wavelengths. (E) Contrast dependency of HS-cell responses for motion in the preferred direction (PD) and null direction (ND). (F) Normalized HS-cell responses to front-to-back and back-to-front for motion on the ipsi- and contralateral side (Adapted from (Schnell et al., 2010)).

velocity (Figure 1.5D) and the contrast (Figure 1.5E) of the visual stimuli. Interestingly, HS-cells located on one hemisphere of the fly brain are also sensitive to motion on the contralateral side (Figure 1.5F).

The **receptive field** of a cell describes how sensitive a cell is to motion at a certain elevation and azimuth angle

All three HS-cells dendrites cover a large portion of the lobula plate. The northern HS-cell (HSN) covers the dorsal, the equatorial HS-cell (HSE) the equatorial and the southern HS-cell (HSS) the ventral part of the lobula plate (Figure 1.6A). The HS-cells have large dendritic spanning fields. HSN, HSE and HSS cover about 70%, 90% and 75% of the total area of the lobula plate, resulting in a large overlap of their dendritic spanning fields. More detailed analysis of visually elicited cell responses indicates that each of the three HS-cells responds best at different elevations, depending on their location in the lobula

plate (Schnell et al., 2010). Hence, HSN responds best to movement in the dorsal part of visual space, whereas HSE and HSS respond best to motion in the equatorial and ventral part of visual space, respectively (Figure 1.6B).

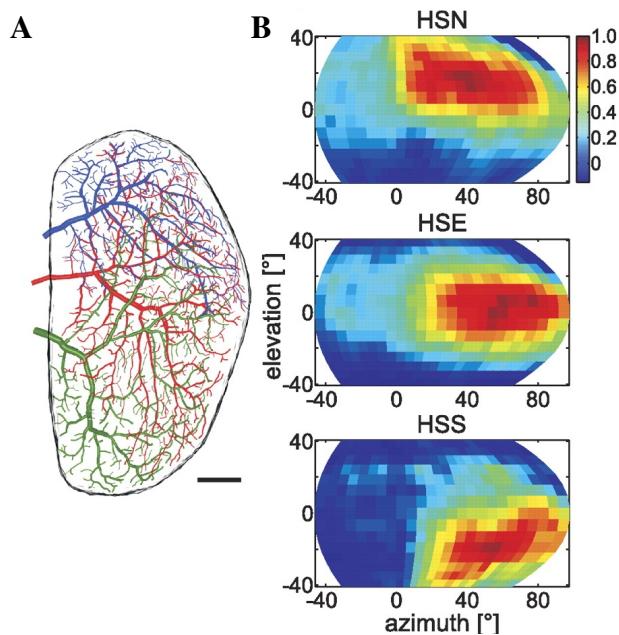


Figure 1.6: Dendritic structure and receptive fields of HS-cells. (A) Reconstruction of the dendritic arborization of HSN (blue), HSE (red), and HSS (green) in the lobula plate (Scale bar: $20 \mu\text{m}$). (B) Receptive fields of the three HS-cells. Response amplitudes (PD–ND), normalized to the maximal response, elicited by a small bar moving horizontally at different elevations (Adapted from (Schnell et al., 2010)).

Because of the similar structure of the optic ganglia and the similar response properties of cells in fruit and blow flies it is intriguing to assume that both flies use a similar strategy to detect motion. This is why several studies on the blow fly can also be used as a reference when studying visually elicited cell and optomotor responses in fruit flies.

1.2.2 Compound Eye: Sensing the Environment

Before lobula plate tangential cells can respond in a direction selective way, the environment has to be sensed, the information needs to be computed and transferred to these cells. For the first step, the detection of changes in luminance in the visual space, flies use their two compound eyes (for a review refer to (Wang and Montell, 2007)).

In *Drosophila*, one compound eye is composed of about 750 “small eyes” called ommatidia. Each ommatidium contains a small lens, a transparent crystalline cone, 8 photoreceptor neurons (R1–R8) and pigment cells (Figure 1.7A).

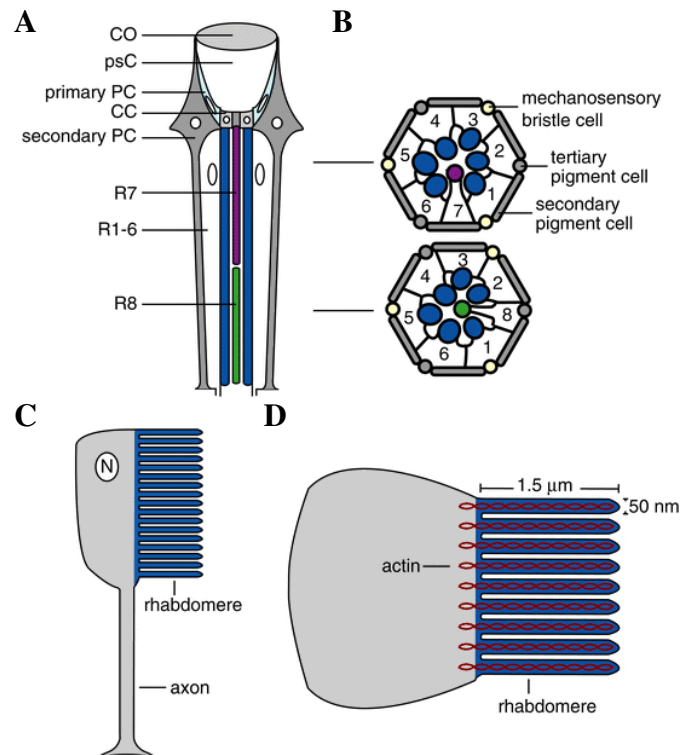


Figure 1.7: Structure of a single ommatidium. (A) A single ommatidium of the compound eye. Schematics depicts: co, cornea; primary PC, primary pigment cell; psC, pseudocone; secondary PC, secondary pigment cell; R1-R6, photoreceptor cells 1-6; R7 and R8, photoreceptor cells 7 and 8. (B) Cross-sections through the distal and proximal regions of the ommatidia. Ovals represent the rhabdomeres and each R cell is numbered. (C) Longitudinal view through a photoreceptor cell. Depicted the rhabdomere, axon, and nucleus (N). (D) Cross-sectional view through a photoreceptor cell with the dimensions of an R1-R6 cell microvillus (Adapted from (Wang and Montell, 2007)).

Each photoreceptor is composed of a rhabdomere, nucleus and an axon (Figure 1.7C). The rhabdomere has a membrane that is folded to a microvilli structure allowing a large membrane surface over a small volume. In each ommatidium, the nuclei of the eight photoreceptors are positioned in a circle with the rhabdomeres pointing towards the center (Figure 1.7B). The rhabdomeres form an axis which composes the rhabdomen. Where the rhabdomeres of R1-R6 occupy the entire length of the retina, R7 and R8 rhabdomeres occupy only the distal and proximal regions with the R7 rhabdomere being on top of the R8 rhabdomere (Figure 1.7A).



To detect the environment, light is focused by the lens and crystalline cone onto the rhabdomen where photons are absorbed by a light-sensitive membrane protein called rhodopsin. Thanks to the large membrane surface of the individual microvilli constituting it, the rhabdomere has a high concentration of rhodopsin (Figure 1.7D; for a review refer to (Hardie and Raghu, 2001)). Rhodopsin is composed of the protein opsin coupled to a light-sensitive chromophore 11-cis retina and is able to absorb photons. The high concentration of rhodopsin present in the rhabdomere maximizes the probability for a photoreceptor to absorb a photon. This allows photoreceptors to be able to respond to single photons (Hardie and Raghu, 2001).

Once a photon is absorbed, the light-sensitive chromophore 11-cis retina is isomerized to all-trans-retinal. This produces a conformational change of the rhodopsin to metarhodopsin. Metarhodopsin binds to a trimeric G-protein with sub-units called α , β and γ (Figure 1.8(1)). Once bound to the trimeric G-protein, metarhodopsin acts as a catalyst and allows for GDP (guanosine diphosphate) to be exchanged with GTP (guanosine triphosphate). After this the GTP-bound α -subunit dissociates (Figure 1.8(2)) and binds to the inhibitor of the phospholipase C (PLC) enzyme. Without its inhibitor, PLC can hydrolyze phosphatidyl inositol biphosphate (PIP₂) to diacylglycerol (DAG) and inositol-3-phosphate (InsP₃) (Figure 1.8(3)). Only after these steps of the phototransduction cascade are the transient receptor potential ion-channels (TRP) opened. Once open, cations can enter the photoreceptor cells, thereby depolarizing them. The exact mechanism opening TRP channels is still unclear. Evidence exists that PLC activity changes the membrane properties of the photoreceptors. The proton released by hydrolysis of PIP₂ by PLC elevates the acidity in the microvilli (Huang et al., 2010). These changes lead to a contraction of the microvilli resulting in mechanical forces that could contribute to the opening of the TRP channels (Hardie and Franze, 2012).

Shortly after the TRP channels have been opened, calcium is rapidly cleared by a sodium-calcium-exchanger (CalX). To bring the cascade back to its initial state, DAG is converted first to phosphatidic acid (PA) by DAG kinase and then PA is converted to PIP₂ by a multienzymatic pathway (Figure 1.8(4)). To inactivate the metarhodopsin it is phosphorylated by rhodopsin kinase and capped by arrestin (Figure 1.8(5)). The G protein and its effector are inactivated by a GTPase activity

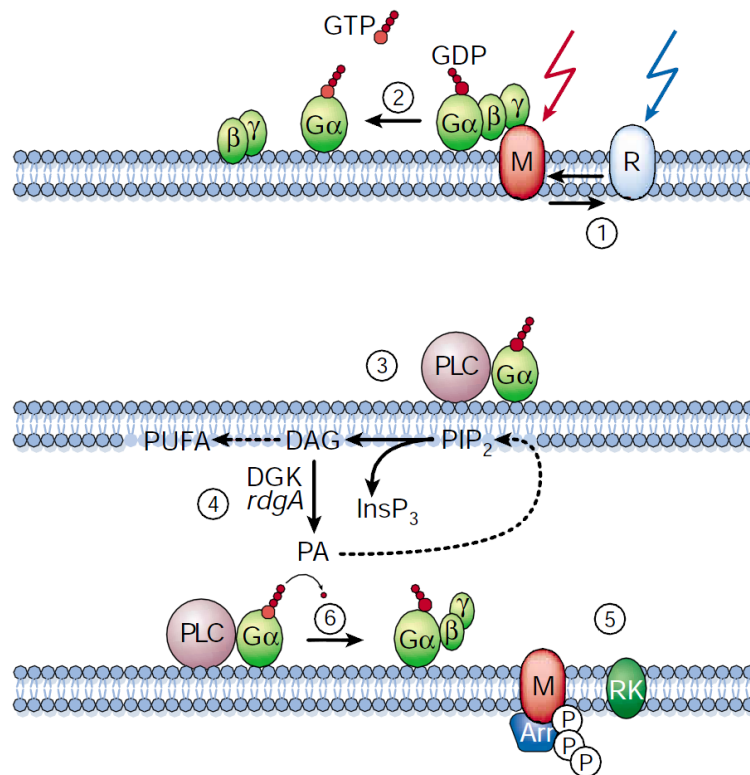


Figure 1.8: The phototransduction cascade. (1) Photoisomerization. Rhodopsin (R) is photoisomerized to thermostable metarhodopsin (M) which can be reconverted to R by long-wavelength light; (2) GTP/GDP exchange. M catalyses exchange of GDP for GTP on the heterotrimeric G protein; active GTP-bound α -subunit dissociates. (3) Activation. G_{α} binds to and activates the effector enzyme PLC which hydrolyses PtdIns(4,5) P_2 (PIP_2) to DAG and Ins(1,4,5) P_3 . DAG is also a potential substrate for DAG lipase, leading to the release of PUFAs. Two classes of channel (TRP and TRPL) are activated by an unknown mechanism. (4) Substrate resynthesis. DAG is converted to phosphatidic acid (PA) by DAG kinase (DGK). PA is converted to PtdIns(4,5) P_2 by a multienzymatic pathway. (5) Metarhodopsin inactivation. M is phosphorylated by rhodopsin kinase (RK) and capped by arrestin. (6) Inactivation of G protein and effector. Effector enzyme and G_{α} are inactivated by the GTPase activity of the G protein, leading to reassociation with $G_{\beta\gamma}$ which is accelerated by PLC (Adapted from (Hardie and Raghu, 2001)).

of the G protein. This leads to a reassociation with $G_{\beta\gamma}$ and is accelerated by PLC (Figure 1.8(6)). For metarhodopsin to transform back to rhodopsin it only needs to absorb light of longer wavelengths (Fig1.8(1)). To make this transformation more



efficient, the eye screening pigments are transparent to long wavelength light, absorbing other wavelengths, and make the fly compound eyes appear red.

Despite the several steps of the phototransduction cascade it is extremely fast and flies have the ability to distinguish flicker of more than 300 Hz from continuous light (Laughlin et al., 1987). This makes watching TV probably an uneventful experience for a fly. Although fast, flies do not have super eyes. Since the 750 ommatidia are used by *Drosophila* to observe almost 180° of visual space, flies have an inter-omatidial angle of as large as 4.6° (Götz, 1965). Therefore, flies have a spatial resolution 500 times lower than the human eye in the fovea.

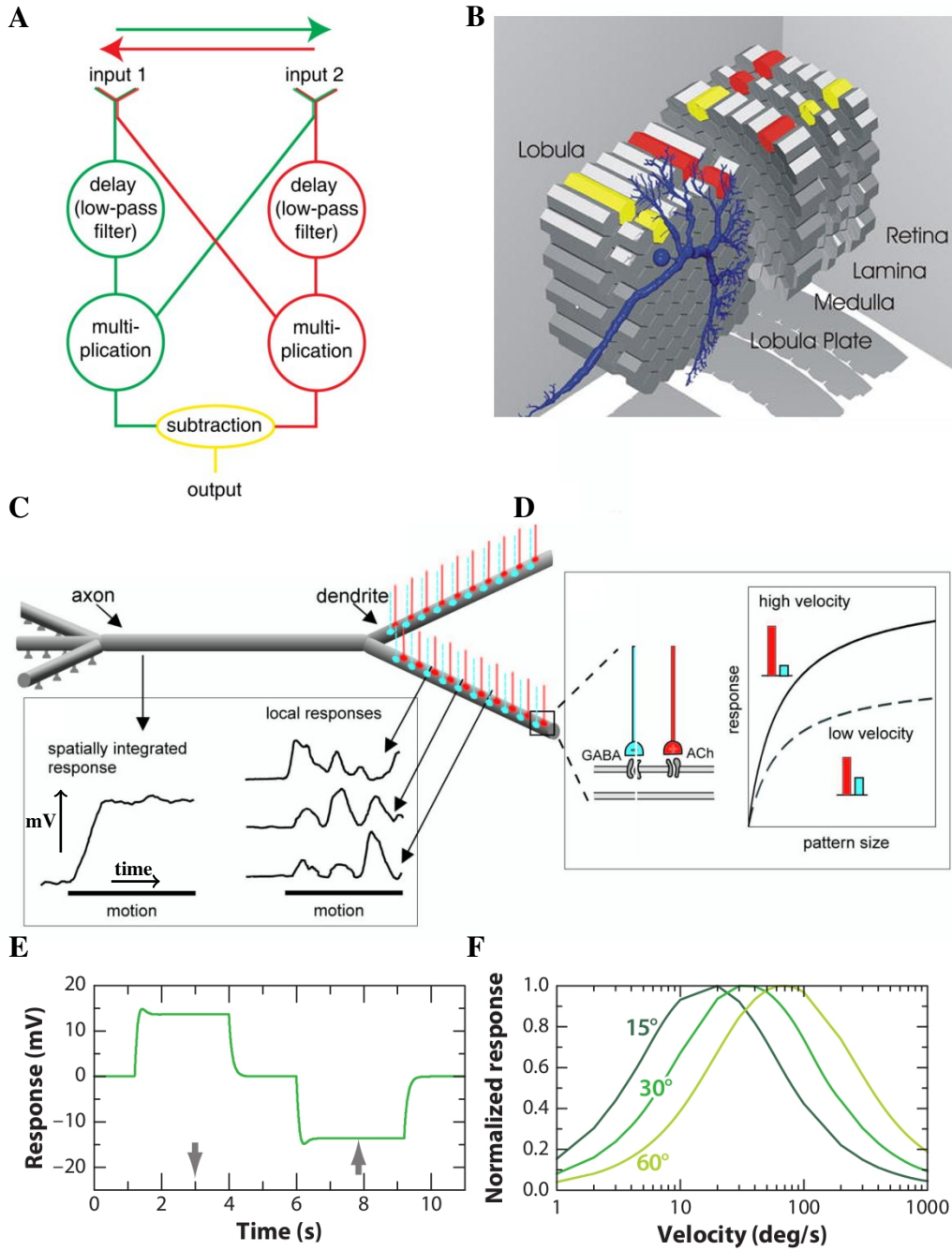
Flies are able to distinguish colors. For this, different opsins sensitive to different wavelengths of light are expressed in the photoreceptors. R1-R6 express the opsin Rh1 with a broad absorption spectrum. R7 expresses one of two opsins sensitive to ultraviolet light, Rh3 or RH4 and R8 expresses Rh5 or RH6 opsins, sensitive to blue and green light, respectively. Using these different combinations in an appropriate way flies are able to distinguish colors (Menne and Spatz, 1977). However not all photoreceptors are thought to take part in color vision. Evidence exists that R1-R6 photoreceptors are primarily used by the fly for motion detection (Yamaguchi et al., 2008) whereas R7 and R8 are used for color vision (Gao et al., 2008). Recent results suggest that these motion and color pathways are not completely separated. Information from R7 and R8 also shapes the motion pathway output improving motion discrimination (Wardill et al., 2012).

1.2.3 Elementary Motion Detectors

Flies need to detect motion. Using their photoreceptors they perceive changes in luminance at certain points in visual space. How do they extract motion from this information? For this one can consider the following: When a bright object moves over a dark background, only those photoreceptors that look at the object depolarize. If this object moves from left to right, the photoreceptors pointing to the left become depolarized earlier than the photoreceptors to the right. This way, when comparing two photoreceptors looking at neighboring points in visual space, the movement of the object will be from the side where the depolarization occurred first towards the second photoreceptor.

Hassenstein and Reichardt proposed a more sophisticated but similar model using their observations from the optomotor responses of the beetle *Clorophanus viridis* (Hassenstein and Reichardt, 1956). This model, known as the correlation-type or elementary motion detector model, consists of two mirror symmetric half detectors (Figure 1.9A). One half detector compares two outputs of two photoreceptors after one of them has been delayed. Mathematically the delay is modeled using a low-pass filter and the comparison is achieved by means of a multiplication stage. If the signal of the delayed line is generated first, it arrives at the multiplication stage at a similar instance in time as does the non-delayed output

Figure 1.9 (facing page): The elementary motion detector model and its properties. (A) Two half detectors and their preferred direction of motion (arrows, red and green). For motion from left to right (green arrow) input 1 occurs before input 2. Since input 1 is delayed in time, both signals reach the multiplication stage at the same instance in time, resulting in a positive output of the multiplication. For motion in the opposite direction, the signal from input 2 reaches the multiplication before input 1 and the multiplication results in a small signal. Same holds true for motion in the opposite direction and the red half detector. Due to the subtraction stage a positive signal is obtained for motion from left to right and negative for motion from right to left (Adapted from (Gabbiani and Jones, 2011)). (B) Schematics of the retina and the three successive neuropiles and a VS-cell (blue). The columnar and the retinotopic projection onto the lobula plate are indicated by red and yellow columns (Adapted from (Borst and Haag, 2002)). (C) and (D) dendritic integration (Adapted from (Egelhaaf, 2009)). (C) Depending on the texture of the environment, motion with constant speed gives differently changing inputs to the lobula plate tangential cells (right traces). By pooling all these varying inputs, an average is taken and the output of the cells is constant over time (left trace). (D) Each lobula plate tangential cell gets inhibitory (GABAergic) and excitatory (cholinergic) input (left). During motion in the preferred direction both types of input are activated. The strength of activation depends on the velocity of motion leading to different saturation levels for different speeds (right traces). (E) and (F) Simulation of an array of elementary motion detectors (Adapted from (Borst et al., 2010)). (E) Output of the elementary motion detectors when motion is presented moving in the directions indicated by the arrows. (F) Dependency of the outputs from an array of elementary motion detectors to sine wave gratings with different spatial wavelengths moving at different velocities.



of the other photoreceptor. In this case the output of the half detector will be a large value since two similar signals were multiplied. When the non delayed photoreceptor is activated first, the signals arrive at the multiplication at different instances in time and the output of the half detector is small. This way, one half detector can detect movement occurring in one direction by giving a positive output for motion in the preferred direction and a small output otherwise. In order to also detect movement in the other direction, a second mirror-symmetrical half detector is used. By subtracting both half detector outputs a fully directionally sensitive detector is obtained. Note that the output of this model depends on the speed of the moving object and delay time. If the speed is such that the delay equals the time needed for the object to reach the non delayed photoreceptor, the output is maximum and smaller otherwise.

When looking at the columnar structure of the visual ganglia it seems to fit perfectly to this model. The image projected onto the retina is projected retinotopically onto the lobula plate (Figure 1.9B). Even after two chiasmata, one between the lamina and the medulla and another one between the medulla and the lobula complex, neighboring columns in the retina remain neighbors in each neuropil. Thus, information from neighboring points in visual space can be processed in the lamina and medulla separately before they reach the lobula and lobula plate.

Studies indicate that lobula plate tangential cells receive excitatory cholinergic as well as inhibitory GABAergic input (Brotz et al., 2001; Raghu et al., 2007; Raghu et al., 2009). The half detector response in the preferred direction is probably passed to the lobula plate tangential cell using excitatory synapses whereas the other half detector response in null direction uses inhibitory synapses (Figure 1.9D, left part). This input scheme allows the cell to be excited by motion in its preferred direction and inhibited by motion in the null direction. Since each elementary motion detector output depends on the texture of the visual scene, changes of the visual environment with constant speed yield changing inputs to the lobula plate tangential cell (Figure 1.9C, right traces). However, since many elementary motion detectors give input to one cell, all outputs are summed and an average is taken making the overall response stable (Figure 1.9C, left trace).

Using this scheme one could expect that the output of lobula plate tangential cells not only depends on the speed of the moving pattern but also on its size,



i.e. the larger the pattern the more input the cell receives. This would make it difficult to distinguish if a big output was due to the speed of the object or simply due to its dimension. However, during motion in the preferred direction inhibitory and excitatory inputs are activated. Since the activation strength depends on the velocity of motion, it leads to different saturation levels of the cells (Borst et al., 1995; Single et al., 1997). This phenomenon, also known as gain control, makes it possible to deduce the speed of motion of patterns with different sizes (Figure 1.9D, right part).

All seems to fit perfectly. However, a model is only useful if it can predict and explain observed phenomena. The elementary motion detector model has been successful in doing this. Interestingly, although this model was proposed using observations of the optomotor responses in the beetle *Clorophanus viridis* it is also able to model optomotor responses of flies (Götz, 1964; Buchner, 1976).

Simulations indicate that pooling elementary motion detectors gives rise to a direction sensitive output (Figure 1.9E) which also shows a temporal frequency optimum (Figure 1.9F; (Borst et al., 2010)). Both of these response characteristics can also be observed in optomotor and cell responses (refer to sections 1.1 and 1.2.1, respectively).

When a step-like velocity change is applied to a resting grating, elementary motion detectors responses during the transient state show transient oscillations at the temporal frequency of the pattern. This also has been observed in lobula plate tangential cells in big and small flies (Egelhaaf et al., 1989; Joesch et al., 2008).

Having a model that can reproduce many observed phenomena raises the question, how are these elementary motion detectors actually implemented, i.e. which neurons form the neuronal network implementing an elementary motion detector?

Cell silencing during behavioural experiments (Rister et al., 2007; Clark et al., 2011) and lobula plate tangential cell recordings (Joesch et al., 2010) have shown lamina cells L1 and L2 to be necessary for motion computation. These cells get their input from photoreceptors R1-R6 located in different neighboring ommatidia pointing at the same location in visual space. Blocking L1-cells eliminates responses to on-edges of lobula plate tangential cells. When blocking L2-cells, lobula plate tangential cells do not respond to off-edges any more. Thus, the vi-

on- and off-edges are luminance increments and decrements of a point in visual space, respectively



separated into subgroups each sensitive to motion on a different axis. According to their preferred direction they give input to the four sublayers of the lobula plate.

When blocking T4- and T5-cells, HS-cells do not respond to motion (Schnell et al., 2012). Selectively blocking T4-cells eliminates off-edge responses, while blocking T5-cells eliminates on-edge responses in lobula plate tangential cells (Maisak et al., 2013). Thus, T4- and L1-cells are necessary for lobula plate tangential cells to respond to on-edges. T5- and L2-cells on the other hand, are necessary for lobula plate tangential cells to respond to off-edges. This suggests that the L1-pathway ends at the T4-cells and the L2-pathway ends at the T5-cells. Since T4- and T5-cells are direction sensitive with velocity tuning similar to lobula plate tangential cells indicates that all the motion computation is done before the lobula plate. Lobula plate tangential cells thus simply pool the directional input from the T4- and T5-cells.

Having strong evidence of the input and output cells of the elementary motion detectors leaves the final question, what is in between? Using electron microscopy a connectome of neurons within the medulla has been reconstructed (Figure 1.10A; (Takemura et al., 2013)).

L1-cells give input to Mi1-, Tm3-, L5-, C2- and C3-cell types. More than half of the synaptic contacts of L1-cells are with Mi1- and Tm3-cell types. Mi1- and Tm3-cells contribute with more than 80% of presynaptic inputs to T4-cells. Thus, the primary on-pathway is composed of the connections of L1- to Mi1- and Tm3-cells which then give input to the T4-cells.

Similar analysis allows to identify neurons composing the off-pathway. L2-cells form strong connections with Tm1-, Tm2- and Tm4-cell types (Takemura et al., 2013). In the lobula, Tm1-, Tm2- and Tm4-cells most likely give input to the T5-cells (Fischbach and Dittrich, 1989).

For this circuit to be able to compute motion it must possess two characteristics. First, visual information from two different points in space need to be analyzed. Second, the information from one of the points needs to be delayed in time. T4-cells receive input from several Mi1- and Tm3-cells (Figure 1.10B; (Takemura et al., 2013)). When calculating the Tm3- and Mi1-cell receptive field components for a T4-cell receptive field as shown in Figure 1.10B, it can be observed that their centers of mass are displaced in the same direction as the directional preference

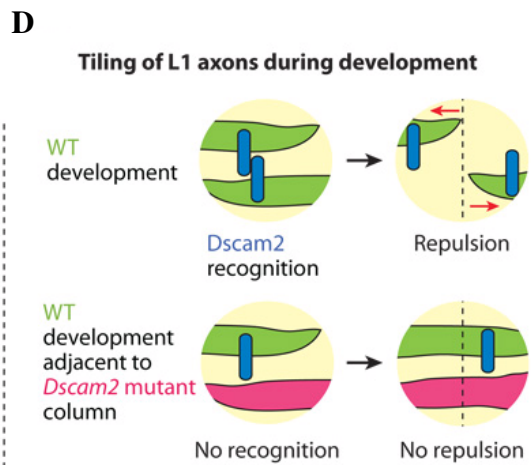
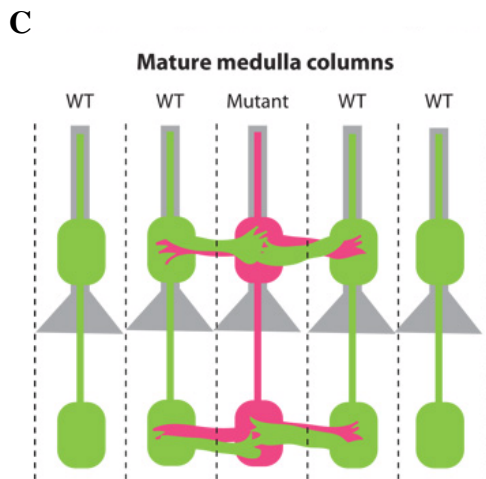
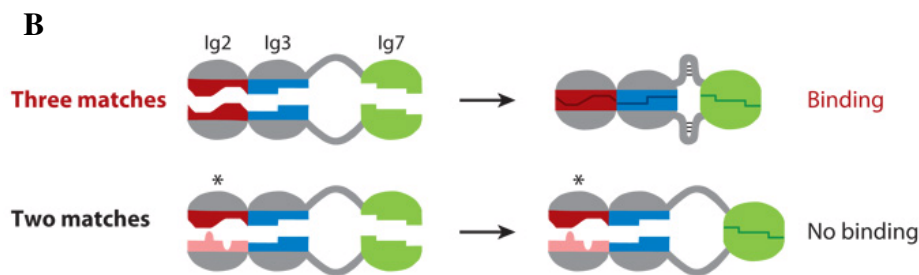
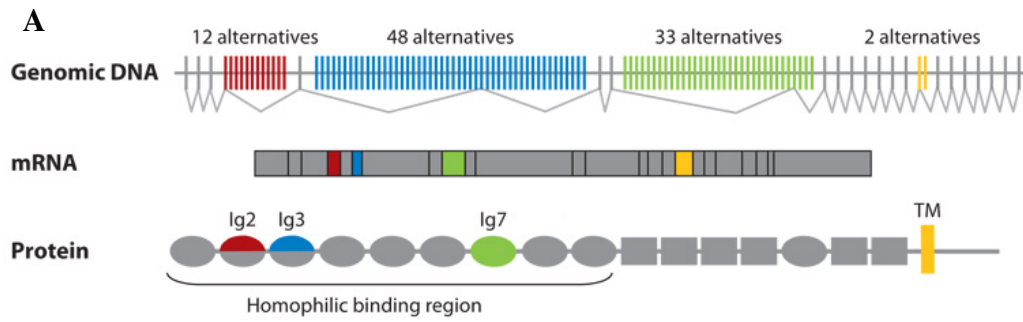
of the T4-cell. Thus, the visual information input to T4-cells incorporates information from two different points in visual space which are weighted through the number of synaptic connections. If the Tm3-arm introduces a longer delay than the Mi1-arm then also the second prerequisite is fulfilled and this circuit could indeed function as an elementary motion detector for off-edges.

1.2.4 Dscam (Down Syndrome Cell Adhesion Molecule) and Neural Circuit Formation

Lobula plate tangential cells become direction selective in only certain areas in visual space by sampling input from elementary motion detectors within a specific area in the visual space. For this, it is essential that the visual space is projected retinotopically onto the lobula plate which is achieved by the columnar organization of the fly visual system.

The importance of this columnar structure and the correct synaptic connec-

Figure 1.11 (facing page): Dscam1 apparently promotes self-avoidance and Dscam2 regulates tiling in the flies visual system. (A) The *Drosophila* Dscam1 gene contains four blocks of alternative exons that encode 12 different variants for the N-terminal half of Ig2 (red), 48 different variants for the N-terminal half of Ig3 (blue), 33 different variants for Ig7 (green), and two different variants for the transmembrane domain (TM) (yellow). Splicing leads to the incorporation of one alternative exon from each block which enables Dscam1 to encode $12 \times 48 \times 33 = 19\,008$ different ectodomains linked to one of two different transmembrane domains. (B) Dscam1 proteins exhibit isoform-specific homophilic binding. Each isoform binds only to its own kind, i.e. to identical isoforms matching at all three Ig domains. (C) Schematic of Dscam2 phenotypes in L1 axons in the fly medulla of the visual system. Wild type (green) L1 axons are restricted to one column, whereas mutant (pink) L1 axons are not. Columns are delineated with dashed lines. (D) Schematic of L1 column development. Dscam2 homophilic binding (blue bars) occurs between wild-type L1 neurites during pupal development. This induces a repulsive signal that results in the retraction of neurites back to their column of origin and the formation of columnar boundaries. Without Dscam2, mutant neurites (pink) cannot interact with wild-type L1 neurites (green) and no homophilic binding can occur. As a consequence, neither mutant nor wild-type L1 neurites can form connections in neighboring columns (Adapted from (Hattori et al., 2008)).



tions of the elementary motion detectors to the lobula plate tangential cells raises the question of how this can be achieved. During development, neurons need to know which way to grow, whether they should avoid or invade neighboring columns and which are the right neurites and cells to finally make synaptic connections with. For this, each neuron can be given a “name tag”. Every time a branch encounters another one during its development, it recognizes which type of neuron the other one belongs to. This allows a neuron to make the correct decision in which direction to grow or if a synaptic connection should be made. Following the above idea, when two neurons belonging to neighboring columns meet, they recognize each other using their name tag and repel each other back to their respective columns.

Since there are a lot of neurons in the fly brain a vast number of name tags are required. Various cell surface recognition molecules have been identified (Tessier-Lavigne and Goodman, 1996) allowing neurons to exchange information and enabling correct growth and patterning during development. As an example, one highly important cell surface protein is Dscam (Down syndrome cell adhesion molecule, for a review refer to (Hattori et al., 2008)).

In *Drosophila* four Dscam genes (Dscam1-4), all members of the immunoglobulin (Ig) superfamily, have been identified. Dscam1 has 24 exons of which 4 can be alternatively spliced giving rise to different variants of the Dscam protein. Each Dscam1 isoform shares the same domain structure with 10 Ig domains, 6 fibronectin type III domains, one transmembrane domain and one cytoplasmic domain (1.11A). Three of the Ig domains are encoded by alternative exon blocks. The first half of Ig2 is encoded by 12 alternative exons, the first half of Ig3 by 48 alternative exons and Ig7 by 33 alternative axons. This gives rise to $12 \times 48 \times 33 = 19\,008$ different isoforms. 18\,048 of these isoforms exhibit isoform-specific homophilic binding which is followed by the repulsion of neurites during development. This large variety of different isoforms as well as their binding specificity allows to generate many of the needed name tags and can be used to give each neuron its own identity. When two identical Dscam1 isoforms on opposing membranes bind, a repulsion of the membranes follows and self-avoidance is achieved (Figure 1.11B).

Whereas Dscam1 is thought to promote self-avoidance and might also pre-

Protein Isoform is one of several different forms of the same protein



vent synapse formation between wrong cells of different populations, Dscam2 promotes tiling, i.e. when branches from different neurons of the same kind meet they repel each other. Studies on the visual system of *Drosophila* have shown that Dscam2 mediates cell-type-specific avoidance between L1 axons in adjacent columns. This restricts each L1 axon to grow within its own column (Figure 1.11C; (Millard et al., 2007)).

1.3 Visual Network

The photoreceptors detect changes in luminance of points in the visual space and the elementary motion detectors implemented in the lamina, medulla and lobula give input to the lobula plate tangential cells. Depending on which layer of the lobula plate these cells are in, they receive direction sensitive input in the corresponding direction of the layer as shown in Figure 1.3B (Maisak et al., 2013). Each cell additionally possesses a specific receptive field which depends on its location and coverage in the corresponding layer of the lobula plate.

However, lobula plate tangential cells do not only receive input from elementary motion detectors. By injecting current in one cell and recording simultaneously the response in another cell, Haag and Borst discovered that these were coupled to each other (Haag and Borst, 2004). Thus far, a large network has been identified and all of the 50 lobula plate tangential cells form a dense network. Cells are connected to each other on the ipsi- and contralateral side using inhibitory and excitatory chemical and electrical synapses (Borst et al., 2010). Figure 1.12A depicts a schematic of this network known to be implemented in *Calliphora*.

These connections explain why the receptive fields of lobula plate tangential cells also incorporate direction sensitivity in other directions than their preferred direction. Figure 1.12B depicts the receptive fields of three VS-cells. It is clear that these are not only sensitive to vertical motion but also to horizontal motion (Wertz et al., 2009). Furthermore, HS-cells receive input from a cell sensitive to back-to-front motion on the contralateral side. This enables them to also be sensitive to back-to-front motion on the contralateral side (Figure 1.5F).

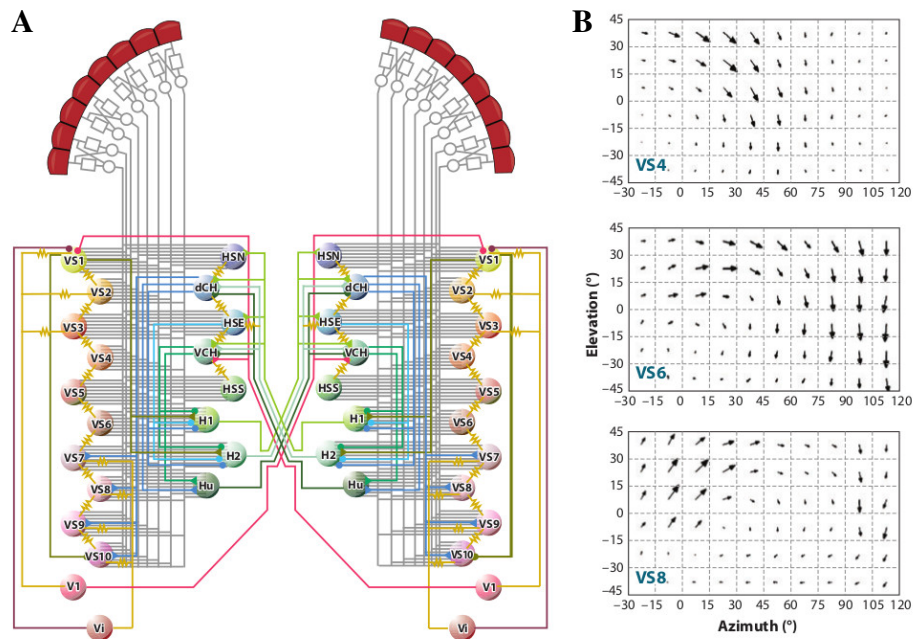


Figure 1.12: Lobula Plate Network. (A) Lobula plate tangential cells form a complicated network. Cells are connected to each other not only on the ipsi-, but also on the contralateral side. These connections are formed via inhibitory (circles) and excitatory (triangles) chemical and electrical (resistors) synapses. (B) Receptive fields of three VS-cells (Adapted from (Borst et al., 2010)).

1.4 Relationship Between Lobula Plate Tangential Cell Responses and Optomotor Responses

The idea that lobula plate tangential cells control optomotor responses has been postulated since Bishop and Keehn made their first electrical recordings of direction sensitive neurons in the visual system (Bishop and Keehn, 1967).

Besides the obvious match of the optomotor response and cell recordings several other observations support the role of lobula plate tangential cells in optomotor responses: i) Mutant fruit flies in which lobula plate tangential cells are missing or defective show a strong reduction in their optomotor response (Heisenberg et al., 1978). ii) Cutting HS-cell axons in adult flies (Hausen and Wehrhahn, 1983) or laser ablating HS precursor cells in larvae (Geiger and Nässel, 1981) significantly



1.4 Relationship Between Lobula Plate Tangential Cell Responses and Optomotor Responses

27

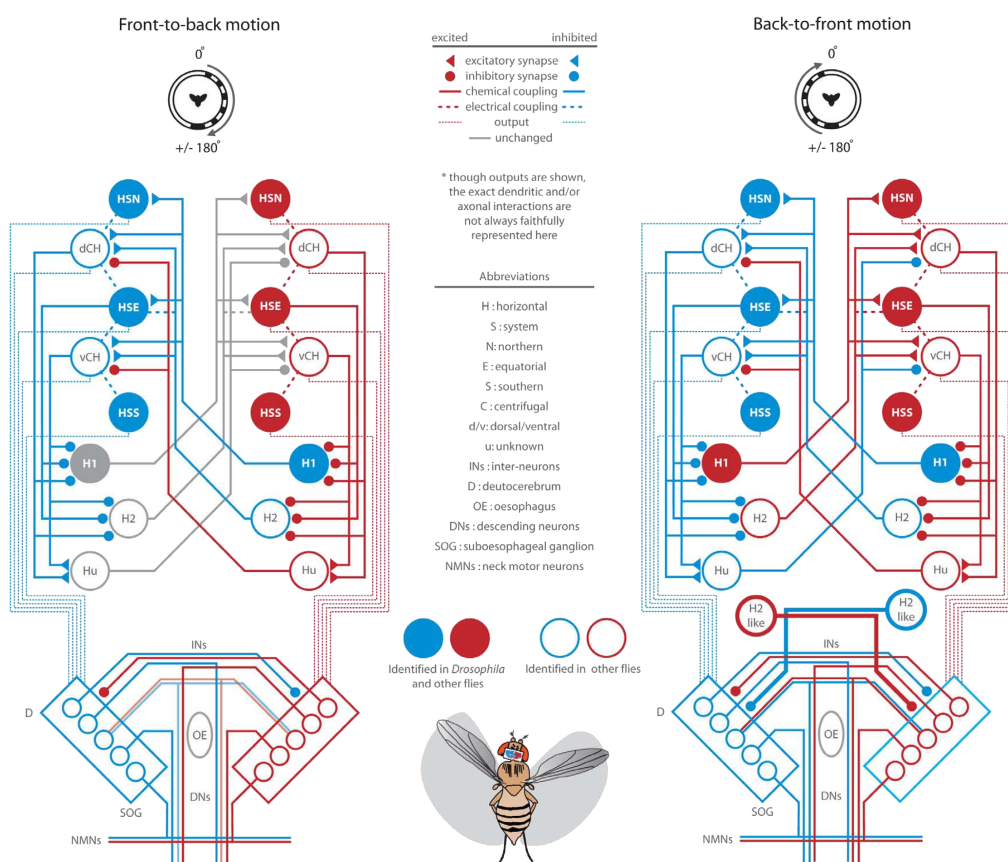


Figure 1.13: Summary diagram of presumed lobula plate tangential cell activation (red = depolarization) and inhibition (blue = hyperpolarization) in response to half-field front-to-back motion (left) and half-field back-to-front motion (right) (Adapted from (Duistermars et al., 2012)).

affects the optomotor response of adult blow flies. iii) Extracellular electrical stimulation of the lobula plate region where HS-cells are located elicits yaw turning responses in blow flies (Blondeau, 1981b).

If the role of HS-cells in optomotor responses has been studied for decades, why have there not been any conclusive results so far? This can be explained when considering the lobula plate cell network (Figure 1.12A). A horizontally moving unilateral whole field visual stimulus activates and inhibits also other cells during front-to-back and back-to-front visual motion (Figure 1.13, left and right, respectively; (Duistermars et al., 2012)). During such motion, additionally to HS-

cells, also Horizontal cell 1 and 2 (H1/2-cells), unknown Horizontal cell (Hu-cell) and horizontal centrifugal cells (CH-cells) are activated or inhibited according to the direction of motion. Of these cells, only H1-cells have been identified in *Drosophila* so far (Bausenwein et al., 1990). During front-to-back visual motion (Figure 1.13, left), the ipsilateral HS-cells are depolarized. This depolarizes through electrical coupling the ipsilateral CH-cells. Furthermore, the ipsilateral H1 and H2-cell, both sensitive to back-to-front motion, become inhibited whereas the Hu-cell is activated. The Hu-cell inhibits contralateral CH-cells which inhibit contralateral HS-cells. During motion in the opposite direction, ipsilateral HS-cells and thus CH-cells become inhibited. At the same time H1 and H2-cells are activated which in turn also excites the contralateral HS-cells. Thus, to infer the role of one cell belonging to the network, its connections to other cells within this network needs to be analyzed.

Additionally to the complex cell network, the pathways downstream of HS-cells have not been identified completely, which complicates the interpretation of HS-cells in optomotor responses. As part of the pathway downstream of the HS-cells in blow flies, a motoneuron of the ventral cervical nerve has been proposed to be a key element of the neck muscular system. This constitutes a rather straightforward link between unilateral HS-cell activation and neck muscle contraction (Haag et al., 2010).

In contrast, much less is known about the circuits underlying turning behaviour during flight (Borst et al., 2010). Unilateral change of wing beat amplitude is controlled by small steering muscles, one of which (M.b1) responds best to whole field motion (Egelhaaf, 1989). This muscle might therefore receive strong input from the HS-system. However, the neural elements that convey the visual information to this and other muscles are yet to be functionally characterized (Gronenberg and Strausfeld, 1990).

1.5 Genetic Approaches

Being all part of a complex network, understanding lobula plate tangential cells in optomotor responses requires specific activation and / or modification of individual lobula plate tangential cells in intact flies. The introduction of the GAL4 /



UAS system, a transcriptional control system in yeast, into *Drosophila* constitutes the necessary genetic approach for doing this. In this system, the GAL4 gene encodes the yeast transcription activator protein Gal4, which binds specifically to the UAS (Upstream Activation Sequence) which then activates gene transcription. Since neither Gal4 nor UAS sequences are present in the *Drosophila* genome, no interaction with other genes are expected. This way when crossing a fly expressing Gal4 in only a few cells (Gal4 line) with another fly having a UAS sequence next to a specific gene X (UAS-line) will allow to express this gene X in only the specific cells with Gal4 expression.

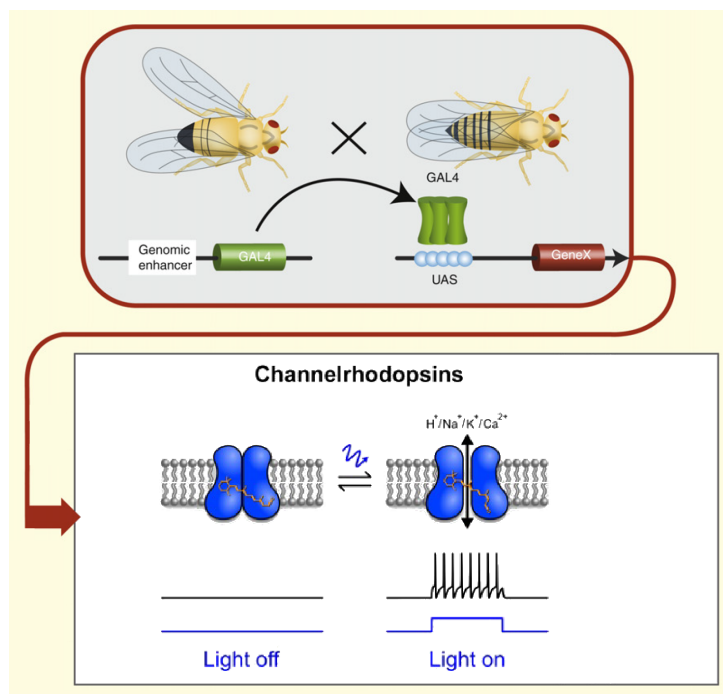


Figure 1.14: Gal4/UAS System. The Gal4/UAS system allows for any gene to be expressed in a population of neurons. Using this system, Channelrhodopsin-2 can be expressed in a population of cells. Using blue light cation channels open and let cations enter the cells, thus, the cell gets depolarized (Adapted and modified from (Borst, 2009) and (Dugue et al., 2012)).

As an example, the Gal4 / UAS system can be used to express Channelrhopsin-2 in specific cells. Channelrhodopsin-2 is a light-gated ion channel and consists of seven transmembrane proteins covalently linked to the chromophore all-trans-

retinal. When a photon of specific wavelength is absorbed by the all-trans-retinal it is isomerized around the 13'-bound which is believed to trigger the opening of the channel (Figure 1.14). Once open, cations pass across the plasma membrane and the cell gets depolarized (for a review refer to (Hegemann, 2008)).

Channelrhodopsin-2 enables the analysis of the function of specific genetically targetable neurons in complex networks. It can be used to specifically activate these neurons and to mimic sensory stimulation at the front end of the circuit. Although conventional Channelrhodopsin-2 allows to depolarize cells it still can be improved. New Channelrhodopsin-2 variants with different properties are engineered through mutations and molecular engineering. In general the goal is to increase the light sensitivity and the peak and steady-state photocurrents, change the kinetics of the photocycle and to shift the peak sensitivity toward longer wavelengths.

Some key positions in Channelrhodopsin-2 have been found. For example mutating the Glutamate at the position 123 to Threonine or Alanine (obtaining the variants E123T and E123A, respectively) has shown to allow faster closing of the channels. However, faster dynamics came along with reduced photocurrent amplitudes when compared with wild-type Channelrhodopsin-2 (Gunaydin et al., 2010). Mutating Cysteine at the position 128 to Threonine, Serine or Alanine (obtaining the variants C128T, C128S and C128A, respectively), has shown to extend the open state lifetime to minutes (Berndt et al., 2009).

Today, many variants exist and can be chosen according to the specific requirements of the experiment. This is important when studying the visual system. The light used to activate neurons is also perceived by the photoreceptors leading to artifacts. The most suited variant would be one sensitive to light at a wavelength not detectable by the photoreceptors. However, such a variant has not yet been engineered. Bi-stable variants are the second choice since only a short light pulse is needed to activate the neurons. Although artifacts are produced during optogenetic light stimulation, long term responses elicited are mostly free of artifacts.



1.6 Project Goals and Achievements

The goal of this study is to understand the role of HS-cells in the generation of optomotor responses. I chose two behavioural readouts, head yaw movements in fixed flies and turning behaviour in tethered flying flies. First, I tested which of the three HS-cells participates in controlling both behaviours. Second, I observed whether optogenetically activating HS-cells was sufficient to elicit optomotor responses as those elicited by front-to-back visual stimulation. Third, I analyzed the importance of the layout of HS-cell receptive fields for yaw turning responses. For this, optomotor responses of flies with genetically modified HS-cell receptive field layouts were analyzed.

First experiments served to get a general idea which of the HS-cells could be participating in head yaw movements in fixed flies and yaw turning behaviour during tethered flight. For this, HS-cell receptive fields and optomotor responses elicited by motion at different elevations were compared. The comparison suggests that HSN and HSE participate in the control of head yaw movements and all three HS-cells control yaw turning behaviour in tethered flying flies.

Second, I considered the following paradigm: When a fly is visually stimulated by a pattern rotating around its vertical body axis, its HS-cells depolarize on the side where motion progresses from front-to-back (Schnell et al., 2010) and the fly displays yaw head movements as well as yaw turning behaviour syndirectional to the stimulus (Duistermars et al., 2012). If HS-cells control both these optomotor responses, unilateral optogenetic depolarization of HS-cells in the absence of any visual stimulus should elicit similar behaviours.

With the help of Maximilian Jösch I generated flies for the expression of the bi-stable Channelrhodopsin-2 variant 'ChR2(C128S)', where a brief pulse of blue light leads to a long-lasting opening of the ion channel lasting up to about 100 seconds (Berndt et al., 2009). In these experiments, activation of HS-cells in one hemisphere of the fly's head elicited head movements towards the stimulated side. When depolarizing HS-cells unilaterally in tethered flying flies turning responses of the fly could be observed. These matched responses normally elicited by front-to-back visual stimulation. These results provide strong causal evidence that HS-cells indeed trigger yaw head movements and yaw turns in *Drosophila*. Results of

this project have been published in (Haikala et al., 2013).

Third, I investigated how motion information from different azimuth positions contribute to the optomotor responses. Responses of flies with genetically modified HS-cell anatomy were compared with optomotor responses of control flies. Preliminary experiments had shown that HS-cells in these flies have missing dendritic branches in the lateral lobula plate corresponding to the frontal field of view. These changes in anatomy come along with a dramatically reduced sensitivity to motion in the frontal region and an enhancement of sensitivity to motion in the lateral field of view of the fly.

Compared to control flies, D(GOF) flies responded significantly weaker to visual stimuli extending over the entire azimuth of the HS-cell receptive fields. Stimulating the flies with additional motion in the rear field of view reduced control optomotor responses significantly whereas D(GOF) flies responded to both visual stimuli equally strongly. Although D(GOF) HS-cells had dramatically reduced sensitivity to motion in the frontal part of visual space, D(GOF) flies still responded robustly to motion in this region. Control and D(GOF) flies also presented differences in head yaw movements. However, neither did these differences correlate with the difference of control and D(GOF) HS-cell receptive fields. These experiments suggest that also other cells participate controlling yaw optomotor responses. During flight the layout of the receptive fields of HS-cells plays an important role for incorporating visual stimuli in the rear field of view to optomotor responses.

In summary, ChR2(C128S) enables analyzing optomotor responses of seeing flies without significant artifacts produced by optogenetic stimulation. Cell responses of HSN- and HSE-cells are used for controlling head yaw movements and of all three HS-cells for controlling turning responses during flight. Depolarization of HS-cells elicits optomotor responses towards the preferred direction of the HS-cells. HS-cells are not the only cells controlling optomotor behaviour and their receptive field layout does not correlate 1 : 1 with yaw optomotor responses.



Chapter 2

Methods

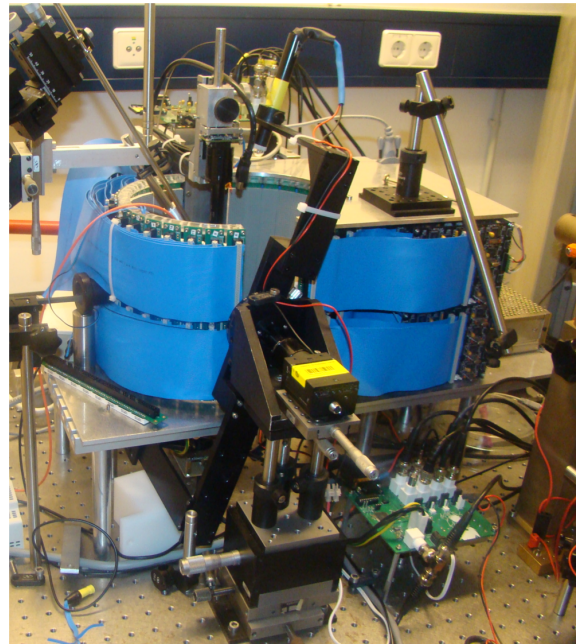
2.1 Setup

2.1.1 Visual Stimulation

An LED-arena engineered and modified according to open-source information of the Dickinson laboratory (Reiser and Dickinson, 2008) was built and used to stimulate the visual system of the flies. The arena consists of 29x8 dot matrix displays (TA08-81GWA, Kingbright) arranged in a cylindrical form. The cylinder has a diameter of 19 cm and covers 348° in azimuth (from -174° to 174°) and 80° in elevation (from -40° to 40°) of the flies visual space. Since each dot matrix display harbors 8x8 individual green (568 nm) LEDs, the spatial resolution at the equator is about 1.5°. Each dot matrix display is controlled by one micro-controller (dot-matrix-controller, Atmega-644, Atmel), combined with a line driver (ULN2804, Toshiba America) acting as a current sink. To control all dot-matrix-controllers synchronously, one main-controller (Atmega-128, Atmel) is used allowing refresh rates of 550 Hz and 16 intensity levels.

Each pattern to be displayed on the arena is generated using Matlab and saved to a Compact Flash card (CF-card). The main-controller reads the pattern information from the CF-card and sends this via I²C to each dot-matrix-controller which save the information into their own external flash memory (AT45DB321D-SU, Atmel). Thus, during experiments, only the frame number to be displayed on the arena is sent by the main-controller to the dot-matrix-controllers. These fetch the frame information from their external flash memory and present the frame on

Figure 2.1: LED arena used for visual stimulation. The cylindrical LED arena is divided into two halves. Both halves are positioned on rails enabling to open and close the arena. Visual stimulation of the flies positioned in the center of the arena is controlled by the main-controller receiving commands via RS-232 from the computer.



the arena until a new command is received. In order to stimulate flies with a moving pattern, consecutive frames are displayed. The speed of the moving pattern is controlled by the main-controller using its own clock.

To analyze recorded optomotor responses elicited with pattern motion, the exact time course of the pattern is recorded. For this, the main-controller toggles one of its outputs every time it sends a new frame number to the dot-matrix-controllers. Using a digital to analog converter (DAC8830IBD, Burr-Brown Corporation), a second main-controller output is generated. This output can take three different values, two to indicate the direction of pattern motion and one to indicate if the pattern stands still. Both signals are recorded with a Data Acquisition Card (PD2-MF-16-150/16H, United Electronic Industries) and are used to align optomotor responses recorded with the same Data Acquisition Card with pattern motion.

During experiments, different sequences of pattern motion can be used. Each sequence is saved as a script on the computer. Using a python interface, each command is sent consecutively via RS-232 to the main-controller. To reliably present each pattern sequence during each trial with the same time course, the clock of the main-controller is used for timing. To overcome the delays produced by the computer and RS-232 communication, the first two commands are sent



to the main-controller when the experiments starts. When the first command has been executed, the main-controller sends a message to the computer and the next command is sent. Thus, the main-controller always knows the current and next command to be executed and no delays are produced.

Positioning flies in the center of the arena turned out to be challenging due to the small diameter of the LED arena. To facilitate this, the arena was divided into two halves. Both halves are positioned on rails enabling opening and closing the arena. To have more room to position measuring devices, e.g. the wing beat analyzer, the arena was additionally positioned about 20 cm above the table (Figure 2.1).

2.1.2 Torquemeter

Inspired by work done by the Dickinson laboratory (Tammero et al., 2004), a torquemeter was built. This consists of a laser beam directed onto a small mirror glued to the tether above the fly. Every time the fly produces yaw torque or a thrust force, the tether is twisted changing the angle between beam and mirror accordingly. The deflection of the beam is measured using two spot detectors, one for horizontal and the other for vertical deflections of the beam. This allows the detection of yaw (horizontal deflection) and thrust (vertical deflection) movements produced by the tethered flying fly.

Tether and Configuration

To measure yaw torque and thrust produced by a tethered flying fly, a small piece of a compact disc acting as a mirror, is glued to the tether. Using a 1.0 mW HeNe 632.8 nm laser (05LHP111, Melles Griot) and two spot detectors (UDT SL5-2, UDT Sensors, Inc.) the movements of the mirror produced by the fly can be detected. For this, the laser beam is first guided using a beamsplitter (10BC17MB.1, Newport) onto the mirror (Figure 2.2A). After being reflected by the mirror, the beam passes again through the beamsplitter and is divided in two at a second beamsplitter (10BC17MB.1, Newport). Each of the resulting beams hit one spot detector. Using the output of the spot detectors, the position of the point of impact of the beam is measured allowing to calculate the deflection of the beam at the

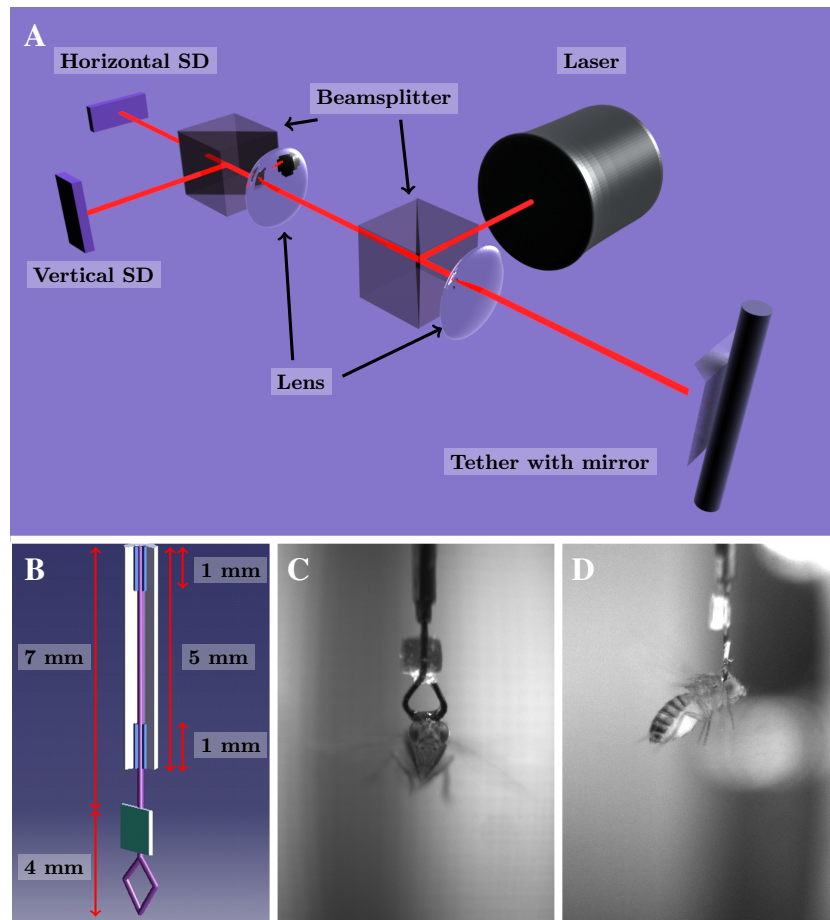


Figure 2.2: Schematic of the torquemeter. (A) A laser beam is directed into the LED-arena and guided using a beamsplitter into the LED arena onto a mirror glued to a tether. When the fly, also glued to the tether, produces thrust forces or torque, the mirror turns and deflects the beam. The deflected beam is divided by a beamsplitter into two beams. Each of the resulting beams hits one of two spot detectors, one positioned horizontally and the other vertically. This arrangement allows measuring the quantity of vertical and horizontal deflection of the beam. (B) Schematic of the tether. A thin tungsten wire is held in place by two steel tubings, allowing the wire to rotate at one end. One end of the wire is bent to a triangular form with one edge pointing downwards. A mirror made of a piece of a compact disc is glued above the triangle. (C) and (D) Pictures with a front and side view, respectively, of a fly glued to the tether.

mirror. Since one spot detector is positioned horizontally and the other vertically, yaw and pitch rotations of the mirror can be detected.



A 130 μm diameter tungsten wire (TW5-3, Science Products) is used as the “spring” for the torquemeter (Figure 2.2B). It has to be long enough for the fly to be able to twitch it, but at the same time not too long in order to return to its initial shape when no torsion is produced. The wire is bent at one end into a triangular shape with one edge pointing downwards. Since the fly is glued to the down pointing edge of the triangle and the mirror at the opposite side, the wire can not be twisted between the mirror and the fly. Thus, the maximum rotation of the mirror is achieved. The long wire is glued to a short steel tube (832000, Science Products) at one end. Horizontal movements are eliminated using another steel tube (832000, Science Products) near the mirror. To keep the friction between wire and tube as low as possible, the lower tube is lubricated using oil. To hold both short tubes in place, these are inserted and glued to another steel tubing (842400, Science Products). Figure 2.2C and D show a fly glued to the tether from the front and side, respectively.

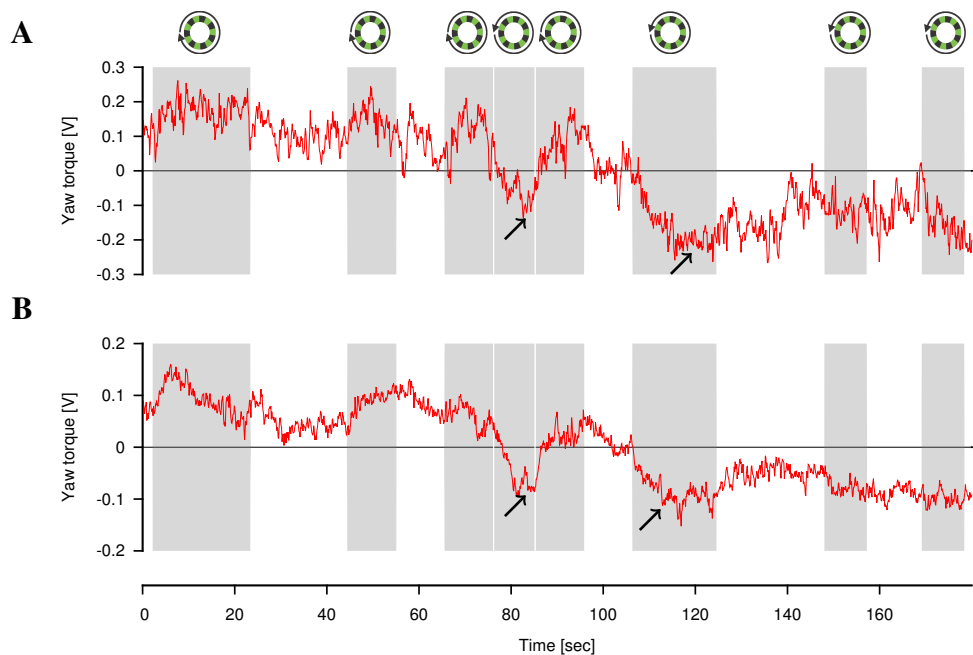


Figure 2.3: Test to find an appropriate tether length for the torquemeter. Mean traces for wild type flies. Gray boxes indicate the time of visual stimulation. (A) and (B) Traces for wild type flies tethered to a 10 mm ($N = 6$) and 7 mm ($N = 12$) long tether, respectively.

To find an appropriate tether length, flies were presented a whole-field squared wave pattern. Each trial started with repetitive clockwise pattern rotations, followed by two clockwise rotations separated by a counter-clockwise rotation. Each trial ended with repeated counter-clockwise rotations (Figure 2.3). The beam deflections measured with a 10 mm tether were greater than when using a 7 mm long tether (compare Figure 2.3A with B). However, the deflection of the laser beam during the first counter-clockwise rotation was smaller compared to the deflection when repeated counter-clockwise visual rotations at the end of the stimuli were presented (Figure 2.3A, arrows). This was considered to be a consequence of a too long tether that did not return to its initial shape when no torque was applied by the fly. For a 7 mm long tether the deflections measured during the first counter-clockwise and the repeated counter-clockwise rotations were closer together (Figure 2.3B, arrows). Even shorter tether lengths were tested, however, these were difficult to build and allowed only small deflections of the mirror which could not be detected with the spot detectors. Therefore, a 7 mm tether was chosen for all experiments (Figure 2.2B).

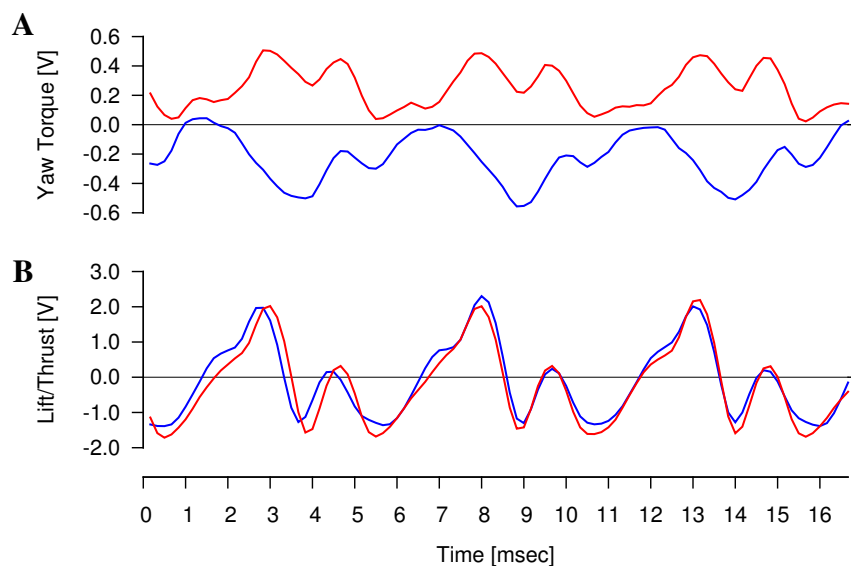


Figure 2.4: Closeup of measured forces using the torquemeter. Individual traces during counter-clockwise (red) and clockwise (blue) rotating visual stimuli. (A) Yaw torque and (B) lift / thrust measured using the spot detectors.



Closer analysis of the measured traces for yaw forces and thrust forces allowed the observation of oscillations (Figure 2.4). These are due to the fact that flies cannot generate long lasting constant forces. The forces generated by flies oscillate according to their wing beat frequency of approximately 200 Hz (Dickinson and Gotz, 1996b).

2.1.3 Wing Beat Analyzer

The torque meter allowed measurements of optomotor-responses. Building the tethers turned out to be laborious and difficult. Even more importantly, it was impossible to make two tethers with identical physical properties such as friction and stiffness. This is a major drawback and prevented the quantitative measurements and comparison of the strength of optomotor responses of a large number of flies. Furthermore, during “fly tethering” the mirror was prone to falling off or the tether to bending, forfeiting its continuous re-use. Hence, an alternative device was built to quantitatively measure the strength of optomotor responses independent of a tether and in large numbers of experimental flies.

Design of the Wing Beat Analyzer

When flies turn during flight, they change their downstroke wing beat amplitude in such a way that the wing on the inside of the turning radius beats with a lower wing beat amplitude (Götz, 1968; Götz et al., 1979). Thus, it is sufficient to measure the wing beat amplitudes of both wings during downstroke and subtract them to measure optomotor responses. Another property of wing beat amplitudes is that when flies fly faster, they beat both wings with a larger downstroke amplitude. Summing up the downstroke amplitudes of both wings is a practical way to obtain lift and thrust.

The design of the wing beat analyzer is based on an existing design described in (Götz, 1987). Using an infrared 870 nm LED (JET-800-10, Roithner Lasertechnik), the shadow of the wings is cast onto a mask with two crescent shaped apertures (Figure 2.5B). Two prisms (BRP-25.4, Newport) are used to reflect the light onto two photodetectors (UDT-555D, Osi Optoelectronics) placed beneath the mask. Depending on the wing beat amplitude, different portions of light

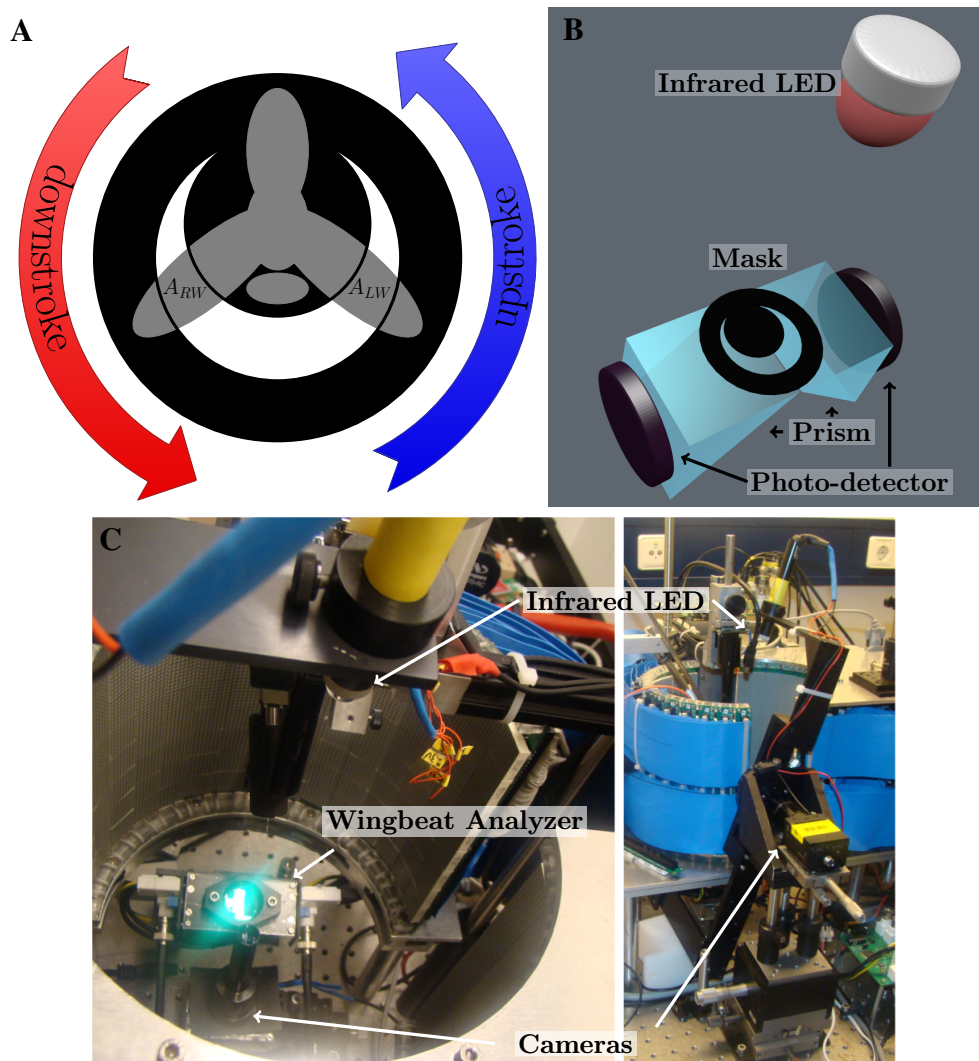


Figure 2.5: Design of the wing beat analyzer. (A) A shadow of the fly is projected onto a mask with two apertures. During downstroke the area covered by the wing grows whereas during upstroke the area decreases. (B) Schematic of the wing beat analyzer design. Using an infrared LED a shadow of the fly is generated onto a mask. The remaining light is projected onto two photodetectors using two prisms. (C) Wing beat analyzer holder. The infrared LED points at the center of the mask. The fly is positioned in the center of the arena between infrared LED and mask using a camera positioned to point at the longitudinal axis of the infrared LED. The holder can be rotated around the lateral axis of the fly changing the angle between fly and LED light beam.



are blocked by the wings turning the measured photo-current at each detector inversely proportional to the wing beat amplitude (Figure 2.5A).

To obtain the wing beat angles, these signals are normalized to their maximum. After detecting the peak of each wing stroke, the moving average of a sliding window of 50 ms duration is calculated. The turning behaviour of the fly is obtained by subtracting the right (RWB) from the left (LWB) wing beat amplitude (Figure 2.6; (Götz, 1968; Götz et al., 1979)). To precisely position the fly in the center of the arena a camera (Dragonfly, PointGrey) with an InfiniStix (1.0X primary magnification, 94mm working distance) video lens (NT55-359, Edmund Optics Ltd) is positioned beneath the fly.

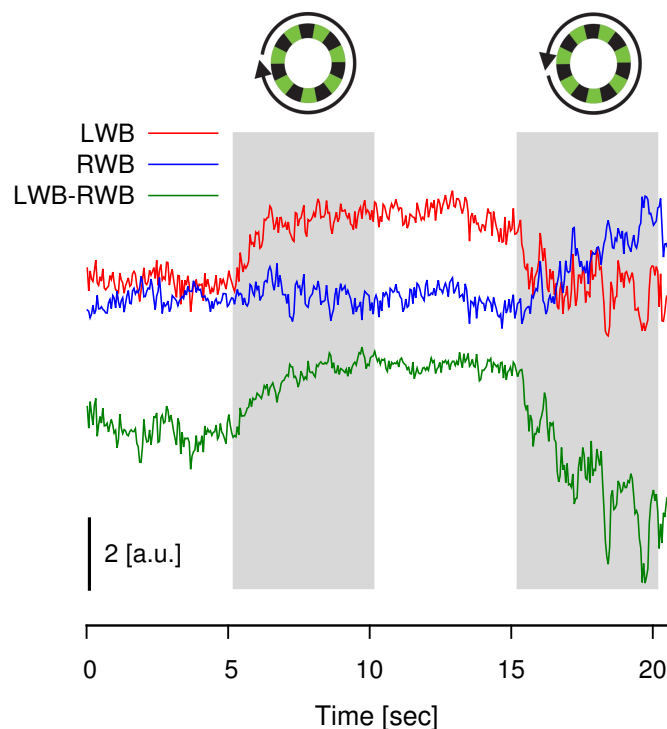


Figure 2.6: Example traces recorded with the wing beat analyzer during clockwise and counter-clockwise visual rotation. Left wing beat (LWB) red, right wing beat (RWB) blue and RWB subtracted from LWB green.

To position the fly in such a way that its shadow could be projected onto the mask proved to be a challenging task. Since an infrared LED was used it was not possible to see the shadow. Additionally, the shadow could be positioned on

the mask by moving the infrared LED, moving the mask or moving the fly. To restrict these degrees of freedom a holder was built (Figure 2.5C, right). This was designed in such a way, that the LED pointed towards the center of the mask. To project the shadow of the fly onto the mask the fly must be centered on the longitudinal axis of the infrared LED. For this a camera (Grasshopper, PointGrey) with an InfiniStix (1.0X primary magnification, 94mm working distance) video lens (NT55-359, Edmund Optics Ltd) is used. The camera is positioned horizontally focusing the longitudinal axis of the LED. When the fly is focused on an image taken by the camera it is close to the correct position. To find the exact position, the entire holder can be moved in all three axes while observing the wing beat signals on an oscilloscope. Additionally, to find the best angle between LED beam and fly, the holder can be rotated around the lateral axis of the fly. Since the longitudinal axis of the camera is positioned to match the axis of rotation of the holder only the angle between LED and fly is changed.

2.1.4 Head Movement Detector

Flies with severe mutations or flies expressing genetically encoded blocks of neuronal activity in visual interneurons tend to no more execute robust flight behaviour. In contrast, head movements are typically still executed by such flies. To be able to also analyze flies carrying more severe genetic manipulations a head movement detector was designed and engineered. A camera is positioned on top of the fly, pointing at the head. Analyzing the images taken during experiments it is possible to record head yaw movements.

For experiments flies are positioned in the center of the arena using a camera (Dragonfly, PointGrey) with an InfiniStix (1.0X primary magnification, 94mm working distance) video lens (NT55-359, Edmund Optics Ltd) to detect head movements. The fly's head is illuminated with an infrared 870 nm LED (JET-800-10, Roithner Lasertechnik). Using another camera (Firefly MV, PointGrey) with an InfiniStix (2.0X primary magnification, 44 mm working distance) video lens (NT55-355, Edmund Optics Ltd), images of the head are taken at 27.8 frames per second. The head is slightly pushed forward using a 130 μm x 76 mm tungsten wire (TW5-3, Science Products) with one end bent to an L shape. This allows to

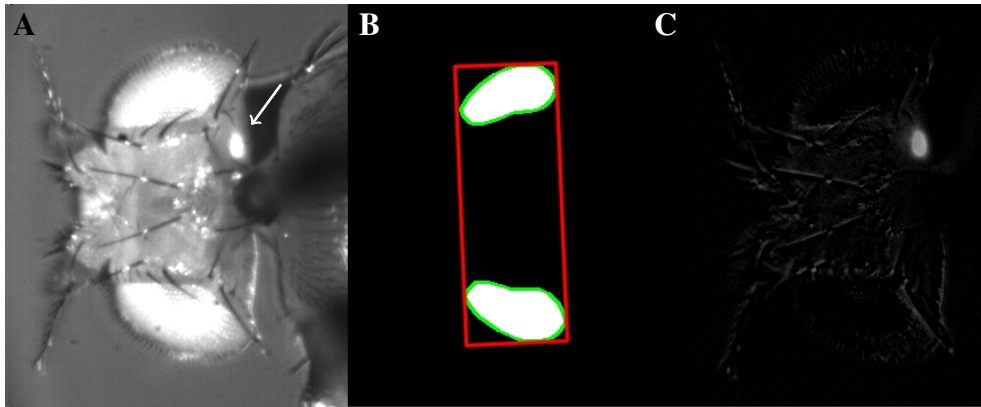


Figure 2.7: Head movement analysis (A) Raw image of fly head (arrow indicates optogenetic light spot). (B) A box is fitted around the contours (green) of a thresholded image shown in (A). (C) Mask used during optogenetic stimulation calculated as the difference of the first image with a light spot and the previous image.

restrict head rotations to the equatorial plane.

The camera is configured to use an external trigger supplied by the arena-controller, to output a strobe signal and to use embedded image timestamps. Embedded image timestamps serve to detect if images are lost during trials. Using the strobe signal of the camera, images, direction of the visual stimuli and optogenetic stimulation can be aligned. Each trial is analyzed offline using OpenCV (Open Source Computer Vision) and python software.

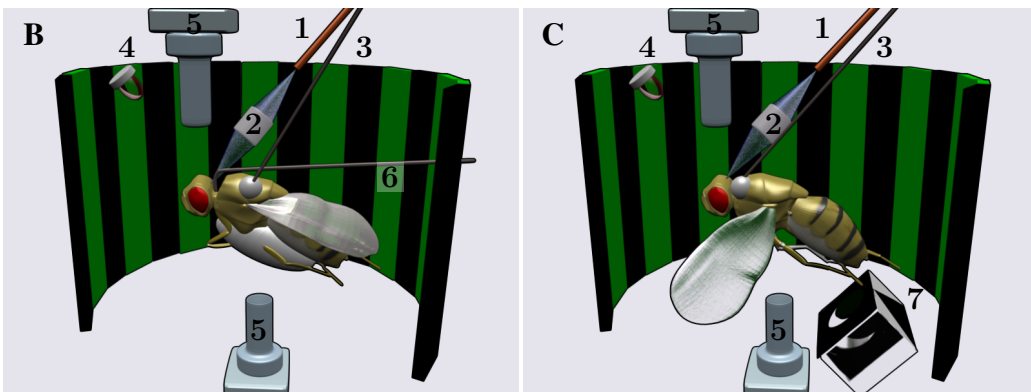
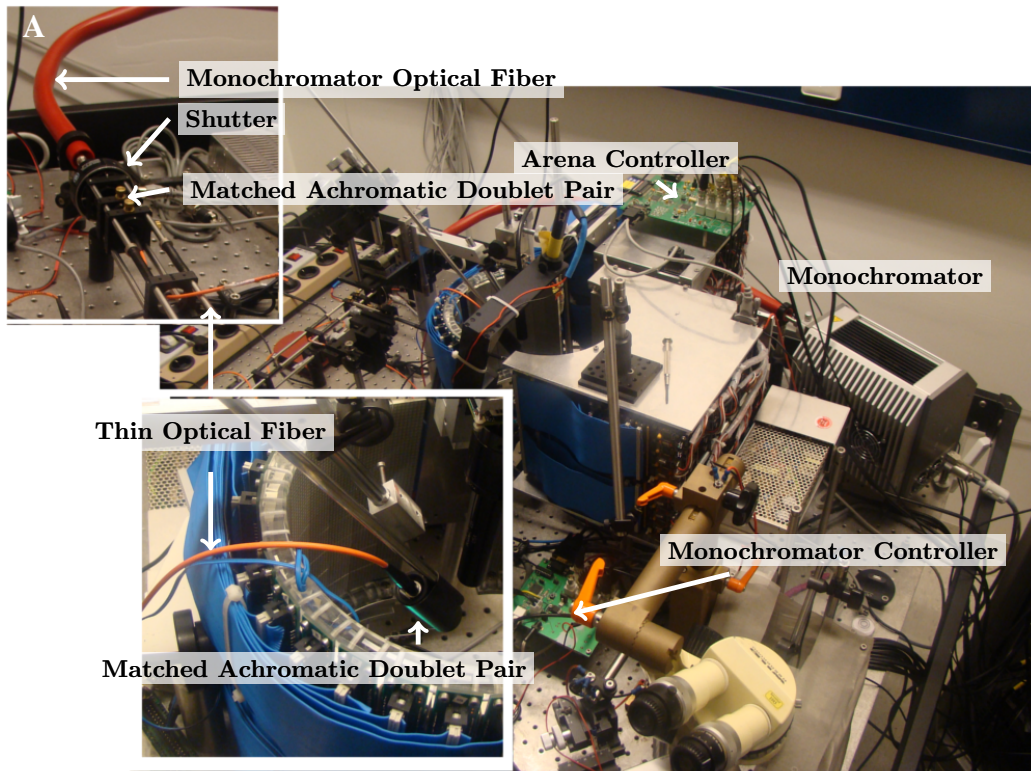
To automatically measure the head angle, the images are divided into two halves, each containing one eye. A threshold is applied to each half. After image thresholding, the eyes of the fly appear white and are identified as the two largest white areas of the thresholded image. Contours are taken of these and a box is fitted around them. The angle of the box corresponds to the angle of the head (Figure 2.7B). During optogenetic light stimulation the light spot (Figure 2.7A, arrow) is removed from the image using a mask calculated as the difference of the first image with a light spot and the previous image (Figure 2.7C).

2.1.5 Optogenetic Activation

In order to activate cells during behaviour a variant of Channelrhodopsin-2 called ChR2(C128S) is specifically expressed in HS-cells. To open and close the channels it is necessary to guide blue and yellow light, respectively, onto the cells. To generate light with different wavelengths a monochromator (Polychrome IV, TILL Photonics Inc) equipped with a glass fiber is used. Wavelength and duration of light pulses are controlled using a micro-controller (Atmega-128, Atmel, monochromator-controller) and a digital to analog converter (LTC 1592ACG, Linear Technology) with a $\pm 10V$ output. Commands to the monochromator-controller are sent via RS-232 from the computer. To synchronize the optogenetic light stimulation with the visual stimuli of the LED-arena, each command is only executed when the monochromator-controller receives a digital signal from the arena-controller.

The light from the monochromator glass fiber is passed through a shutter, controlled with a single channel shutter driver (VCM-D1, Uniblitz) and the monochromator-controller. A matched achromatic doublet pair (MAP051919-A, Thorlabs) is positioned between the head and the thin fiber with a 50 μm core (M14L01, Thorlabs). Another matched achromatic doublet pair (MAP051919-A, Thorlabs) is positioned between head and thin fiber to focus the outcoming light of the thin optical fiber onto the fly's head (Figure 2.7A, arrow). To align the lenses and optic fibers, the light intensity at the tip of the thin fiber are maximized. The light intensity and spectral wavelength are measured using a power and energy

Figure 2.8 (facing page): Optogenetic activation setup. (A) Blue and yellow light are generated using a monochromator equipped with a glass fiber. The wavelength and duration of the light pulses are controlled using the monochromator controller. The light is guided using a matched achromatic doublet pair into a thin fiber. To turn the light off, a shutter controlled with the monochromator controller is used. A matched achromatic doublet pair is used to focus the light of the thin fiber onto the head of the fly. (B) Setup used to analyze head movement (C) Apparatus for tethered flight experiments. For (B) and (C) 1: Thin light-fiber, 2: Matched achromatic doublet pair, 3: Tether, 4: Infrared LED, 5: Camera, 6: Head positioner, 7: Wing-beat-analyzer consisting of a mask, two prisms (white) and two photodetectors (not shown)



meter console (PM100D, Thorlabs) and a compact spectrometer (CCS200, Thorlabs), respectively. During optogenetic stimulation experiments described in the following chapter, light intensities at the tip of the thin fiber for blue and yellow light were 10 μ W and 6 μ W, respectively.

2.2 Experimental Preparation

2.2.1 Fly Strains and Genetics

For the optogenetic stimulation experiments two Gal4 driver lines were used: *R27B03-Gal4* (Chiappe et al., 2010), which expresses Gal4 in all three HS-cells and *DB331-Gal4* (Joesch et al., 2008) with Gal4 expression in all HS- and VS-cells (plus additional cells in other neuropiles). Additionally, *norpA⁷* flies with dysfunctional phototransduction were used as a control (Hotta and Benzer, 1970). ChR2(C128S)-YFP was first amplified via PCR with additional EcoRI restriction sites and cloned into pUAST. After a P-element mediated germ-line transfection (Spradling and Rubin, 1982) a line with strong expression of ChR2(C128S)-YFP on the third chromosome was identified. *R27B03-Gal4* and ChR2(C128S)-YFP flies were additionally crossed into a *CantonS-wt* background. To maximize the expression of ChR2(C128S) homozygous ChR2(C128S) flies were used for all the experiments, except tethered flying *norpA⁷* flies.

For head yaw experiments *w⁺; +; R27B03-Gal4::UAS-ChR2(C128S)-YFP, norpA⁷; +; R27B03-Gal4::UAS-ChR2(C128S)-YFP* and *DB331-Gal4; +; UAS-ChR2(C128S)-YFP* were used as experimental flies and *w⁺; +; R27B03-Gal4, norpA⁷; +; R27B03-Gal4* and *DB331-Gal4; +; +* as control flies. For tethered experimental flight experiments *w⁺; +; R27B03-Gal4::UAS-ChR2(C128S)-YFP, norpA⁷; +; R27B03-Gal4::UAS-ChR2(C128S)-YFP/tm6b* and *DB331-Gal4; +; UAS-ChR2(C128S)-YFP* were used as experimental flies and *w⁺; +; R27B03-Gal4, norpA⁷; +; +/tm6b* and *DB331-Gal4; +; +* as control flies.

For Dscam experiments *DB331-Gal4* and *UAS-mCD8::GFP/CyO* (Bloomington #5137) as a marker were used. For tethered flight experiments *DB331-Gal4/x; UAS-mCD8::GFP/Bl; UAS-Dscam11.31.25.1/+* were used as experimental flies and *DB331-Gal4/x; UAS-mCD8::GFP/Bl; +/+* as control flies. Head movement



experiments were performed using *DB331-Gal4/2EYFP; UAS-mCD8::GFP/+; UAS-Dscam11.31.25.1/+* as experimental flies and *DB331-Gal4/2EYFP; UAS-mCD8::GFP/+; +/tm6b* as control flies.

2.2.2 Fly Preparation

Flies were raised at 25° and 60 % humidity on standard cornmeal agar medium with a 12 / 12 hr light / dark cycle and selected 1-3 days after eclosion. Before each experiment flies were cooled down at 5°C and fixed to the tether. For tethered flight a 130 μm x 76 mm tungsten wire (TW5-3, Science Products), reinforced with two hypodermic stainless steel tubings (843600 and 832000, Science Products), was glued between head and thorax using UV sensitive glue. For the automatic detection of head movements the same tether was waxed to the thorax whereas legs and wings were waxed to the abdomen.

Channelrhodopsin-2 is a light-gated ion channel. It consists of seven transmembrane proteins covalently linked to a chromophore, all-trans-retinal (ATR). Photons of specific wavelength are absorbed by the ATR and it is isomerized. This conformational change in the structure is believed to trigger the opening of the channel. Since ATR is not available in *Drosophila* it must be fed to the flies before each experiment. Thus, for optogenetic stimulation experiments, after selection, female flies were additionally fed (unless otherwise stated) with a yeast-water mix containing all-trans retinal (ATR) (R2500, Sigma Aldrich) and kept for 2 days in a dark vial. The flies were prepared for the experiments under red light. For tethered flight, the wire was positioned between head and thorax and waxed to the thorax. A drop of nail polish on the tip of the wire prevented head movements during flight.

2.2.3 Data Analysis

All data are given as mean \pm s.e.m. The significance of differences between datasets are given as P-values of a two sided Mann-Whitney rank test.

Optomotor responses of flying tethered flies were defined as the mean turning behaviour during front-to-back visual motion minus the mean turning behaviour during back-to-front visual motion. The response to wide-field visual stimulation

was calculated as the mean turning behaviour during clockwise rotation minus the mean turning behaviour during counter-clockwise rotation.

To ensure all flies analyzed during optogenetic activation experiments were able to turn their head in both directions, for head movement detection only those trials were used in which the mean head angle during clockwise and counter-clockwise rotation was positive and negative, respectively. The only exception to this being *norpA⁷* flies for which all trials were used. Number of flies and trials used were as follows (fly/ flies tested/ trials/ flies used/ trials used): (*w⁺*; +; *R27B03-C128S*/ 44/ 116/ 34/ 61), (*w⁺*; +; *R27B03-C128S* (no ATR)/ 34/ 102/ 33/ 64), (*w⁺*; +; *3HS*/ 34/ 100/ 29/ 59), (*norpA⁷*; +; *R27B03-C128S*/ 15/ 33/ 15/ 33), (*norpA⁷*; +; *R27B03-C128S* (no ATR)/ 19/ 65/ 19/ 65), (*norpA⁷*; +; *R27B03*/ 15/ 47/ 15/ 47), (*DB331*; +; *C128S*/ 31/ 152/ 30/ 78), (*DB331*; +; *C128S* (no ATR)/ 25/ 147/ 24/ 71) and (*DB331*/ 36/ 193/ 35/ 109). Similar to head detection, tethered fly trials were only used if a fly had at least two positive trials and, except for *norpA⁷* flies, the responses for clockwise and anticlockwise rotation were positive and negative, respectively. Data presented is composed of (*w⁺*; +; *R27B03-C128S*/ 46/ 235/ 27/ 105), (*w⁺*; +; *R27B03-C128S* (no ATR)/ 33/ 165/ 27/ 86), (*w⁺*; +; *R27B03*/ 35/ 200/ 27/ 95), (*norpA⁷*; +; *R27B03-C128S/tm6b*/ 29/ 94/ 26/ 91), (*norpA⁷*; +; *R27B03-C128S/tm6b* (no ATR)/ 31/ 84/ 26/ 79), (*norpA⁷*; +; *3HS/tm6b*/ 29/ 101/ 27/ 99), (*DB331*; +; *C128S*/ 16/ 70/ 16/ 52), (*DB331*; +; *C128S* (no ATR)/ 16/ 59/ 16/ 46) and (*DB331*/ 19/ 69/ 16/ 41). Trials obtained from a single fly were averaged and the mean was used as the fly's optomotor behaviour. Responses for blue light activation were defined as the mean signal (head angle or turning behaviour) between the onset of blue light and the onset of yellow light, minus the mean of the signal during the last second before blue light onset. The response to blue light of an individual fly was calculated as the mean of the responses during each trial.

2.3 Genetic Modification of HS-cell Responses

For the experiments presented in the following chapter, HS-cell properties were genetically modified. First, Chr2(C128S) was expressed in HS-cells allowing to optogenetically activate these. Second, a *Dscam1* isoform was over-expressed



in HS-cells modifying their anatomy and receptive field layouts. The following sections summarize the work performed in our laboratory relevant for the interpretation of the results obtained in this work.

2.3.1 Switchable Optogenetic Depolarization of HS-cells using ChR2(C128S)

The ChR2(C128S)-YFP fly line was generated together with Maximilian Jösch and patch-clamp recordings of this section were performed by Alex Mauss

Optogenetic stimulation has become the method of choice to specifically activate genetically defined neuron types and to study their role in behaviour. However, applying optical stimulation in the *Drosophila* visual system will also activate photoreceptors and hence produce undesired artifacts interfering with visual processing. To reduce this problem, the use of the bi-stable Channelrhodopsin-2 variant C128S (ChR2(C128S); (Berndt et al., 2009)) with severely slowed off-kinetics was explored. ChR2(C128S) has the advantage over conventional Channelrhodopsin-2 that the channel opening and closure can be gated by brief blue and yellow light pulses, respectively, and thus leaving neurons in a depolarized state between these light pulses. The inter stimulus period can then be used to observe the effect of the activated cells on behaviour. The artifact in behaviour caused by the optogenetic stimulation should be minimized.

A transgenic fly strain carrying ChR2(C128S)-YFP under UAS control was generated and patch-clamp recordings from lobula plate tangential cells expressing this construct were performed. In order to assay the direct impact of ChR2(C128S) on membrane potential of the recorded cell and to reduce network artifacts from stimulating photoreceptors or other ChR2(C128S) expressing cells, the following recording conditions were chosen: First, the preparation was bathed in a Ca^{2+} -free external solution with high Mg^{2+} (20 mM) to suppress synaptic activity; second, *norpa*⁷-mutant flies with dysfunctional phototransduction, which do not show any visual responses at the level of lobula plate tangential cells, were used.

Stimulation of lobula plate tangential cells expressing ChR2(C128S) with blue

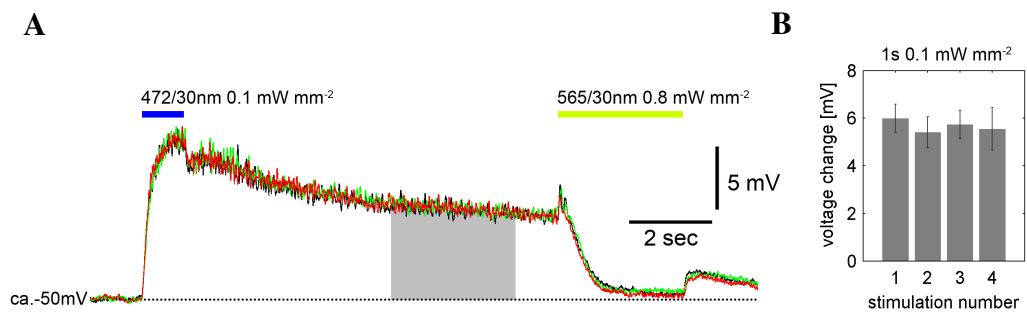


Figure 2.9: Electrophysiological recordings from lobula plate tangential cells expressing ChR2(C128S). (A) Three consecutive sample recordings of the same cell expressing ChR2(C128S) in zero Ca^{2+} / high Mg^{2+} external solution. A blue light pulse (1 s, 472 / 30 nm) light elicits a prolonged depolarization of the cell. A yellow light pulse (3 s, 565 / 30 nm) interleaved by a 9 s interval without repolarizes the membrane potential back to baseline. Amplitude and dynamics of the membrane potential changes remain constant across trials. (B) Mean responses \pm s.e.m. for one *DB331-Gal4*; + ; *UAS-ChR2(C128S)* fly and three *norpa⁷*; + ; *R27B03-Gal4*, *UAS-ChR2(C128S)* flies for four repetitive trials. Mean responses are calculated as the mean during a 3 s interval starting 5 s after blue light offset (gray box in A; Data: Alex Mauss).

light pulses (1 s, 472 / 30 nm, 0.1 mW/mm²) led to depolarizations of about 6 mV \pm 1.2 mV on average, as measured 5 s to 8 s after the offset of the optogenetic stimulus (Figure 2.9A). This value is in the range of a solid visually evoked depolarization of the membrane potential of HS-cells during preferred direction visual stimuli (Schnell et al., 2010).

One concern was a possible photocurrent loss over consecutive stimulations, as has been published for hippocampal pyramidal cells expressing ChR2(C128S) and related ChR2 variants (Schoenenberger et al., 2009). The results show that in the *Drosophila* visual system, ChR2(C128S)-mediated membrane depolarizations do not significantly attenuate during repetitive stimulation with blue and yellow light. This was shown for at least four consecutive blue light pulses, which were interleaved after 9 s by longer wavelength light flashes to terminate the conducting state of the channel (Figure 2.9B). Thus, ChR2(C128S) permits the effective and repetitive activation of lobula plate tangential cells by brief light pulses applied directly to the lobula plate of a fly preparation.



2.3.2 Over-Expressing Dscam1 in HS-cells Modify Cell Morphology and Responses

This section summarizes the work of Jing Shi (fly genetics and imaging), Friedrich Förstner (cell reconstruction), Bettina Schnell (cell recordings)

Precise growth of neurites as well as synapse formation are required to integrate visual information for the control of flight maneuvers. Mechanisms like self-avoidance and axonal or dendritic arborization enable cells to optimize wiring and efficiently cover the sensory space. For this, Dscams play an important role in the development (Schmucker and Chen, 2009; Hattori et al., 2007) of the fly (Millard et al., 2007; Millard et al., 2010) and vertebrate visual system (Fuerst et al., 2008; Fuerst et al., 2009). Thus, over-expressing a single Dscam1 isoform in a given neuron should change its morphology and thus its wiring to other cells. This hypothesis was tested in HS-cells. HS-cells have constant location and shape between different individuals which facilitates the detection of possible effects of over-expressing a single Dscam1 isoform in these cells.

Using the DB331-Gal4 driver line (Joesch et al., 2008), a specific Dscam1 isoform (11.31.25.1) was over-expressed in all HS- and VS-cells. In total 16 different flies were analyzed by anti-GFP-immunolabeling and 16 HSN- and HSE-cells were reconstructed from confocal stacks. It could be observed that over-expressing Dscam caused changes in the morphology of HS-cells with varying degree, not only between different flies but also between the two hemispheres of the same fly (2.10A, left column). HS-cells showed a reduced dendritic spanning field, i.e. covered the lobula plate to a smaller extent when compared with control HS-cells. A consequence of this reduced dendritic spanning field was a reduction of the overlap of HSE- and HSN-cells in the lobula plate (both effects quantified in Figure 2.10B and C).

Having quantified the effects of the Dscam gain-of-function D(GOF) on HS-cell anatomy in the lobula plate provided the opportunity to analyze changes in HS-cell response properties. As discussed in section 1.2.3, each HS-cell sums up horizontally sensitive elementary movement detectors in different areas of the receptive field (i.e. different elevation). This suggests that HS-cells with reduced

The Dscam1 isoform (11.31.25.1) will be referred to as Dscam

HS-cells over-expressing Dscam will be referred to as D(GOF) HS-cells

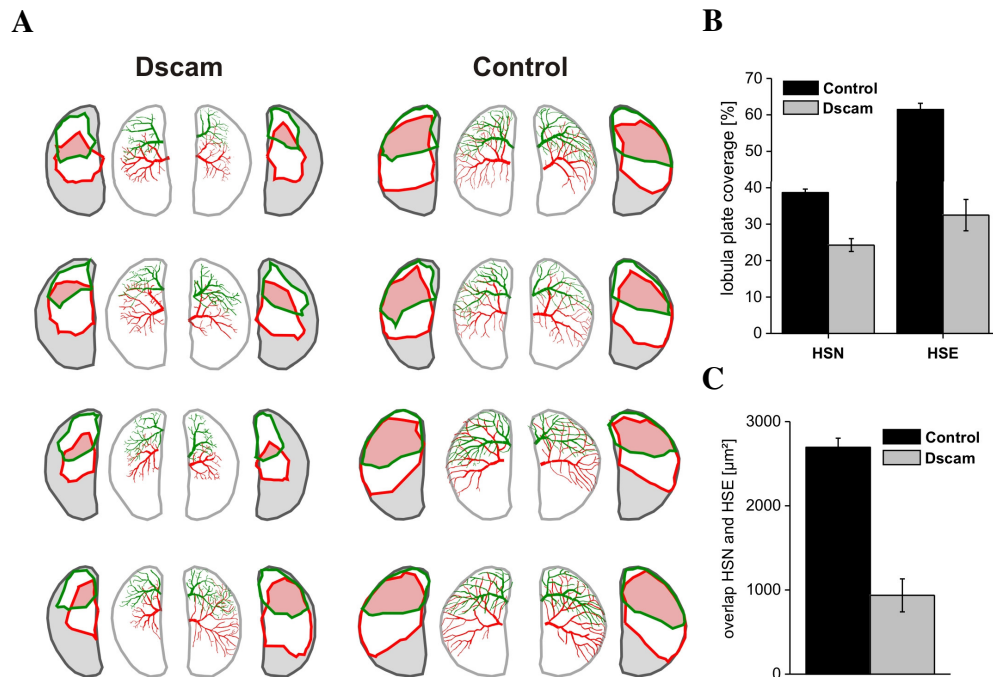


Figure 2.10: Overexpression of a single Dscam1 isoform in HS-cells reduces dendritic branching and enhances unoccupied territory in the lobula plate.

(A) Reconstruction of the dendritic arborizations of HSN-cells (green) and HSE-cells (red) in the lobula plate of control (right) and Dscam (left) flies. (B) Overexpression of Dscam causes a significant reduction of the occupied area of HSN and HSE in the lobula plate. HSN and HSE cover 38.6% and 61.5% (N=10 each) of the lobula plate in control flies and 24.3% and 32.5% (N=8 each), respectively, in D(GOF) flies. (C) Over-expression of Dscam causes a significant reduction of the area in which the dendrites of HSN and HSE overlap. The mean size of this area is $2695\mu\text{m}^2$ and $936\mu\text{m}^2$ in control and D(GOF) flies, respectively (Data: Friedrich Förstner).

dendritic arbor that covers less of the lobula plate, should receive less input and show deficits in its response properties. These deficits should be most detectable when analyzing the receptive fields of D(GOF) HS-cells by patch-clamp recordings.

Electrophysical recordings indicated that D(GOF) HS-cell responses did not differ from control HS-cell responses when a whole-field drifting grating was presented to the flies (Figure 2.11A). Measurements of the receptive fields, on the other hand revealed a significant difference between D(GOF) HS-cells and control

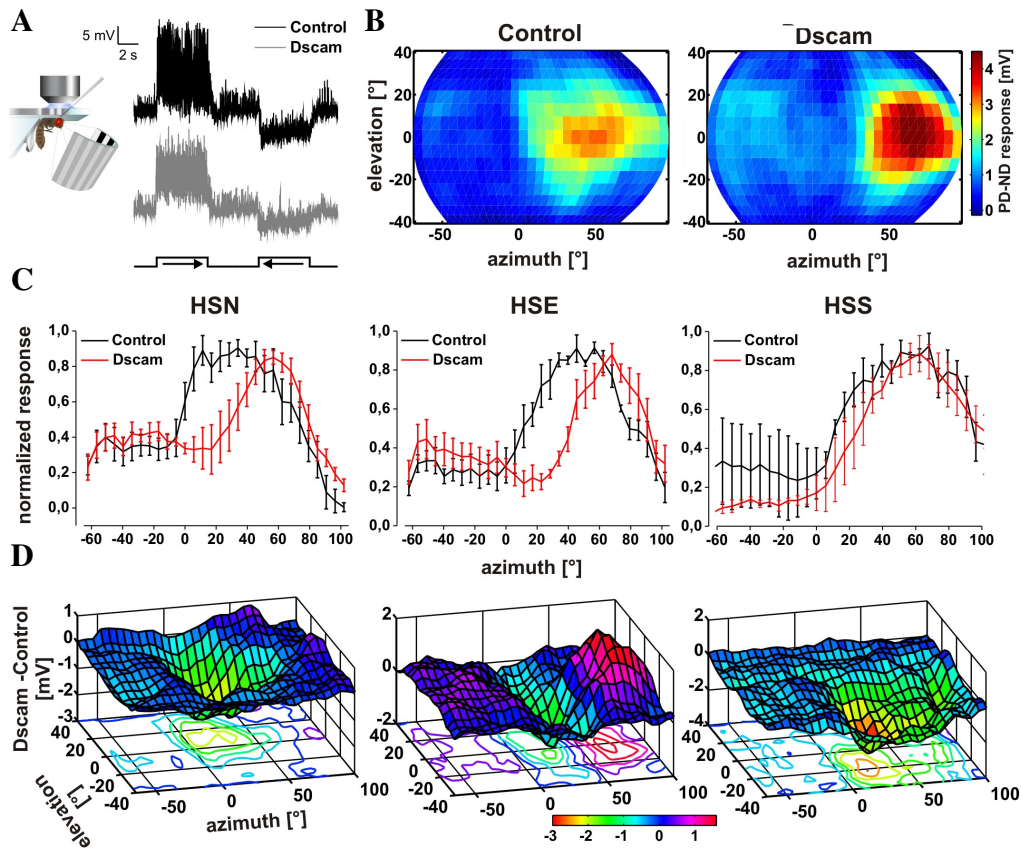


Figure 2.11: Overexpression of a single Dscam1 isoform in HS-cells causes a gap in the frontal receptive field. (A) Responses of control (black) and D(GOF) (gray) HS-cells to a drifting whole-field grating moving in the preferred and null direction of the HS-cell. (B) Receptive fields of a control ($N = 4$) and D(GOF) ($N = 6$) HSE-cell. Depicted in false color code are the responses (preferred minus null direction responses) elicited by a small, horizontally moving bar presented at different positions in the visual field of view. (C) Normalized response profiles of the three HS-cells for control (black) and Dscam (red) flies. Data from different elevation are averaged along the azimuth, bin size 5° . (D) Difference in the receptive field of control and D(GOF) flies (Data: Bettina Schnell).

HS-cells. Although D(GOF) HS-cells were most sensitive at their corresponding elevations (HSE receptive field shown in Figure 2.11B) they had a reduced sensitivity in the frontal region of the visual space. D(GOF) HSE-cells additionally were much more sensitive to motion in the lateral field of view when compared with control HS-cells (Figure 2.11D).

Chapter 3

Results

3.1 Comparison of HS-cell Activity and Yaw Optomotor Responses

First, experiments were designed to study which of the three HS-cells participate in controlling yaw turns during flight and yaw head movements in fixed flies. Optomotor responses elicited with visual motion at different elevation angles were compared with the receptive fields of HS-cells. Tethered flying flies responded to motion presented at every elevation. Fixed flies responded to motion at the equatorial and dorsal parts of visual space, but did not robustly follow with their head motion at the ventral regions of visual space. These observations suggest that tethered flying flies use all three HS-cells for controlling yaw turns whereas only HSN and HSE are used for controlling head yaw movements.

HS-cell response properties are modulated by flight activity (Maimon et al., 2010; Chiappe et al., 2010; Jung et al., 2011). To investigate the strength of modulation during both behaviours the optomotor responses to visual motion at different velocities were compared to HS-cell responses of immobilized flies. These experiments suggest that the temporal frequency profile is more modulated during flight than during head yaw movements.



Several studies have reported optomotor responses being similar to lobula plate tangential cell responses (Bishop and Keehn, 1967; Hausen and Wehrhahn, 1989; Duistermars et al., 2007; Duistermars et al., 2012). Since the three HS-cells are sensitive to horizontal visual motion, they are believed to control yaw turning behaviour. The three HS-cells are most sensitive in different parts of the visual space. HSN responds best to dorsal horizontal motion whereas HSE and HSS respond best to equatorial and ventral motion, respectively (Schnell et al., 2010). To investigate which of the three HS-cell control yaw turning behaviour of the head and whole body, wild type flies were tested. Horizontal motion stimuli were presented at different elevations and the optomotor responses elicited were compared to the receptive fields of HS-cells.

A square wave pattern restricted to approximately 10° in elevation was presented to the flies. This pattern was presented at 8 different elevations, rotating clock and counter-clockwise for 5 s each to activate, as specifically as possible, a single HS-cell. To elicit responses in only HS-cells on one hemisphere, each stimulus was presented unilaterally omitting the overlap region of HS-cells ($\pm 15^\circ$; (Schnell et al., 2010)).

Turning responses generated during tethered flight were measured using the wing beat analyzer (Methods 2.1.3). Flies responded best to horizontal motion at the equator. Responses were slightly weaker for movements towards the dorsal and ventral regions of visual space (Figure 3.1A, red curve). Fixed flies, able to move their heads only, responded in a similar way to motion above the equator. Beneath the equator the responses were the smaller the further ventral the position of the pattern, disappearing at the most ventral part of the visual space (Figure 3.1A, blue curve). Since HSS-cells show strongest sensitivity at the ventral regions, the weak responses in this region suggest that of the three HS-cells only HSN- and HSE-cells participate in controlling head movements. Similar analysis of yaw turning responses suggests that during tethered flight all HS-cells control yaw turning responses.

To study how different HS-cell responses elicited during head yaw movements and tethered flight were compared to HS-cells responses of immobilized flies further experiments were performed. In fixed *Drosophila*, HS-cells (Schnell et al., 2010) and VS-cells (Joesch et al., 2008) show a temporal frequency optimum

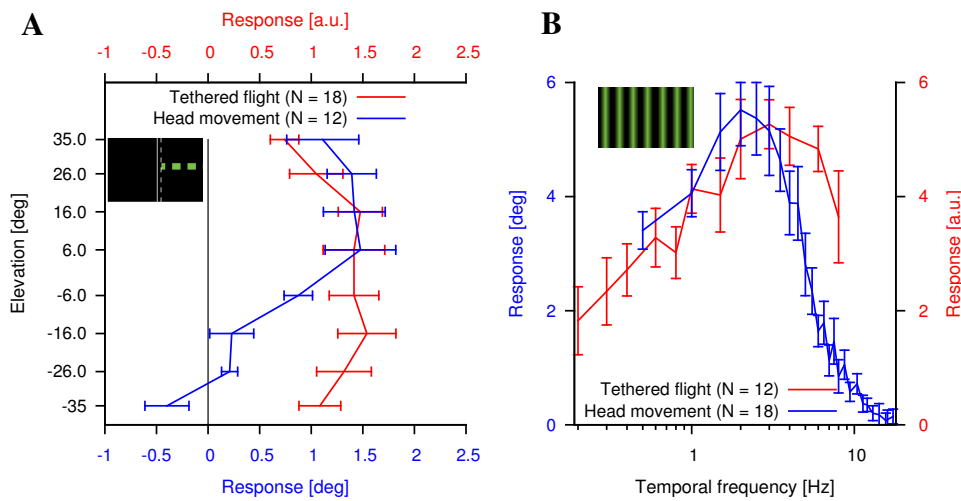


Figure 3.1: Comparison of head yaw responses in fixed flies with yaw turning responses in tethered flying flies. Mean \pm s.e.m. responses for yaw turns (red) and head yaw movements (blue). (A) Yaw responses for a monocular square wave pattern (excluding 15° of frontal visual view), extending approximately 10° in elevation and moving horizontally at eight different elevations. (B) Yaw responses elicited with a sine wave grating with spatial wavelength of 24° rotating horizontally at different velocities around the fly.

of 1 Hz. A qualitatively similar velocity dependence on the speed and layout of moving gratings has also been observed in flying and walking tethered flies. In these experiments different temporal frequency optima were observed. Walking flies show strongest responses to frequencies of 3 Hz (Götz and Wenking, 1973). Classical experiments have reported flying tethered *Drosophila* to respond best to a 1 Hz (Götz, 1964) temporal frequency. More recent experiments have reported an optimum temporal frequency of 4-9 Hz (Duistermars et al., 2007; Duistermars et al., 2012).

Cell recordings in behaving animals have given some insight into why different optima have been obtained. When flies are active, the membrane potential of lobula plate tangential cells shifts towards more positive values (Maimon et al., 2010). Activity of the flies also modulates the temporal frequency curve, shifting the temporal frequency optimum of the cells towards higher frequencies (Chiappe et al., 2010; Jung et al., 2011). Thus, the greater the shift in temporal frequency,



higher membrane potential of the cells are expected. The behavioural setup used in this study involved the same LED arena as in the electrophysiology experiments where a temporal frequency optima of 1 Hz was obtained (Schnell et al., 2010; Joesch et al., 2008). This gave the opportunity to compare cell responses with yaw torque and yaw head movements of the fly under identical conditions when changing the activity level of the flies.

The responses to a sine wave grating with spatial wavelength of 24° rotating at different velocities were investigated for tethered flying flies using the torquemeter (Methods 2.1.2). Flies responded qualitatively equally strong to temporal frequencies in the range of 2 Hz to 6 Hz (Figure 3.1B, red curve). For head movement responses in fixed flies, a similar curve with a maximum in the range of 1.5 Hz to 3 Hz was obtained (Figure 3.1B, blue curve). Both response curves were compared with the response curve of HS-cell recordings in *Drosophila* (Schnell et al., 2010). The activity level of the flies flattened the response curve, i.e. the responses for temporal frequencies close to the optimum did not decline as fast as for HS-cell responses in immobilized flies. Compared to cell recordings, the modulation of the response curve was stronger for flying flies than fixed flies moving their heads.

3.2 Optogenetic Activation of HS-cells

When a fly is visually stimulated by a pattern rotating around the vertical axis of the fly the HS-cells depolarize on the side where motion progresses from front-to-back (Hausen and Wehrhahn, 1989; Schnell et al., 2010). At the same time the fly displays yaw head movements (Duistermars et al., 2012) as well as yaw turning behaviour syndirectional to the stimulus (Blondeau, 1981a; Hausen and Wehrhahn, 1989; Duistermars et al., 2012).

If HS-cells control both these optomotor responses, then unilateral depolarization of HS-cells in the absence of any visual stimulus should mimic these following reactions. To test this idea, flies expressing a bi-stable Channelrhodopsin-2 variant called ‘ChR2-(C128S)’ (Berndt et al., 2009) in HS-cells were generated. When HS-cells were optogenetically activated in one hemisphere of the

fly's head, fixed flies turned their head towards the stimulated side. Tethered flying flies showed turning responses towards the stimulated side as well.

3.2.1 Activation of HS-cells Elicits Head Yaw Movements in the Preferred Direction of the Cell

Having confirmed that application of short light pulses to lobula plate tangential cells expressing ChR2(C128S) leads to a prolonged depolarization of the cells (Methods, section 2.3.1), the effect of this depolarization on head movements could be tested. In blow flies, a possible optomotor pathway has been described (Haag et al., 2010): three muscles controlling yaw head movements receive input from the ventral cervical nerve, comprised of the axons of three motor neurons, which in turn receive visual input from two of the three HS-cells (HSE and HSN).

In a first set of experiments a Gal4 driver line (*R27B03*; (Chiappe et al., 2010)) specifically targeting the three HS-cells in the lobula plate was used to express ChR2(C128S) in all three HS-cells. In the beginning of each trial, flies were stimulated by a square wave pattern rotating for 5 s first in the clockwise and then in the counter-clockwise direction. Flies responded to these stimuli by head movements with an amplitude of about 4° in the direction of the pattern motion (Figure 3.2A_i, left part). After the clockwise rotation had stopped, the flies' head remained in the position until the counter-clockwise rotation started. When HS-cells in the right hemisphere were depolarized by means of a 1 s pulse of blue light, flies on average showed head movement in the clockwise direction (Figure 3.2A_i, right part). In contrast, control flies that had the same genotype but were not fed the cofactor all-trans-retinal (ATR) did not show a significant response to the blue light pulse. The same holds true for the second group of control flies that did not carry the transgene encoding ChR2(C128S). These responses were quantified as the difference between the mean head angle between blue light and yellow light onsets and the mean head angle within the last second before blue light onset (see Methods). Responses of the experimental flies were highly significant, as compared to both groups of control flies (Figure 3.2A_{ii}).

To further investigate the role of HS-cells in head turning responses, I used

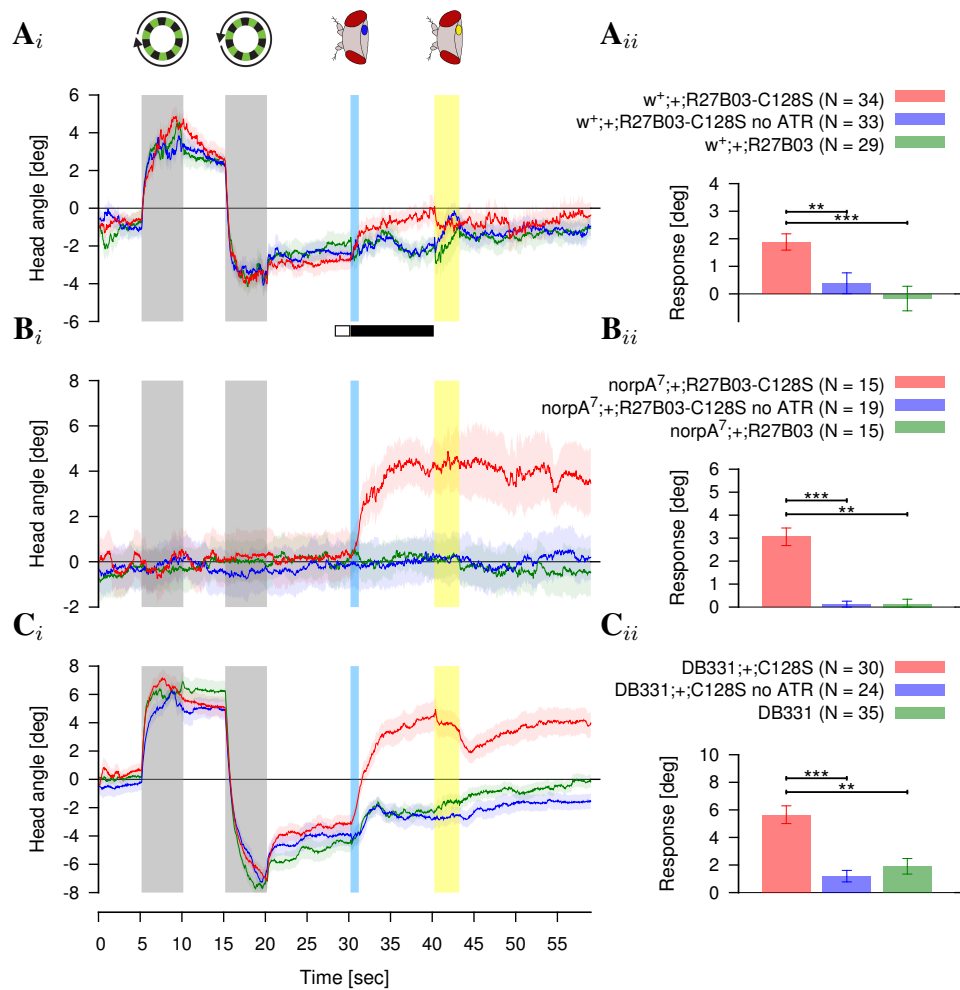


Figure 3.2: Optogenetic activation of HS-cells elicits head yaw movement in the preferred direction of the cell in fixed flies. Head movement analysis. Panels to the left represent mean traces \pm s.e.m., gray boxes indicate the time of visual stimulation, blue and yellow boxes show timing of optogenetic light stimulation. Right figures represent the mean \pm s.e.m response to the blue light pulses for (A) *R27B03-Gal4*, (B) *norpA⁷; +; R27B03-Gal4* and (C) *DB331-Gal4* experimental and control flies. Experimental flies expressed ChR2(C128S) and were fed with all-trans-retinal (ATR) (red traces), control flies had either the same genotype, but were not fed ATR (blue traces) or did not carry the ChR2(C128S) transgene (green trace). Mean responses are calculated as the difference between the mean head angle between blue light and yellow light onsets (black box in A) and the mean head angle within the last second before blue light onset (white box in A). $P^* < 0.01$, $P^{**} < 0.001$, $P^{***} < 0.0001$

mutant flies defective in phototransduction (*norpA*⁷) and combined them with the *R27B03* driver line to specifically express ChR2(C128S) exclusively in HS-cells. As expected, no responses to visual stimulation could be observed (Figure 3.2B_i, left part). In contrast, a blue light pulse elicited strong head turning towards the illuminated side in experimental flies, whereas both groups of control flies did not show any reaction (Figure 3.2B_i, right part). This response was again highly significant (Figure 3.2B_{ii}) and provides further support for the notion that activation of HS-cells in one hemisphere is indeed coupled to the execution of head movements towards the activated side.

To rule out the possibility that the observed effects were caused by unspecific expression of ChR2(C128S), i.e. in neurons other than HS-cells, a different independent Gal4 line with an expression pattern including HS- and VS-cells (*DB331*; (Joesch et al., 2008)) was used. Again, flies executed head movements following the grating motion (Figure 3.2C_i, left part). Upon application of a one second pulse of blue light to the right hemisphere, experimental flies showed head turning in the clockwise direction that were significantly larger than those of control flies (Figure 3.2C_{ii}). These responses were more pronounced than in the previous experiment where a driver specific for HS-cells was used (compare Figure 3.2C_{ii} with A_{ii}).

3.2.2 Activation of HS-cells Elicits Yaw Optomotor Responses in Tethered Flying *Drosophila*

To explore whether the HS-cell output also control thoracic motor circuits underlying flight steering maneuvers, the same experiment as described above was performed in tethered flying flies. To produce torque during flight, flies reduce their wing-beat amplitude on the side they turn to while enlarging it on the opposite side (Götz, 1968; Götz et al., 1979). HS-cells are known to synapse onto descending neurons that connect to the motor centers in the thoracic ganglion (Gronenberg and Strausfeld, 1990), which in turn might impinge on muscles controlling the wing beat (Egelhaaf, 1989).

To test this, flies of the same genotypes as in Figure 3.2A (*R27B03*), i.e. expressing ChR2(C128S) exclusively in HS-cells, and the same stimulus protocol as

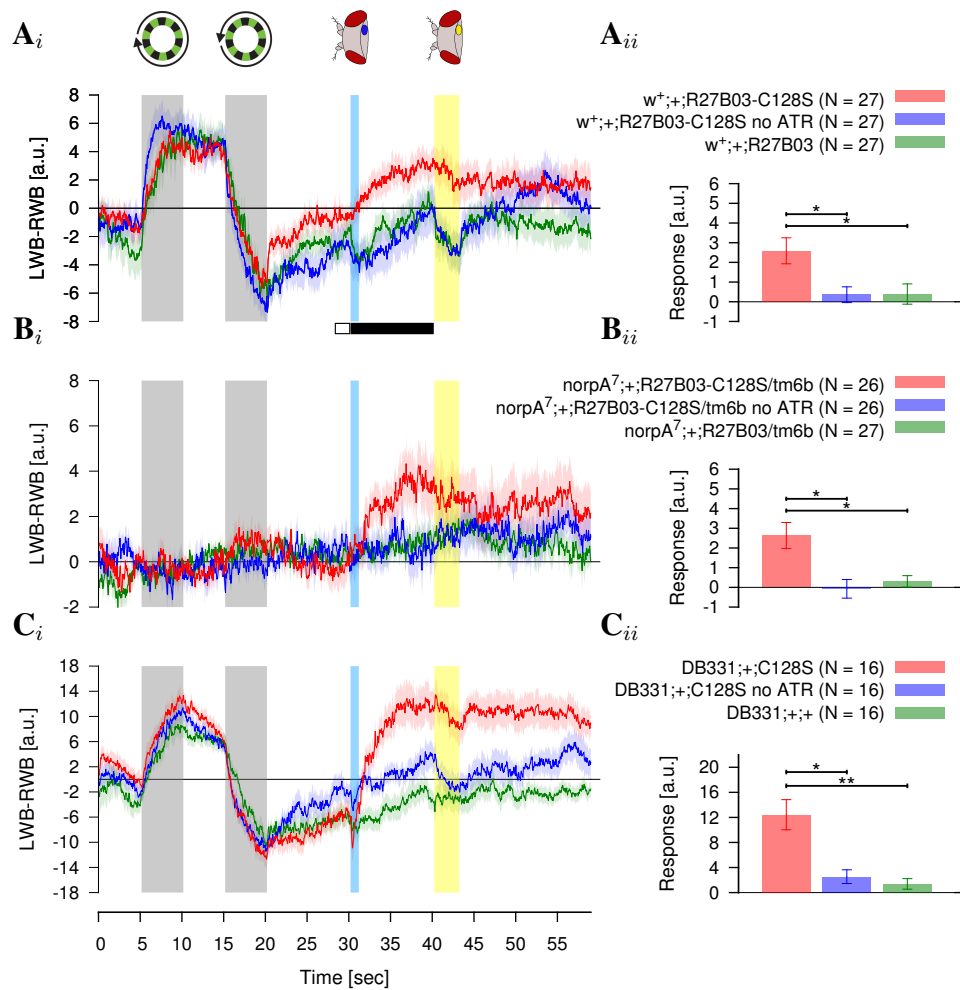


Figure 3.3: Optogenetic activation of HS-cells during tethered flight elicits yaw turning responses in the preferred direction of the cell. Wing beat analysis. Left figures represent mean traces \pm s.e.m., gray boxes indicate the time of visual stimulation, blue and yellow boxes show timing of optogenetic light stimulation. Right figures represent the mean responses \pm s.e.m. for experimental flies (A) *R27B03-Gal4* (B) *norpA⁷; + ; R27B03-Gal4* and (C) *DB331-Gal4* and control flies. Experimental flies expressed ChR2(C128S) and were fed with all-trans-retinal (ATR) (red traces), control flies had either the same genotype, but were not fed ATR (blue traces) or did not carry the ChR2(C128S) transgene (green trace). Mean responses are calculated as the difference between the mean turning behaviour between blue light and yellow light onsets (black box in A) and the mean turning behaviour within the last second before blue light onset (white box in A). $P^* < 0.01$, $P^{**} < 0.001$

for the observation of head movements were used. This time, however, the flies were allowed to fly with their head fixed to the thorax and their turning behaviour was quantified with use of the wing-beat analyzer (using the difference between left and right wing beat amplitude as measure, see Methods).

As observed for head turning, flies showed a strong and reliable wing response to the visual stimuli that would lead to a body turn in the direction of visual motion (Figure 3.3A_i, left part). Following delivery of a blue light pulse to the right hemisphere, only flies expressing ChR2(C128S) in their HS-cells and fed ATR showed strong turning behaviour towards the stimulated side (Figure 3.3A_i, right part). Responses were quantified as the difference between the mean turning behaviour between blue light and yellow light onsets and the mean turning behaviour within the last second before blue light onset (see Methods). This response was highly significant (Figure 3.3A_{ii}). In contrast, both types of control flies had no directional bias in their responses (Figure 3.3A_i, right part; Figure 3.3A_{ii}).

As done previously for the study of head movements, the experiments were repeated in flies with defective phototransduction (in *norpA*⁷). During clockwise and counter-clockwise rotations of the visual panorama, no responses were detectable (Figure 3.3B_i, left part). This changed upon hemisphere specific delivery of blue light pulses; only those flies that expressed ChR2(C128S) in HS-cells and that were fed with ATR showed a turning behaviour towards the stimulated side. Neither of the two groups of control flies revealed consistent unilateral response in their wing beat amplitudes (Figure 3.3B_i, right part; Figure 3.3B_{ii}).

Finally, flies with same genotype as in Figure 3.2C were tested. All flies followed the grating motion (Figure 3.3C_i, left part). Depolarization of cells on the right hemisphere using a 1 s pulse of blue light elicited turning responses in the clockwise direction that were significantly larger than those of control flies (Figure 3.3C_{ii}). As observed during head movement experiments, these responses were more pronounced than in the previous experiment where another driver, specific for HS-cells, had been used (compare Figure 3.3C_{ii} with A_{ii}).



3.3 Role of HS-cell Receptive Fields for Yaw Optomotor Behaviour

Having established the participation of HS-cells in optomotor behaviour, I next tested how optomotor responses change when the HS-cell anatomy / receptive field layout is genetically modified. For this, optomotor responses of flies with gain-of-function of a single Dscam1 isoform in HS-cells were compared to control fly optomotor responses (Dscam gain-of-function, D(GOF)). Compared to control HS-cells, D(GOF) HS-cells are smaller, less sensitive to horizontal motion in the frontal region and more sensitive to motion in lateral part of visual space.

First, tethered flying flies were tested. D(GOF) flies responded much weaker than control flies to visual stimulation covering the entire azimuth extension of HS-cell receptive fields. Motion in the rear part of visual space elicited a strong inversion of the optomotor responses in control flies. This inversion could not be observed for D(GOF) flies. Despite the reduced sensitivity of D(GOF) HS-cells in the frontal field of view, D(GOF) displayed robust following movements to motion in front of the fly.

D(GOF) and control flies also showed differences in head yaw movements which, however, did not correlate with the specific deficits of HS-cells in D(GOF) flies. In summary, thus, while D(GOF) flies show aberrant optomotor responses in yaw flight responses and head movements, these alterations are not confined to the frontal part of the visual field where HS-cells of D(GOF) flies have a strong deficit. This result suggests that other cells participate in controlling yaw optomotor responses as well. Therefore, the receptive field of HS-cells and the sensitivity of the optomotor responses do not correspond 1:1.

3.3.1 Changes in HS-cell Receptive Fields Modify Turning Behaviour in Tethered Flying Flies

As seen in section 3.2.2, when HS-cells are optogenetically activated during flight, flies show a following reaction towards the depolarized side. How do the optomotor responses change when the HS-cells' receptive fields have changed as described for flies with a Dscam gain-of-function in HS-cells (D(GOF) flies, refer to Methods, 2.3.2)? Are flies unable to react to motion in regions where HS-cells show strongly reduced sensitivity to motion? Do flies show stronger optomotor responses in regions where HS-cells respond stronger when compared to control flies?

Analysis of Tethered Flight using Stimuli Excluding the Frontal Region of the Visual Space

Tethered flying flies were stimulated with visual stimuli while simultaneously recording their wing beat kinematics. D(GOF) flies were expected to respond weaker than control flies to motion in the frontal region of visual space. The effect of Dscam gain-of-function on HS-cells was variable among HS-cells on both hemispheres of the same fly (Figure 2.10A, left column). One concern was that "healthy" HS-cells might compensate for possible reduction in optomotor responses. In the frontal region, where the strongest reduction in sensitivity was observed in D(GOF) HS-cells, all 6 HS-cells perceive motion. This is because of the largely overlapping receptive fields of HS-cells on one hemisphere (refer to Figure 1.6 or (Schnell et al., 2010)) and because of the binocular overlap of HS-cells. It was not possible to reduce the possible compensatory effects of HS-cells on the ipsilateral side, but the binocular overlap was eliminated by presenting unilateral visual stimuli excluding $\pm 15^\circ$ of the flies' visual space. For all following experiments a square wave pattern with spatial wavelength of 24° rotating at $30^\circ / \text{s}$ (a temporal frequency of 1.24 Hz) was used.

First the contrast sensitivity of the flies was tested measuring the optomotor response strengths elicited with a square wave pattern with different contrasts. Each trial began and ended with a bilateral whole-field stimulus with maximum contrast rotating for 5 s in each direction. Between these whole-field stimuli,

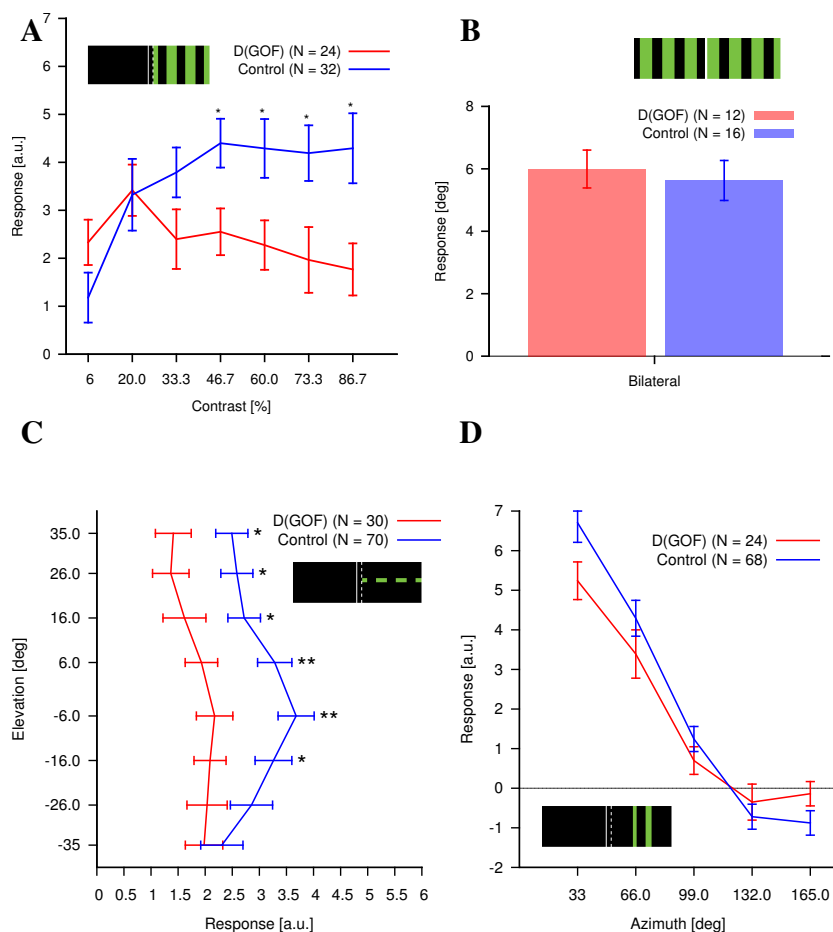


Figure 3.4: Effects of Dscam gain-of-function in tethered flying flies for a stimulus excluding the frontal region of the visual field. Mean \pm s.e.m optomotor responses for D(GOF) flies (red) and control flies (blue) for a square wave pattern with spatial wavelength of 24° rotating at $30^\circ / \text{s}$ (a temporal frequency of 1.24 Hz) excluding $\pm 15^\circ$ of visual space. (A) Contrast dependency for unilateral pattern motion. (B) Yaw torque responses for a whole-field pattern with maximum contrast (same flies used for (A)). (C) Responses to a square wave pattern extending about 10° in elevation centered at eight different elevations. (D) Responses to a square wave pattern extending 33° in azimuth centered at 4 different azimuth angles ($P^* < 0.05$, $P^{**} < 0.01$).

seven unilateral square wave patterns with different contrasts were presented to each hemisphere of the fly. These rotated for 2 s in the null direction, 5 s in the preferred and 5 s in the null direction. Since presented unilaterally, all three

HS-cells in one hemisphere were activated. Optomotor responses of control and D(GOF) flies increased with increasing contrast of the pattern. At low contrasts, both genotypes responded equally well. For higher contrasts the responses saturated at a different level amounting for D(GOF) flies to only about 50 % of control flies (Figure 3.4A). Responses to a bilateral square wave grating presented in the beginning and end of each trial elicited yaw responses of approximately equal strength in control and D(GOF) flies (Figure 3.4B).

The monocular stimulus activated all three HS-cells at the same time. To study the participation of individual HS-cells in the optomotor responses a square wave grating restricted to about 10° in elevation was used. This small grating was presented at 8 different positions in elevation. As for the stimulus with varying contrast (Figure 3.4A), each elevation was presented randomly moving for 2 s in the null direction, 5 s in the preferred direction and then in the null direction again. Both genotypes were able to follow the small drifting square wave pattern in elevation. The strength of the responses of D(GOF) flies were weaker than for control flies, especially for motion at the equator (Figure 3.4C).

D(GOF) HS-cell responses, when compared to control HS-cell responses, were weaker in the frontal and stronger in the lateral part of visual space. Similar differences were expected for optomotor responses. To investigate this, a grating extending the entire elevation and restricted to 33° in azimuth was presented to the flies at 5 different azimuth angles. No significant difference in response strength could be observed between D(GOF) and control fly optomotor responses (Figure 3.4D). Control and D(GOF) flies responded strongest to motion in the frontal part of visual space. Motion in the rear part of visual space elicited negative responses.

Tethered Flight Including the Frontal Region of Visual Space

The results of the first experiments indicated that D(GOF) flies present qualitatively similar but weaker optomotor responses to monocular visual motion. Due to the missing sensitivity of D(GOF) HS-cells in the frontal region of visual space, the largest differences between control and D(GOF) optomotor responses were expected to be to motion in this region. However, the frontal $\pm 15^\circ$ region of visual space of view had been excluded in the previous experiments in order to exclude



the binocular overlap of the HS-cells. To investigate the effect of motion in the frontal region of visual space on the optomotor responses one of the fly's eyes was painted black. This allowed to include the frontal region of the visual space and at the same time to exclude the participation of the contralateral HS-cells in the optomotor responses.

First, square wave gratings with spatial wavelength of 24° rotating at $30^\circ / \text{s}$ (a temporal frequency of 1.24 Hz) extending the entire elevation and over four different azimuth angles (from -30° to 15° , 90° and 165°) were tested. Each trial started and ended with a whole-field square wave grating rotating 5 s in each direction. Between the whole-field stimuli the three stimuli with different azimuth extensions were presented. These rotated for 2 s in the null direction and then in preferred and null direction for 5 s each.

When motion was presented only in the frontal region (-30° to 15°) control and D(GOF) flies followed the visual motion (Figure 3.5A) at about the same strength. This was not expected since D(GOF) HS-cells had, compared to control HS-cells, strongly reduced sensitivity to motion in this region. A significant difference in optomotor response strength was observed for an azimuth expansion from -30° to 90° (Figure 3.5A). This approximately corresponds to the azimuth extension at which HS-cells are sensitive to motion (Schnell et al., 2010). The incorporation of visual motion in the rear part of visual space ($>90^\circ$) strongly reduced the responses for control flies. For D(GOF) flies there was no change in response strength when additionally stimulating the rear part of visual space (compare responses to pattern motion between -30° and 90° with motion between -30° and 165° ; Figure 3.5A).

Tethered flying flies were presented square wave gratings, centered at 90° in azimuth, extending the entire elevation and 45° , 90° , 135° and 180° in azimuth. Control flies followed significantly stronger a square wave grating centered at 90° and extending 135° in azimuth than D(GOF) flies (Figure 3.5B). The incorporation of the frontal and rear regions of visual space enhanced the response strength of D(GOF) to a larger extent than control flies (compare responses for control and D(GOF) flies to a pattern extension of 135° with 180° ; Figure 3.5B).

Finally, the responses to a bilateral square wave pattern were analyzed. Due to the painted black eye, the entire azimuth and elevation extensions of the visual

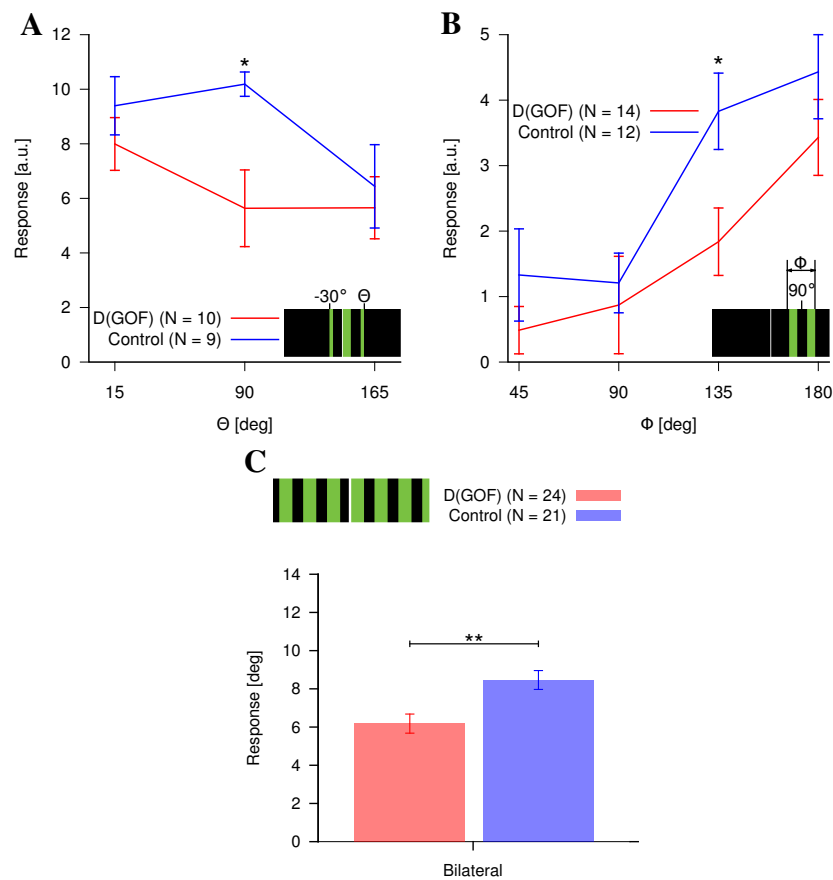


Figure 3.5: Effects of Dscam gain-of-function in tethered flying flies with one eye painted black, using a stimulus including the frontal region of the visual field. Mean \pm s.e.m. optomotor responses for D(GOF) flies (red) and control flies (blue) for a square wave pattern with spatial wavelength of $\lambda = 24^\circ$ rotating at $30^\circ / \text{s}$ (a temporal frequency of 1.24 Hz). (A) Responses to a square wave pattern extending from -30° to 15° , 90° and 165° in azimuth and the entire elevation. (B) Responses to a square wave pattern centered at 90° and extending 45° , 90° , 135° and 180° in azimuth and the entire elevation. (C) Responses to a bilateral square wave pattern motion ($P^* < 0.05$, $P^{**} < 0.01$).

field of HS-cells in only one hemisphere were stimulated. Control flies showed stronger responses than D(GOF) flies (Figure 3.5C). For control flies these responses were stronger than those elicited with flies able to use both eyes. D(GOF) flies exhibited the same strength in optomotor response regardless if one eye had been painted black or not (compare Figure 3.4B with Figure 3.5C).



3.3.2 Changes in HS-cell Receptive Fields Modify Head Yaw Movements

The experiments with flying tethered flies presented so far suggest that a modification of the anatomy of HS-cell dendrites and concomitant changes in their receptive fields is indeed linked to changes in optomotor responses. To test if this is also the case for head yaw movements new experiments were performed. During these experiments flies turn their head and the presentation of the stimuli used for tethered flying flies does not allow to stimulate only certain regions of fly's field of view. Two new stimuli had to be designed to correlate the possible deficits in optomotor responses to the reduced and enhanced sensitivity of D(GOF) HS-cells in the frontal and lateral part of visual space, respectively.

The results presented in section 3.1 suggest that of the three HS-cells, only HSN and HSE are used to control head yaw movements. Assuming that HS-cell responses correlate with the optomotor responses in a linear way, then the sum of the receptive fields of HSN and HSE-cells should correlate with the strength of the executed yaw head movements. Thus, the difference of the receptive fields for head movement of D(GOF) and control flies (Figure 3.6C) should match the differences in head movements of D(GOF) and control flies.

The sum of the receptive fields of HSN and HSE-cells will be referred to as the receptive field for head movement

Closer inspection of the difference in receptive fields for head movement of control and D(GOF) flies suggested that the loss of sensitivity in the frontal region of visual space is not constant for all elevations (Figure 3.6C). The largest reduction in sensitivity in the frontal region of visual space was located at the equator. For azimuth angles above about 50° , D(GOF) flies were expected to be more sensitive to motion than control flies. For azimuth angles below about 50° , the opposite was expected. To investigate this, three angles of elevation were chosen to present motion (30° to 40° , 0° to 10° and -20° to -10°). For each extension in elevation, the difference of the receptive field for head yaw movement were calculated for each azimuth angle (Figure 3.6D).

Two new stimuli were designed to compare the cell recordings (Figure 3.6D) with head yaw movements. The first stimulus (null direction stimulus, ND-stimulus; Figure 3.7A) consisted of a square wave pattern restricted to about 10° in elevation superimposed by a black curtain opening behind the fly. The square

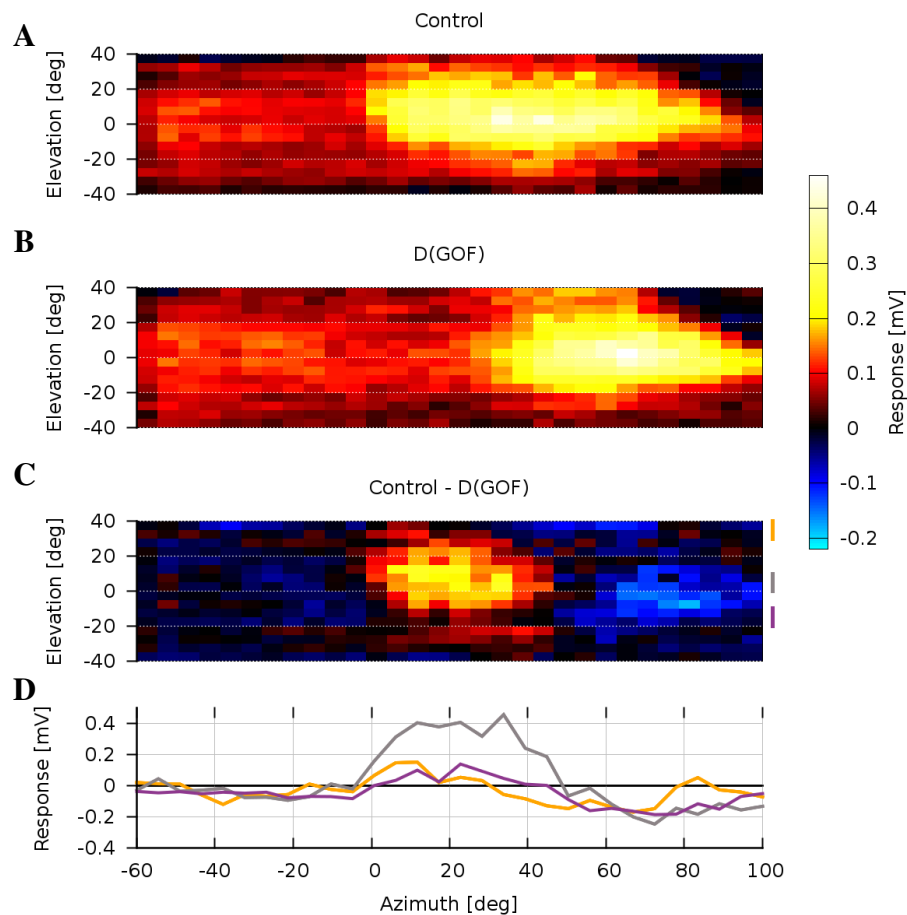


Figure 3.6: Comparison of the sum of HSN and HSE receptive fields for control and D(GOF) flies. Sum of the mean receptive fields of HSN and HSE for control (A) and D(GOF) flies (B). (C) Difference of the receptive fields shown in (A) and (B). (D) Sum in elevations between 30° and 40° (red), 0° and 10° (blue), -30° and -20° (green) of the receptive fields in (C). (Data: Bettina Schnell)

wave pattern rotated counter-clockwise with identical speed as the curtain opened. During the first part of the stimulus, the fly experiences increasing back-to-front motion (Figure 3.7A_{ii}) until the leading edge of the square wave pattern reaches the front of the fly (Figure 3.7A_{iii}). From this instance on, the right eye of the fly perceives back-to-front motion while the left eye experiences increasing front-to-back motion (Figure 3.7A_{iv}).

For presenting front-to-back motion in the first half of the stimulus a second stimulus was designed (preferred direction stimulus, PD-stimulus; Figure 3.7B).

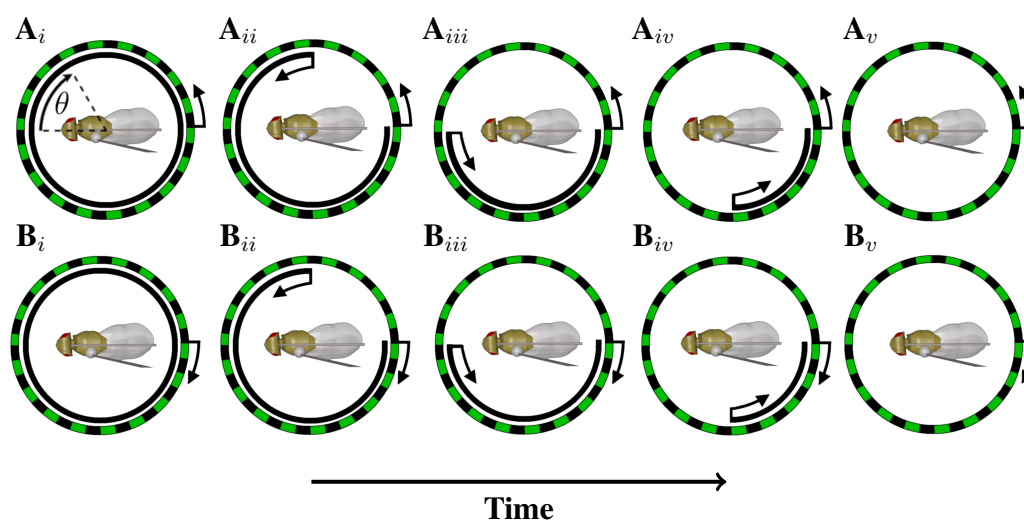


Figure 3.7: Stimulus used for head movement experiments with D(GOF) flies.

At stimulus begin a square wave pattern restricted to about 10° in elevation rotating (A) counter-clockwise and (B) clockwise is covered by a black “curtain”. The curtain starts to open clockwise with the same speed as the square wave pattern is rotating, revealing the covered square wave pattern motion. Positive head angles and position of the curtain edge (θ) were defined positive towards the right side of the fly (A_i).

This consisted of a clockwise rotating square wave pattern restricted to about 10° in elevation covered with a black curtain opening counter-clockwise with identical speed. During the first half of this stimulus, due to the square wave pattern, the fly experiences increasing front-to-back motion. The leading edge of the curtain is perceived by the fly as back-to-front motion (Figure 3.7B_{ii}). In the second half of the stimulus, motion on the right side is perceived as front-to-back motion, while the left eye experiences an increasing back-to-front motion together with a front-to-back moving edge (Figure 3.7B_{iv}).

To test the general ability of the flies to follow horizontal movement, a whole-field square wave pattern moving for 5 s in each direction was presented before each stimulus. The order of the directions had to be chosen in such a way that the second pattern motion was in the opposite direction of the stimulus to be presented. Since the ND-stimulus consisted of an increasing counter-clockwise rotation (Figure 3.7A), each trial started with a counter-clockwise followed by

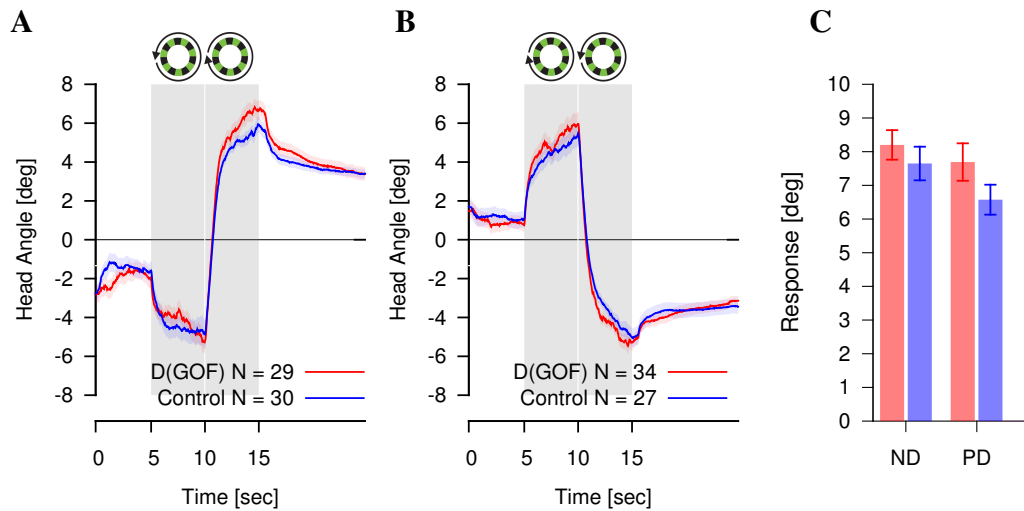


Figure 3.8: Comparison of head yaw movement traces \pm s.e.m. and responses \pm s.e.m. of D(GOF) (red) and control (blue) flies elicited by a whole-field square wave pattern. Gray boxes indicate direction of rotation. (A) Whole-field visual stimulation presented during ND-stimulus trials moving first clockwise then counter-clockwise. (B) Whole-field visual stimulation presented during PD-stimulus trials moving first counter-clockwise then clockwise. (C) Responses to whole-field rotation shown in (A) and (B).

a clockwise whole-field rotation. After the whole-field stimulus the arena was turned off for 10 s and the ND-stimulus was presented. For experiments using the PD-stimulus consisting of an increasing clockwise rotation (Figure 3.7B), each trial started with a clockwise followed by counter-clockwise whole-field rotation and ended after a 10 s dark period with the presentation of the PD-stimulus.

First, the following movements of the head elicited by the whole-field stimulus were analyzed. Control and D(GOF) flies were able to follow the whole-field motion stimulus presented during the first part of each experiment (mean trace for ND-stimulus Figure 3.8A and PD-stimulus Figure 3.8B). Since D(GOF) flies seemed to respond somewhat stronger to the visual stimulus, the responses were analyzed in further detail. The responses were not statistically different ($P = 0.4$ for ND- and PD-stimulus trials) which is consistent with the flying tethered experiments where no significant difference in optomotor responses was observed for whole-field stimulation. Thus, D(GOF) flies did not show evident motor defi-



ciencies.

During these experiments flies turn their heads, which leads to the perception of the visual stimuli not being equal in time across trials. To compare the head yaw movement elicited with the ND-stimulus and PD-stimulus each recorded trace was shifted in time. Time point zero corresponds to the instance in time at which the leading edge of the stimulus had reached the front of the fly (angle 0° with respect to the fly's head).

Control and D(GOF) flies started to follow motion before the edge of the square wave grating had been revealed for azimuth angles smaller than 100° (Figure 3.9, blue and red traces for times smaller than about -7 s). The fact that HS-cells are sensitive to motion for azimuth angles up to about 100° suggests that these following movements were elicited by other cells than HS-cells. These following movements were in the back-to-front direction for both tested stimuli. This was unexpected for the PD-stimulus since it consisted of an increasing square wave rotating in the front-to-back direction. Thus, the curtain edge, moving from back-to-front also elicited following movements of the head. Since the following movements were in the back-to-front direction suggests that the cell eliciting the following movement of the head must be sensitive to back-to-front visual motion.

Control and D(GOF) showed slight differences to both stimuli (Figure 3.9A and B, green traces), however no evident correlation between the difference of control and D(GOF) HS-cell receptive fields with the difference in head yaw movements could be observed. To investigate this in a more detailed way, the differences in head yaw movement of control and D(GOF) flies (Figure 3.9, green traces) were compared with the difference of control and D(GOF) cell responses (Figure 3.6D). Since HS-cells had been recorded only for azimuth angles between -60° to 100° , the cell response curves (Figure 3.6D) for positive angles were symmetrically used for negative angles. Thus, obtaining the cell responses for azimuth angles between -100° to 100° in azimuth.

For head yaw movements the following movement was considered stronger at a certain angle if the head angle was smaller during the ND-stimulus and larger during the PD-stimulus. For a positive difference between control and D(GOF) flies to indicate a stronger following movement of control flies, the difference of control and D(GOF) flies during head yaw movement elicited by the ND-

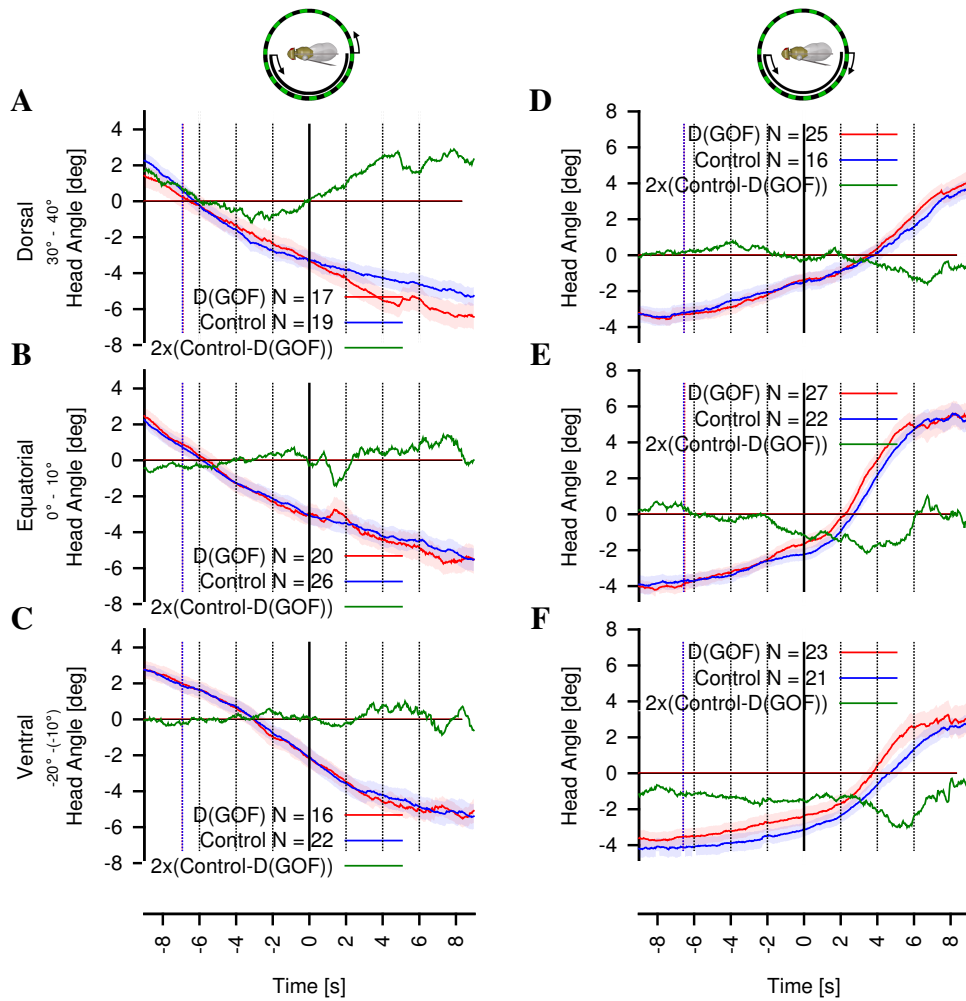


Figure 3.9: Comparison of head yaw traces \pm s.e.m. of D(GOF) (red) and control flies (blue), elicited using the ND-stimulus (A-C) and PD-stimulus (D-F). Schematics on top depict convention of positive head and curtain edge angle (blue), direction of square wave rotation (green/black arrow) and direction of curtain edge movement (black arrow). Stimulus restricted to (A and D) 30° to 40°, (B and E) 0° to 10°, (C and F) -20° to -10° in elevation. Depicted in green the difference between control and D(GOF) fly traces multiplied by 2. Traces are shifted in time and time zero corresponds to time instance when the leading edge of the pattern reached the front of the fly. Blue vertical lines indicate mean time when leading edge reaches 100° respect to the fly's head.

stimuli was multiplied by -1. Since the visual stimulus rotated at 15° / s, the time axis of Figure 3.9 was multiplied by -15 to get an approximation of the posi-

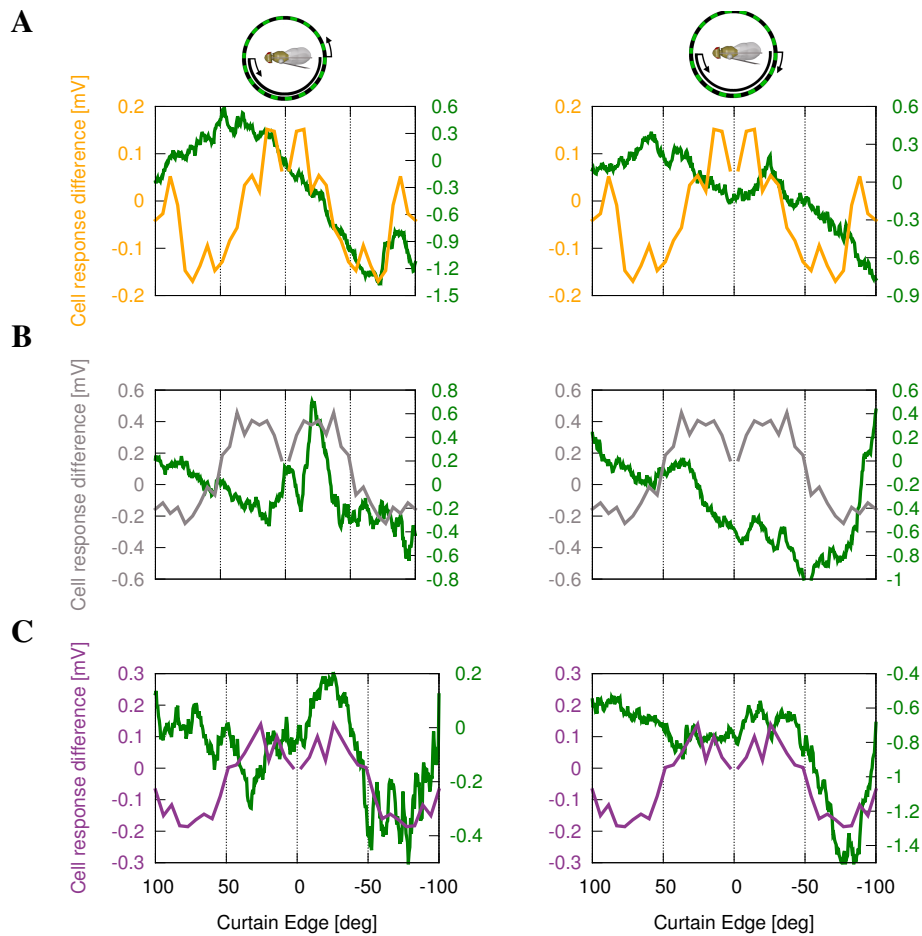


Figure 3.10: Comparison of the response difference in head yaw movement of D(GOF) and control flies with the difference of the receptive fields of D(GOF) and control flies (Figure 3.6D). Depicted in orange, gray and purple the difference between D(GOF) and control receptive fields and in green the difference between D(GOF) and control head yaw movement. Left column depicts results for the ND- (multiplied by -1), right for PD-stimulus. Pattern movement restricted to (A) 30° to 40°, (B) 0° to 10°, (C) -20° to -10° in elevation.

tion of the leading edge in degrees consistent with the angle convention shown in Figure 3.7A_i.

When the rotating square wave grating was revealed in the back of the visual field, the difference in behaviour was the opposite of what was expected, i.e when D(GOF) HS-cells were more sensitive to motion than control HS-cells (negative

difference in cell response) D(GOF) flies showed weaker following movement of the head (increasing difference of green traces). When the edge of the stimulus reached the other hemisphere of the fly the expected behaviour of the difference in head yaw movement could be observed, i.e. when control HS-cells were more sensitive compared to D(GOF) flies (positive difference in cell response) control flies showed a stronger following head yaw movements (increasing difference of green traces).



Chapter 4

Discussion

When confronted with a large-field stimulus rotating around the vertical body axis, flies display a following behaviour. Three large tangential horizontal cells (HS-cells) of the lobula plate have been identified as prime candidates to be the neural control elements for these so called ‘optomotor responses’. In this work the role of HS-cells for optomotor responses was investigated. HS-cell response properties were genetically manipulated and the resulting optomotor responses analyzed.

First, experiments were performed to deduce which of the three HS-cells could be participating in head yaw movements in fixed flies and yaw turning behaviour during tethered flight. Optomotor responses to motion at different elevations were recorded and compared with the HS-cell receptive fields. These experiments suggest that all three HS-cells control turning responses in flight, but only HSN and HSE are involved in the control of head yaw movements.

Second, to investigate whether HS-cells are sufficient to elicit optomotor responses a bistable Channelrhodopsin-2 variant was expressed specifically in HS-cells. This allowed for unilateral activation of HS-cells in intact flies while simultaneously recording their optomotor responses. The main finding of these experiments was that unilateral activation of HS-cells elicits yaw turning be-

haviour of the head and of the whole fly according to the preferred direction of the activated cell.

Third, the role of HS-cell anatomy / receptive field layout for optomotor responses was investigated. For this, optomotor responses of flies with a gain-of-function of a single *Dscam1* isoform in HS-cells (D(GOF) flies) were analyzed. HS-cells of these flies have missing dendritic branches in the lateral lobula plate corresponding to the frontal field of view. These anatomical changes come along with dramatically reduced sensitivity to motion in the frontal and increased sensitivity to motion in the lateral part of visual space. Optomotor responses of flying tethered flies were analyzed. Compared to control flies, D(GOF) flies responded significantly weaker to visual motion presented over the entire azimuth extension of the receptive fields of HS-cells. The observed responses were significantly reduced for control flies when the entire hemisphere of the fly was stimulated. On the other hand, the incorporation of motion to the rear part of visual space had no effect on D(GOF) optomotor responses. Although D(GOF) HS-cells have dramatically reduced sensitivity in the frontal region of the visual field, D(GOF) flies were able to follow visual motion in front of the fly. D(GOF) and control flies also showed differences in head yaw movements. These differences did not correlate 1 : 1 with the difference between the HS-cell receptive field layouts of control and D(GOF) flies.

4.1 Comparison of HS-cell Activity and Yaw Optomotor Responses

The similarity of lobula plate tangential cell responses and yaw optomotor responses has been observed in several studies (Bishop and Keehn, 1967; Hausen and Wehrhahn, 1989; Duistermars et al., 2007; Duistermars et al., 2012). Using this as a reference, the first experiments were performed to get an insight into the



role of HS-cells in optomotor responses.

Comparison of Optomotor Responses to Motion at Different Angles of Elevation with the Receptive Field Layout of HS-cells

First experiments served to identify which of the three HS-cells participate in head yaw movements and in turning responses of flying flies. For this, the receptive field layouts of HS-cells (Schnell et al., 2010) were compared to optomotor responses elicited with local horizontal motion stimuli moving at different elevations.

Wild type flies did not exhibit robust head following reactions for patterns moving in their ventral part of visual space (Figure 3.1A, blue curve). Optomotor responses of flying tethered flies were symmetric with respect to the elevation of the presented stimulus (Figure 3.1A, red curve; (Duistermars et al., 2007)). A possible and likely explanation for this observation is that head yaw movements are controlled only by the HSN- and HSE-cells, whereas during flight, yaw torque is in addition controlled by the HSS-cells. This is in agreement with a possible optomotor pathway suggested in blow flies (Haag et al., 2010). Three muscles controlling yaw head movements receive input from the ventral cervical nerve, comprised of the axons of three motor neurons. These in turn receive visual input from only two of the three HS-cells (HSE and HSN).

The experiments performed suggest that *Drosophila* uses the same kind of neural wiring as blow flies for head yaw movements. This might be useful when flies walk. During walking the optic flow elicited by the relative motion of the floor is strong. Ignoring this information might make flies more sensible to movements in the dorsal part of the visual space. During flight all the optic flow is important and would explain why flies also use the optic flow in the ventral part of visual space. Disconnecting the HSS-cell from the visual-motor pathway during walking would be an effective way of achieving this.

Comparison of Optomotor Responses to Motion with Different Speed with HS-cell Responses

A qualitative experiment was performed to study whether HS-cell responses during head yaw movement and flight could be expected to be similar to HS-cell responses of immobilized flies. For this the following was considered. The temporal frequency optimum of HS-cells in walking flies (Chiappe et al., 2010) and H1-cells in flying flies (Jung et al., 2011) is shifted towards higher frequencies when compared to cell recordings in immobilized flies. Besides the change in the temporal frequency optimum also the membrane resting potential rises with higher activity levels of the fly (Maimon et al., 2010). Both observations have been explained by the release of octopamine when flies get active (Chiappe et al., 2010; Jung et al., 2011). Thus, compared to HS-cell recordings, the higher the shift in temporal frequency optimum is, the higher the resting potential of the HS-cells turns out to be.

HS-cells present a temporal frequency optimum of 1 Hz and the responses decline for lower and higher temporal frequencies (Schnell et al., 2010). During the behavioural experiments performed in this work the same LED arena was used as in these HS-cells recordings. Thus, it was possible to compare cell responses with yaw torque and yaw head movements of the fly under identical conditions with different activity levels of the flies.

For head yaw movements, a temporal frequency optimum of 2 Hz was observed. Temporal frequencies between 1.5 and 3 Hz elicited qualitatively equally strong responses (Figure 3.1B, blue curve). The strongest responses for tethered flying flies were to a temporal frequency of 3 Hz. However, the response strength to temporal frequencies between 2 Hz and 6 Hz were qualitatively equally strong (Figure 3.1B, red curve). Thus, the higher the activity level of the fly was, the slower the responses declined for temporal frequencies below and above the optimum. This suggests, that the activity profile of HS-cell responses during head yaw movements is more similar to HS-cell responses in immobilized flies than during flight. Using head yaw movements as readout possibly reflects HS-cell recordings in immobilized flies more precisely than yaw turning responses during flight.

These experiments revealed an activity-dependent modulation of the visual



system similar to previous work (Chiappe et al., 2010; Jung et al., 2011). The temporal frequency profile is even more modulated during flight than during head yaw movements. This suggests that the modulation is not simply turned on and off when a fly moves but increases with activity. This makes sense, since during flight higher image speeds need to be detected than during walking or when a fly stands still. It would be interesting to additionally perform these experiments with walking tethered flies and observe whether the modulation strength during walking is in between the observed during head yaw movement and flying tethered flies.

4.2 Optogenetic Activation of HS-cells

Extra-cellular electrical stimulation of the lobula plate region where HS-cells are located elicits yaw turning responses (Blondeau, 1981b). However, the observed yaw turning responses are in the opposite direction of what HS-cell responses would predict.

The above experiment suggests that lobula plate tangential cells are sufficient for optomotor reactions. However, the experiment lacks precise and non-invasive manipulation which might explain why the elicited responses using extra-cellular electrical stimulation were in the opposite direction as expected. To investigate whether this was due to the unspecific activation of the HS-cells using extra-cellular electrical stimulation or simply due to the fact that a depolarization of HS-cells has a more complicated effect on the system than expected, I decided to use optogenetics in *Drosophila*.

Although optogenetic methods have been successfully applied in a number of studies involving different species like *C. elegans* (Nagel et al., 2005), zebrafish (Douglass et al., 2008; Arrenberg et al., 2010; Schoonheim et al., 2010) and mice (Arenkiel et al., 2007; Matyas et al., 2010), its use in adult *Drosophila* (Zimmermann et al., 2009; Yaksi and Wilson, 2010) has been rather limited, in particular for analyzing visual circuits. One reason for this is the difficulty of delivering light to activate light-sensitive ion channels or pumps without directly stimulating the photoreceptors and, thus, interfering with the visual processing to be studied. To avoid this problem, optogenetic stimulation has been performed

in blind flies (de Vries and Clandinin, 2012). This strategy raises potential concerns as to whether the circuits are compromised by visual deprivation and using blind flies does not allow the simultaneous visual probing of the system. In this respect, the development of switchable, bi-stable Channelrhodopsin-2 variants (Berndt et al., 2009) represents a major breakthrough. One of these variants, ChR2(C128S), allows for prolonged and repeated excitation of cells. I decided to use this specific Channelrhodopsin-2 variant since it allowed to activate cells by means of only a short pulse of light and later deactivate these with another pulse of light at a different wavelength. Thereby, artifacts produced by optogenetic activation were minimized and observations of optomotor responses free of an external stimulus were possible.

I could show that optogenetic stimulation of HS-cells is sufficient to evoke both yaw head movements as well as flight turning responses of the whole animal. However, due the small size of *Drosophila* even a small optogenetic activation light spot was visually perceived by flies. This led to transient physiological and behavioural artifacts. Nevertheless, long-lasting responses were only observed in animals expressing functional ChR2(C128S) which is in agreement with the bi-stable nature of this channel. Optogenetic activation of ChR2(C128S) depolarized the membrane potential of HS-cells and elicited yaw turning behaviour comparable to visually elicited optomotor responses. The direction of the behavioural responses toward the stimulated side can be interpreted as an attempt to counteract perceived unintended yaw body rotations.

Data Selection

HS-cells are located close to the back of the head. To reach the back of the head of the flies during head yaw experiments, the head was pushed forward using a thin tungsten wire. If the wire was not positioned correctly, flies did not turn their head in both directions when stimulated with a whole-field visual stimulus. Similar to head yaw experiments, preparation of flies for tethered flight experiments might have prevented flies to turn in both directions. To ensure that all flies analyzed were able to move their heads in both directions during head yaw experiments and to present turning behaviour in both directions during tethered flight experiments,



only a subgroup of the flies tested were selected for final analysis (refer to chapter 2: Methods). This was considered necessary, since when showing that control flies do not turn their head or fly towards the stimulated side it is essential to show that they are actually able to do so. The same holds true for experimental flies. If they are not able to turn away from the stimulated side the analysis of responses is misleading.

To ensure that the results presented are not only true for the selected flies, the data of all flies was analyzed. It could be observed that the responses to whole-field visual stimulation were not equally strong for all fly genotypes. This was expected, since for different genotypes a different number of flies did not show a robust following movement of the whole-field pattern. Nevertheless, the responses to optogenetic stimulation of experimental flies were significantly different to control fly responses when all the flies were analyzed as described in chapter 2, Methods.

Stronger Effect of Optogenetic Activation in Flying Flies than Fixed Flies

The responses elicited by optogenetic depolarization of HS-cells in flying flies seemed to be stronger than those observed for head yaw movements (compare Figure 3.2A with 3.3A). In fact *norpA*⁷ flies, heterozygous for ChR2(C128S), did not show head yaw turning responses to blue light (data not shown) but did show yaw turning responses to blue light in flying flies (Figure 3.3B).

A possible explanation could be the shift in the response gain at the level of lobula plate tangential cells in behaving flies (Chiappe et al., 2010; Maimon et al., 2010; Jung et al., 2011) making them possibly more sensitive for ChR2(C128S) activation. Experiments in wild type flies (section 3.1) corroborates that flies able to move only their heads are in a calmer behavioural state than flying flies. This might result in a lower resting potential of the HS-cells when compared with HS-cells in flying flies. Since HS-cells were not recorded during the experiments this is only a speculative conclusion.

Yaw Turns Do Not End When the HS-cell Membrane Potential Returns to Baseline

For head yaw movements flies did not return their head to baseline level after a yellow light pulse was applied (Figure 3.2 A_i - C_i, right part). According to patch clamp recordings (Figure 2.9) yellow light did reliably close the channels. The same could also be observed for visually elicited yaw head responses, i.e. flies did not return their head to baseline level after visual stimulation in one direction (Figure 3.2 A_i and C_i, left part), ruling out an artifact of optogenetic activation.

This observation could be explained by the fact that flies were not allowed to actually turn or move neither wings nor halteres. Under these experimental conditions the yaw head movements were smooth and continuous whereas when flies were allowed to beat their wings and halteres the head yaw movements presented saccadic movements. This suggests, together with the presented results, that HS-cells only elicit following head yaw movements and another signal is necessary to return the head to baseline level.

The above could also be observed for tethered flying flies. Neither after visual stimulation nor after closing of the ChR2(C128S) channels with yellow light did flies return to a straight flight course (Figure 3.3). Increasing and decreasing haltere movement has an effect on the saccadic behaviour observed in tethered flight when the fly is able to physically turn (Bender and Dickinson, 2006a). This hints towards visual information triggering turns and self motion detected by the halteres controlling the termination of the turns.

Strong Responses to Optogenetic Activation of Blind Flies

Optogenetic activation of HS-cells resulted in stronger responses in blind flies as compared with visually intact flies (compare Figure 3.2A with B).

This could be an artifact produced by the optogenetic stimulation. Visually intact flies also responded to the blue light stimulus giving rise to a competing reaction which might have attenuated the effect of HS-cell depolarization. Another possible explanation for the weaker responses elicited in visually intact flies in comparison to blind flies, could be that stationary visual signals from the inactive arena provided stable reference points antagonizing the effect of HS-cell



activation.

Closer inspection of the reactions might allow for separating the response to blue light and the response elicited by HS-cell depolarization. Using patch clamp recordings in HS-cells, it is possible to observe that, when using blue light, the onset of the opening of the channels and the input from the photoreceptors are separated by approximately 10 ms (experiments performed by Alex Mauss). During this time window the behaviour should be free of artifacts produced by the blue light. An analysis of the dynamics in optomotor responses would be interesting. However, for head yaw detection a frame rate of 30 frames per second was used which is too slow to separate the two responses. During tethered flight the fly flaps its wings twice during the 10 ms time window which makes it difficult to separate both responses simply analyzing the mean traces.

***DB331* Flies Responded More Strongly to Blue Light Than *R27B03* Flies**

DB331 flies responded more strongly to blue light than *R27B03* flies. One reason is the much higher expression level of ChR2(C128S) in the HS-cells when using *DB331* as Gal4 driver instead of *R27B03*. Second, the Gal4 expression of *DB331-Gal4* is not specific for HS-cells. In the lobula plate Gal4 is expressed apart from HS-cells also in VS-cells. This might indirectly enhance the effect of optogenetic activation of HS-cells. VS-cells might additionally also elicit yaw turning responses themselves. It is also not possible to rule out cells extrinsic to the lobula plate contributing to the response strength. Again, since cells were not recorded during the experiments this is only a speculative conclusion.

Apart from higher and unspecific expression level, the above can also partly be explained by the stronger responses to visual stimuli of *DB331* than *R27B03* flies observed for head yaw movements and tethered flight experiments (compare Figure 3.2A with C and Figure 3.3A with C).

Remarks

While all three HS-cells were stimulated as a functional unit it is not necessarily the case that they are functionally equivalent. For instance, HS-cells can be distinguished by their receptive fields both in elevation and azimuth (Hausen, 1982;

Schnell et al., 2010). While HSN responds best to optic flow in dorsal retinal locations, HSE and HSS are tuned to motion mostly in horizontal and ventral parts in the visual field, respectively. Moreover, HSN and HSE receive contralateral input rendering them particularly sensitive for yaw rotation. In contrast, HSS lacks contralateral input. This might be the reason why among the HS-cells HSS encodes translation-related optic flow parameters that could be utilized for estimating distance (Karmeier et al., 2005; Liang et al., 2012). By refining the specificity of genetic driver lines to be able to manipulate one HS-cell at a time it should be feasible to dissect such functional specializations in the future.

These experiments do not yield the whole picture and they do not insinuate that every time HS-cells are depolarized the fly turns to the stimulated side. If this were so, flies could for example not fly close to a wall. The optic flow produced by the wall would elicit a turning response towards the wall. If the fly was not willing to land it would crash. This problem could be resolved by using a second more important mechanism for flight course stabilization. In closed loop, allowing the fly to control the position of a stripe, a fixation of the stripe can be observed, i.e. flies try to fly or walk towards the stripe (Reichardt and Wenking, 1969; Wehner, 1972; Bahl et al., 2013). Following movements of a pattern and fixation behaviour are controlled by different neuronal pathways. When blocking T4 and T5 neurons using *shibire* (blocking the input to HS-cells), flies are not able to follow whole-field visual motion (Bahl et al., 2013). Flies, however, still are able to fixate a stripe. When a fly is fixating a stripe in closed loop and additionally a whole-field stimulus is presented in the surrounding, the stripe is not fixed in front of the fly but slightly shifted in the direction of the whole-field motion. This indicates that both mechanisms are active at the same time. Both observations make it feasible, that flies primarily fixate an object during straight flight and only if the object is lost, e.g. due to a gust of wind, do flies rely on the optomotor response elicited by the HS-cells. Additional evidence for this hypothesis exists. When *Drosophila* is presented an expanding visual flow field it turns away from it. This turning behaviour away from the expanding visual stimulus can be overwritten when placing an object in the focus of the expanding pattern (Reiser and Dickinson, 2010).



4.3 Role of HS-cell Receptive Field Layout for Yaw Optomotor Behaviour 87

4.3 Role of HS-cell Receptive Field Layout for Yaw Optomotor Behaviour

Cutting HS-cell axons in adult flies (Hausen and Wehrhahn, 1983) or laser ablation of HS precursor cells in larvae (Geiger and Nässel, 1981) significantly affects the optomotor responses of adult flies. Using these methods it is possible to show that HS-cells are part of the sensory-motor pathway, but only allow to study the system when the complete pathway is disrupted. Thus, it is not possible to infer specific functions of the HS-cell within the network. In this work, flies with modified dendritic anatomy in HS-cells were used. Those changes in the anatomy come with modified HS-cell receptive field layout and, thus, allowed to investigate the detailed role of the HS-cell receptive field layout for optomotor responses.

During development Dscams play an important role in achieving the specific structure of the visual ganglia (Fuerst et al., 2008; Fuerst et al., 2009). Through alternative splicing the *Dscam1* gene can encode for a vast number of *Dscam1* isoforms. Different combinations of *Dscam1* isoforms give each neuron its own identity. When two identical *Dscam1* isoforms on opposing membranes bind, a repulsion of the membranes follows and self-avoidance is achieved. Considering the complex neuronal wiring of the visual system it is not surprising that a single *Dscam1* isoform gain-of-function (D(GOF)) on HS-cells has an effect on the morphology of HS-cells. D(GOF) HS-cells show a reduced dendritic spanning field. Electrophysiological recordings indicate that these anatomical defects are accompanied by a reduction in HS-cell sensitivity to motion in the frontal region and an enhancement of sensitivity in the lateral region of the fly's visual field of view. D(GOF) HS-cell responses to whole-field visual stimuli are not affected when compared to control HS-cell responses. In summary, D(GOF) have functional HS-cells which differ from control HS-cells in their smaller receptive fields. Thus, analysis of D(GOF) optomotor responses provides an adequate approach for investigating the role of HS-cell receptive fields for optomotor responses.

D(GOF) flies were compared to control flies in terms of optomotor response. Patch clamp recordings in fixed flies performed by Bettina Schnell had shown that D(GOF) HS-cells have a reduced sensitivity to motion in the frontal region and enhanced sensitivity to motion in the lateral field of view. The behaviour

setup did not allow simultaneous electrical cell recordings during behaviour and it was not possible to show that D(GOF) and control HS-cells in behaving flies presented the same difference in HS-cell responses as measured in immobilized flies. Although fly activity modulates the temporal frequency curves of lobula plate tangential cells (Chiappe et al., 2010; Jung et al., 2011) the global direction sensitivity remains unchanged (Maimon et al., 2010). Thus, it was assumed that the receptive field properties of HS-cells were unchanged during the behavioural experiments.

4.3.1 Changes in HS-cell Receptive Fields Modify Turning Behaviour in Tethered Flying Flies

First, optomotor responses of tethered flying flies were analyzed. Since D(GOF) HS-cells were less sensitive in the frontal region of visual space unilateral stimulation was expected to elicit weaker responses in D(GOF) flies than in control flies. HS-cells have a binocular overlap, i.e. the contralateral HS-cells respond to motion on the ipsilateral side in the frontal field of view. Since the effect of Dscam gain-of-function on HS-cells was variable among both hemispheres of the same fly, the possible reduction in optomotor responses might have been compensated by an HS-cell not affected by the Dscam gain-of-function on the contralateral side. To eliminate the participation of HS-cells of the contralateral side, the frontal region (0° to 15° ; (Schnell et al., 2010)) of the unilateral stimuli was omitted for the first stimuli.

Responses to Motion With Different Pattern Contrast

Presenting a square wave grating with different pattern contrast served to analyze how flies performed when the input to the HS-cells got stronger (Schnell et al., 2010). At low contrasts, control and D(GOF) flies responded equally well. For higher contrasts the responses of control and D(GOF) flies saturated at a different level. D(GOF) fly responses amounted to only about 50 % of control fly optomotor strength (Figure 3.4A).

The weak responses (about 3°) of D(GOF) flies to pattern motion with high contrast cannot be attributed to any motor deficiency. D(GOF) flies were able to



4.3 Role of HS-cell Receptive Field Layout for Yaw Optomotor Behaviour 89

respond as strongly as for 5° , as can be observed in the response strengths to a square wave grating restricted to an azimuth extension of 33° centered at 33° in azimuth (Figure 3.4D).

Why did D(GOF) flies respond as strongly as control flies to pattern motion with low contrast and much weaker to pattern motion with high contrast? This could be a consequence of the neuronal network and participation of other cells in optomotor responses. In flying tethered flies the responses to front-to-back motion increase with increasing pattern contrast. For back-to-front visual motion the optomotor responses decrease with increasing pattern contrast. In contrast to responses to front-to-back motion, responses to back-to-front motion also exhibit a slower onset in wing and head steering that peak at low contrasts (Duistermars et al., 2012). These differences in response characteristics between front-to-back and back-to-front visual stimulation suggests that these responses involve also different cells.

It would be interesting to analyze the responses elicited with front-to-back and back-to-front motion in more detail. Since in these experiments front-to-back and back-to-front visual motion was presented consecutively it is difficult to separate both responses. The response elicited by back-to-front motion always incorporates part of the response elicited with front-to-back motion. Detailed analysis could indicate whether responses to motion in only one direction or both directions of rotation were affected in D(GOF).

Optomotor Responses to Motion at Different Angles of Elevation

Flying control flies responded to motion presented at different elevations qualitatively similarly to wild type flies (compare Figure 3.4C to figure 3.1A or to (Duistermars et al., 2007)). Compared with the response strength of control flies, flying D(GOF) flies presented weaker responses at every elevation tested (Figure 3.4C). The most significant reduction was observed when the grating was presented at the equator (square waved pattern centered at 6° and -6° in elevation). Responses to motion at lower elevations centered at -26° and -35° showed no statistically significant reduction (two-sided Mann-Whitney-U test).

The largest reduction at the equator might be explained considering that in this

region all three HS-cells show directional sensitivity and participate in eliciting yaw optomotor responses (refer to section 3.1). Since a *Dscam* gain-of-function on HS-cells did not always reduce the the HS-cell size to the same extent, the probability of having more than one cell with greatly reduced dendrites participating in the yaw response is largest in the equatorial region. In the upper visual field ($>10^\circ$ in elevation) only HSE and HSN participate in the yaw response. This makes it less likely to have two cells with deficits. This should also apply for the lower visual field. However, the cells that participate in this region are the HSE and HSS of which only HSE showed a strong reduction in cell responses (Figure 2.11C and D).

If the lobula plate network in *Drosophila* is similar to the network described for *Calliphora vicina*, then another possible reason arises for the weak reduction in optomotor strength in the lower region. HSS-cells do not get any input from other lobula plate tangential cells whereas HSE and HSN receive excitatory input from the contralateral H1-cell (Borst et al., 2010). H1-cells have been identified in *Drosophila* (Bausenwein et al., 1990). Thus, it is possible that a similar connection exists also in *Drosophila*. This could indicate that the reduction in optomotor responses observed for visual motion in the dorsal part of visual space is also a product of a modified cell-network.

Optomotor Responses to Motion at Different Azimuth Angles

For the last experiment a squared wave grating extending 33° in azimuth and the whole elevation was presented at different azimuth angles to the fly. These stimuli were used in order to possibly reveal the existence of differences in optomotor responses in the frontal and rear part of visual field as observed for HS-cell responses (Figure 2.11). Visual stimulation restricted to the frontal part of visual space elicited the strongest responses in control and D(GOF) flies. Motion in the rear part of visual space (165°) elicited weak negative optomotor responses in both flies (Figure 3.4D).

The lack of significant reduction in the frontal region was unexpected. It is possible that in this region together with HS-cells also other cells elicit optomotor responses. In blow flies, the comparison of optomotor responses with HSE-cell



4.3 Role of HS-cell Receptive Field Layout for Yaw Optomotor Behaviour 91

responses has shown both to be qualitatively similar for several visual stimuli. The only exception found is for visual stimulation at different azimuth angles (Hausen and Wehrhahn, 1989). For visual stimulation at different azimuth angles also other cells, the figure detection cells (FD-cells), need to be accounted for. Although FD-cells have not been identified in *Drosophila*, it is possible that *Drosophila* also uses other cells when controlling optomotor responses to visual stimuli at different azimuth angles.

Responses to a Whole-field Stimulus When Painting One Eye Black

The responses to whole-field stimuli of control and D(GOF) flies with one eye painted black were compared. Since flies had one eye painted black only HS-cells on one hemisphere were stimulated. D(GOF) flies performed equally well for a bilateral whole-field motion when able to use both eyes and with one eye painted black. Control flies showed stronger responses to a whole-field stimulus when only using one of their eyes (compare Figure 3.4B with Figure 3.5C).

Wild type flies show stronger responses to unilateral front-to-back visual motion compared to bilateral motion (Duistermars et al., 2012). The presented experiment suggests that the frontal region of the HS-cells, where D(GOF) flies have strongly reduced sensitivity to motion, plays an important role for this behaviour.

Optomotor Responses to Motion In Front of the Flies

Since one eye of the fly was painted black it was possible to present motion restricted to the frontal region of the fly's visual space. D(GOF) HS-cells in this region, when compared to control HS-cells, have strongly reduced sensitivity to motion. Visual motion in this region was expected to elicit, when compared to control flies, much weaker following responses of D(GOF) flies. D(GOF) flies, however, showed robust following movements to visual motion in the frontal region of field of view (Figure 3.5A).

As discussed above, this could be explained if the FD1-cell sensitive to motion in the frontal region also controls optomotor responses.

Another possible explanation arises when considering that flying flies with missing HS-cell (Geiger and Nässel, 1981) and walking flies in which the input to

HS-cells has been blocked (Bahl et al., 2013) are still able to follow a stripe. Considering the HS-cell overlap, flies in this experiment were able to see the square wave grating extending 30° in azimuth (from -15° to 15°). Since the square wave grating had a spatial wavelength of about 24° , the flies perceived practically only a stripe. This could lead to a fixation of a stripe rather than a following movement, thus, explaining the robust responses to motion in the frontal field of view of D(GOF) flies.

Effect of Motion in the Rear Part of Visual Space on Optomotor Responses

The responses to motion in the frontal field of view (-30° to 90°) and responses to motion extending -30° to 165° in azimuth were compared. The incorporation of the rear part (90° to 165°) reduced the response strength of control flies significantly (Figure 3.5A, blue curve; two-sided Mann-Whitney-U test $P = 0.03$). This is consistent with motion in the rear part of visual space in wild type flies generating counter directional turning responses (Tammero et al., 2004). For D(GOF) flies the incorporation of visual motion in the rear part of visual space did not reduce the responses as observed for control flies (Figure 3.5A, red curve; two-sided Mann-Whitney-U test $P = 0.9$).

The weaker responses to visual stimuli in the rear part of visual field could simply be because of the stronger cell responses of D(GOF) HS-cells in the lateral part of visual space eliciting stronger responses. However, D(GOF) and control HS-cell responses to whole-field motion were qualitatively similar. It would be expected that the HS-cell responses are already saturated when presenting visual motion between azimuth angles of -30° and 90° and incorporating the rear part should not additionally enhance the response strength of HS-cells. This indicates that the anatomy / receptive field layout of the D(GOF) HS-cells plays an important role in the observed responses.

Effect of Motion in the Rear and Frontal Part of Visual Space on Optomotor Responses

Responses to visual motion extending from 22.5° to 157.5° in azimuth were compared with responses to motion extending from 0° to 180° in azimuth. Control



4.3 Role of HS-cell Receptive Field Layout for Yaw Optomotor Behaviour 93

flies responded equally strong to both visual stimuli (Figure 3.5B, blue curve; two-sided Mann-Whitney-U test for control $P = 0.5$). D(GOF) flies responded more strongly to the stimuli extending over the entire hemisphere of the fly visual field (Figure 3.5B, red curve; two-sided Mann-Whitney-U test $P = 0.05$).

The incorporation of the frontal field of view had a large effect on optomotor responses of D(GOF) flies. As discussed above, this suggests that also other cells sensitive to visual motion in the frontal field of view participate in controlling optomotor responses.

4.3.2 Changes in HS-cell Receptive Fields Modify Head Yaw Movements

Since HS-cells also control head yaw movements, D(GOF) flies, when compared to control flies, were expected to show modified head yaw responses. Analyzing head yaw movements had two advantages over tethered flight. First, since almost all flies present robust head yaw movements, analysis is much faster than when using flying flies which not always like to fly. Second, as discussed in section 4.1, HS-cell responses in fixed flies only moving their head might be more alike to HS-cell responses of immobilized flies than of flying flies.

To compare the difference in HS-cell responses with a possible difference in optomotor responses, a receptive field for behaviour was calculated. Since during head yaw movements only HSE and HSN seem to be participating in optomotor responses (discussed in section 4.1) only the receptive fields of HSE and HSN were considered for analysis. The participation of each HS-cell in the optomotor responses was considered to be linear which allowed to add both receptive fields.

Responses to Whole-Field Stimuli

Before each trial, a whole-field stimulus rotating in both directions was presented to the flies. D(GOF) flies seemed to respond more strongly to the visual stimulus. Analysis of the responses however indicated that the differences observed were not statistically different ($P = 0.4$ for ND- and PD-stimulus trials, Figure 3.8). This is consistent with experiments in flying flies where no evident difference in behaviour could be observed for a whole-field stimulus.

Responses to Motion in the Rear Part of Visual Space

When presenting the ND- and PD-stimulus, flies started to turn their head before the edge of the visual stimulus had reached an angle of 100° respect to the head of the fly. For both stimuli these following movements were in the back-to-front direction.

HS-cells are sensitive to motion for azimuth angles roughly up to 100° (Schnell et al., 2010). This suggests that also other cells participate in head yaw movements. The following movements were in back-to-front direction, which suggests that the cells eliciting these responses to motion in the rear part of visual field are sensitive to motion in the back-to-front direction as well. These could be the H1 and H2 cells, of which H1 has been identified in *Drosophila* (Bausenwein et al., 1990). In blowflies, the H1-cell receives indirect inhibitory input through CH-cells from the HS-cells and additionally direct inhibitory input from the HSE-cell on the ipsilateral side. H1-cells give direct and through CH-cells indirect excitatory input to the HSE- and HSN-cell on the contralateral side (Borst et al., 2010). In *Calliphora vicina*, H1-cells have a broad receptive field (about 0° to 150°) responding to back-to-front motion (Krapp et al., 2001).

In blow flies (Haag et al., 2010) three muscles controlling yaw head movements receive input from the ventral cervical nerve, comprised of the axons of three motor neurons, which in turn receive visual input from two of the three HS-cells (HSE and HSN). If *Drosophila* uses the same optomotor pathway for head yaw movements, then during back-to-front motion the hyperpolarization of the ipsilateral HSE- and HSN-cell relaxes the muscles on the ipsilateral side. The excitatory input of the H1-cell excites the contralateral HSE- and HSN-cell which in turn contracts the muscles of the contralateral side.

Comparison of the Difference in Receptive Fields of HS-cells and Yaw Head Movements of Control and D(GOF) Flies

For the PD- and ND-stimuli the difference in behaviour of control and D(GOF) flies were similar (Figure 3.10). During the first part of both stimuli, when the square wave grating was revealed to the flies in the region in which D(GOF) HS-cell responses were stronger than control HS-cell responses, D(GOF) flies



4.3 Role of HS-cell Receptive Field Layout for Yaw Optomotor Behaviour 95

followed the pattern more weakly than control flies. When the square wave pattern was additionally revealed to one of the eyes of the fly in the region in which D(GOF) HS-cells are less sensitive to motion than control HS-cells, D(GOF) flies started to follow the grating motion more strongly than control flies. The opposite was observed when revealing the square wave grating also to the other hemisphere of the fly. When motion was presented in the frontal field of view, D(GOF) followed the pattern motion more weakly than control flies. Motion in the lateral part of visual space elicited stronger responses for D(GOF) flies than control flies. Thus, the difference in the receptive field layout of control and D(GOF) flies correlated inversely with the difference in head yaw movement of control and D(GOF) flies during the first half of both stimuli and correlated during the second half of both stimuli.

During the first part of the ND-stimulus, one eye of the fly perceived increasing back-to-front motion. The second half of the ND-stimulus consists of increasing front-to-back visual motion. This suggests that the difference of D(GOF) and control HS-cell receptive field layout correlates with the difference in head yaw movements for front-to-back pattern motion. For back-to-front motion an inverse correlation was found. This could be explained if considering that HS-cells control head yaw movement only in the preferred direction and for back to front motion the optomotor responses are elicited by the H1-cells.

However, the opposite was observed for the PD-stimulus, which consisted of front-to-back motion in the first half of the stimulus and back-to-front motion in the second half. Thus, a positive correlation would have been expected during the first half of the PD-stimulus. This contradiction might be explained by the curtain edge, moving in the opposite direction as the square wave pattern, eliciting stronger responses than the square wave pattern.

Another observation is that during the first half of both stimuli the fly was stimulated unilaterally whereas during the second half the stimulation was bilateral. Thus, it could be that the difference of D(GOF) and control HS-cell receptive field layouts only correlates with the difference of their head yaw movements for bilateral motion and correlates inversely for unilateral motion.

4.4 Conclusions

The introduction of ChR2(C128S) in *Drosophila* enabled to study for the first time the sufficiency of HS-cells in intact seeing flies, producing reduced artifacts by the optogenetic activation. Optimizing light delivery for the optogenetic activation might reduce these artifacts. In the future, this tool can be used to test the sufficiency of other cells for optomotor responses.

HS-cells control head yaw movements and turning responses during flight towards the preferred direction of the HS-cells. The turning responses are not stopped after the membrane potential of HS-cells returns to baseline level. Thus, other sensory input, e.g. information from the halteres, must trigger the ending of the turns.

Drosophila and blow flies probably use a similar visuo-motor pathway for head yaw movements. For motion in the front-to-back direction, HS-cells of the ipsilateral side contract the ipsilateral neck muscles and the fly turns its head following the visual motion. For motion in the opposite direction H1-cells get activated and excite contralateral HS-cells. These contract the contralateral neck muscles and the fly turns its head following the visual motion. For the interaction between H1-cells and HS-cells, the layout of the receptive fields of HS-cells plays an important role since flies with modified HS-cell receptive fields display modified head yaw movements.

Flying tethered flies use all three HS-cells and other cells sensitive to visual motion in the frontal part of visual space for flight course control. Counter turns to visual motion in the rear part of visual space were significantly reduced in D(GOF) flies. This could be due to changed interactions between H1 and HS-cells produced by the modified HS-cells anatomy / receptive field layout.

The experiments performed in this work provide an insight into the complex system flies rely on to perform correct flight maneuvers. Yaw optomotor responses seem to be controlled by the combined responses of H1- and HS-cells. Thus, to obtain a detailed view of yaw turning responses, the role of H1-cells for optomotor responses should be studied in the future. Additionally, the role of the receptive field in the interaction between HS- and H1-cells needs to be investigated in detail.

Bibliography

Arenkiel, B. R., Peca, J., Davison, I. G., Feliciano, C., Deisseroth, K., Augustine, G. J., Ehlers, M. D. and Feng, G. (2007). In vivo light-induced activation of neural circuitry in transgenic mice expressing channelrhodopsin-2. *Neuron* 54, 205–218.

Arrenberg, A. B., Stainier, D. Y., Baier, H. and Huisken, J. (2010). Optogenetic control of cardiac function. *Science* 330, 971–974.

Bahl, A., Ammer, G., Schilling, T. and Borst, A. (2013). Object tracking in motion-blind flies. *Nat. Neurosci.* 16, 730–738.

Bausenwein, B., Buchner, E. and Heisenberg, M. (1990). Identification of H1 visual interneuron in *Drosophila* by [3H]2-deoxyglucose uptake during stationary flight. *Brain Res.* 509, 134–136.

Bender, J. A. and Dickinson, M. H. (2006a). A comparison of visual and haltere-mediated feedback in the control of body saccades in *Drosophila melanogaster*. *J. Exp. Biol.* 209, 4597–4606.

Bender, J. A. and Dickinson, M. H. (2006b). Visual stimulation of saccades in magnetically tethered *Drosophila*. *J. Exp. Biol.* 209, 3170–3182.

Berndt, A., Yizhar, O., Gunaydin, L. A., Hegemann, P. and Deisseroth, K. (2009). Bi-stable neural state switches. *Nat. Neurosci.* 12, 229–234.

Bishop, L. G. and Keehn, D. G. (1967). Neural correlates of the optomotor response in the fly. *Biol. Cybern.* 3, 288–295.

- Blondeau, J. (1981a). Aerodynamic Capabilities of Flies, as Revealed by a New Technique. *J. Exp. Bio.* 92, 155–163.
- Blondeau, J. (1981b). Electrically evoked course control in the fly *Calliphora erythrocephala*. *J. Exp. Bio.* 92, 143–153.
- Blondeau, J. and Heisenberg, M. (1982). The three-dimensional optomotor torque system of *Drosophila melanogaster*. *J. Comp. Physiol. A* 145, 321–329.
- Borst, A. (1986). Time Course of the Houseflies' Landing Response. *Biol. Cybern.* 54, 379–383.
- Borst, A. (2009). *Drosophila's* view on insect vision. *Curr. Biol.* 19, 36–47.
- Borst, A., Egelhaaf, M. and Haag, J. (1995). Mechanisms of dendritic integration underlying gain control in fly motion-sensitive interneurons. *J. Comput. Neurosci.* 2, 5–18.
- Borst, A. and Euler, T. (2011). Seeing things in motion: models, circuits, and mechanisms. *Neuron* 71, 974–994.
- Borst, A. and Haag, J. (2002). Neural networks in the cockpit of the fly. *J. Comp. Physiol. A* 188, 419–437.
- Borst, A., Haag, J. and Reiff, D. F. (2010). Fly motion vision. *Annu. Rev. Neurosci.* 33, 49–70.
- Brotz, T. M., Gundelfinger, E. D. and Borst, A. (2001). Cholinergic and GABAergic pathways in fly motion vision. *BMC Neurosci* 2, 1.
- Buchner, E. (1976). Elementary detectors for vertical movement in the visual system of *Drosophila*. *Biol. Cybern.* 24, 85–101.
- Buchner, E., Buchner, S. and Bülthoff, I. (1984). Deoxyglucose mapping of nervous activity induced in *Drosophila* brain by visual movement. *J. Comp. Physiol. A* 155, 471–483.
- Card, G. and Dickinson, M. (2008). Performance trade-offs in the flight initiation of *Drosophila*. *J. Exp. Biol.* 211, 341–353.

Chiappe, M. E., Seelig, J. D., Reiser, M. B. and Jayaraman, V. (2010). Walking modulates speed sensitivity in *Drosophila* motion vision. *Curr. Biol.* *20*, 1470–1475.

Clark, D. A., Bursztyn, L., Horowitz, M. A., Schnitzer, M. J. and Clandinin, T. R. (2011). Defining the computational structure of the motion detector in *Drosophila*. *Neuron* *70*, 1165–1177.

Collett, T. S. and Land, M. F. (1975). Visual Control of Flight Behaviour in the Hoverfly, *Syritta pipiens* L. *J. Comp. Physiol.* *99*, 1–66.

de Vries, S. E. and Clandinin, T. R. (2012). Loom-sensitive neurons link computation to action in the *Drosophila* visual system. *Curr. Biol.* *22*, 353–362.

Dickinson, M. H. and Gotz, K. G. (1996a). The wake dynamics and flight forces of the fruit fly *Drosophila melanogaster*. *J. Exp. Biol.* *199*, 2085–2104.

Dickinson, M. H. and Gotz, K. G. (1996b). The wake dynamics and flight forces of the fruit fly *Drosophila melanogaster*. *J. Exp. Biol.* *199*, 2085–2104.

Douglass, A. D., Kraves, S., Deisseroth, K., Schier, A. F. and Engert, F. (2008). Escape behavior elicited by single, channelrhodopsin-2-evoked spikes in zebrafish somatosensory neurons. *Curr. Biol.* *18*, 1133–1137.

Dugue, G. P., Akemann, W. and Knopfel, T. (2012). A comprehensive concept of optogenetics. *Prog. Brain Res.* *196*, 1–28.

Duistermars, B. J., Care, R. A. and Frye, M. A. (2012). Binocular interactions underlying the classic optomotor responses of flying flies. *Front. Behav. Neurosci.* *6*, 6.

Duistermars, B. J., Chow, D. M., Condro, M. and Frye, M. A. (2007). The spatial, temporal and contrast properties of expansion and rotation flight optomotor responses in *Drosophila*. *J. Exp. Biol.* *210*, 3218–3227.

Egelhaaf, M. (1989). Visual afferences to flight steering muscles controlling optomotor responses of the fly. *J. Comp. Physiol. A* *165*, 719–730.

Egelhaaf, M. (2009). Insect Motion Vision. *Scholarpedia of Computational Neuroscience* 4, (11):1671.

Egelhaaf, M., Borst, A. and Reichardt, W. (1989). Computational structure of a biological motion-detection system as revealed by local detector analysis in the fly's nervous system. *J. Opt. Soc. Am. A* 6, 1070–1087.

Fermi, G. and Reichardt, W. (1963). Optomotorische Reaktionen der Fliege *Musca Domestica*. *Biol. Cybern.* 2, 15–28.

Fischbach, K. F. and Dittrich, A. (1989). The optic lobe of *Drosophila melanogaster* I. A Golgi analysis of wild-type structure. *Cell Tissue Res.* 258, 441–475.

Fry, S. N., Sayaman, R. and Dickinson, M. H. (2003). The aerodynamics of free-flight maneuvers in *Drosophila*. *Science* 300, 495–498.

Fuerst, P. G., Bruce, F., Tian, M., Wei, W., Elstrott, J., Feller, M. B., Erskine, L., Singer, J. H. and Burgess, R. W. (2009). DSCAM and DSCAML1 function in self-avoidance in multiple cell types in the developing mouse retina. *Neuron* 64, 484–497.

Fuerst, P. G., Koizumi, A., Masland, R. H. and Burgess, R. W. (2008). Neurite arborization and mosaic spacing in the mouse retina require DSCAM. *Nature* 451, 470–474.

Gabbiani, F. and Jones, P. W. (2011). A genetic push to understand motion detection. *Neuron* 70, 1023–1025.

Gao, S., Takemura, S. Y., Ting, C. Y., Huang, S., Lu, Z., Luan, H., Rister, J., Thum, A. S., Yang, M., Hong, S. T., Wang, J. W., Odenwald, W. F., White, B. H., Meinertzhagen, I. A. and Lee, C. H. (2008). The neural substrate of spectral preference in *Drosophila*. *Neuron* 60, 328–342.

Geiger, G. and Nässel, D. R. (1981). Visual orientation behaviour of flies after selective laser beam ablation of interneurons. *Nature* 293, 398–399.

- Götz, K. G. (1964). Optomotorische Untersuchung des visuellen systems einiger Augenmutanten der Fruchtfliege *Drosophila*. *Kybernetik* 2, 77–92.
- Götz, K. G. (1965). Die optischen Übertragungseigenschaften der Komplexaugen von *Drosophila*. *Biol. Cybern.* 2, 215–221.
- Götz, K. G. (1968). Flight control in *Drosophila* by visual perception of motion. *Kybernetik* 4, 199–208.
- Götz, K. G. (1975). The Optomotor Equilibrium of the *Drosophila* Navigation System. *J. Comp. Physiol.* 99, 187–210.
- Götz, K. G. (1987). Course-control, metabolism and wing interference during ultralong tethered flight in *Drosophila melanogaster*. *J. Exp. Biol.* 128, 35–46.
- Götz, K. G., Hengstenberg, B. and Biesinger, R. (1979). Optomotor control of wing beat and body posture in *Drosophila*. *Biol. Cybern.* 35, 101–112.
- Götz, K. G. and Wenking, H. (1973). Visual control of locomotion in the walking fruitfly *Drosophila*. *J. Comp. Physiol.* 85, 235–266.
- Gronenberg, W. and Strausfeld, N. J. (1990). Descending neurons supplying the neck and flight motor of Diptera: physiological and anatomical characteristics. *J. Comp. Neurol.* 302, 973–991.
- Gunaydin, L. A., Yizhar, O., Berndt, A., Sohal, V. S., Deisseroth, K. and Hegemann, P. (2010). Ultrafast optogenetic control. *Nat. Neurosci.* 13, 387–392.
- Haag, J. and Borst, A. (2004). Neural mechanism underlying complex receptive field properties of motion-sensitive interneurons. *Nat. Neurosci.* 7, 628–634.
- Haag, J., Wertz, A. and Borst, A. (2010). Central gating of fly optomotor response. *Proc. Natl. Acad. Sci. U.S.A.* 107, 20104–20109.
- Haikala, V., Joesch, M., Borst, A. and Mauss, A. S. (2013). Optogenetic control of fly optomotor responses. *J. Neurosci.* 33, 13927–13934.
- Hardie, R. C. and Franze, K. (2012). Photomechanical responses in *Drosophila* photoreceptors. *Science* 338, 260–263.

Hardie, R. C. and Raghu, P. (2001). Visual transduction in *Drosophila*. *Nature* 413, 186–193.

Hassenstein, B. and Reichardt, W. (1956). Systemtheoretische analyse der zeit-, reihenfolgen-und vorzeichenbewertung bei der bewegungsperzeption des rüsselkäfers *chlorophanus*. *Z. Naturforsch* 11, 513–524.

Hateren, J. H. and Schilstra, C. (1999). Blowfly flight and optic flow. II. Head movements during flight. *J. Exp. Biol.* 202 (Pt 11), 1491–1500.

Hattori, D., Demir, E., Kim, H. W., Viragh, E., Zipursky, S. L. and Dickson, B. J. (2007). Dscam diversity is essential for neuronal wiring and self-recognition. *Nature* 449, 223–227.

Hattori, D., Millard, S. S., Wojtowicz, W. M. and Zipursky, S. L. (2008). Dscam-mediated cell recognition regulates neural circuit formation. *Annu. Rev. Cell Dev. Biol.* 24, 597–620.

Hausen, K. (1982). Motion sensitive interneurons in the optomotor system of the fly: II. The Horizontal Cells: Receptive Field Organization and Response Characteristics. *Biol. Cybern.* 46, 6779.

Hausen, K. and Wehrhahn, C. (1983). Microsurgical lesion of horizontal cells changes optomotor yaw responses in the blowfly *Calliphora erythrocephala*. *Proc. R. Soc. Lond. B* 219, 211–216.

Hausen, K. and Wehrhahn, C. (1989). Neural circuits mediating visual flight control in flies. I. Quantitative comparison of neural and behavioral response characteristics. *J. Neurosci.* 9, 3828–3836.

Hegemann, P. (2008). Algal sensory photoreceptors. *Annu. Rev. Plant. Biol.* 59, 167–189.

Heisenberg, M., Wonneberger, R. and Wolf, R. (1978). Optomotor-blindH31 – a *Drosophila* mutant of the lobula plate giant neurons. *J. Comp. Physiol.* 124, 287–296.

Hengstenberg, R. (1993). Multisensory control in insect oculomotor systems. *Rev. Oculomot. Res.* 5, 285–298.

Hotta, Y. and Benzer, S. (1970). Genetic dissection of the *Drosophila* nervous system by means of mosaics. *Proc. Natl. Acad. Sci. U.S.A.* 67, 1156–1163.

Huang, J., Liu, C. H., Hughes, S. A., Postma, M., Schwiening, C. J. and Hardie, R. C. (2010). Activation of TRP channels by protons and phosphoinositide depletion in *Drosophila* photoreceptors. *Curr. Biol.* 20, 189–197.

Joesch, M., Plett, J., Borst, A. and Reiff, D. F. (2008). Response properties of motion-sensitive visual interneurons in the lobula plate of *Drosophila melanogaster*. *Curr. Biol.* 18, 368–374.

Joesch, M., Schnell, B., Raghu, S. V., Reiff, D. F. and Borst, A. (2010). ON and OFF pathways in *Drosophila* motion vision. *Nature* 468, 300–304.

Jung, S. N., Borst, A. and Haag, J. (2011). Flight activity alters velocity tuning of fly motion-sensitive neurons. *J. Neurosci.* 31, 9231–9237.

Karmeier, K., Krapp, H. G. and Egelhaaf, M. (2005). Population coding of self-motion: applying bayesian analysis to a population of visual interneurons in the fly. *J. Neurophysiol.* 94, 2182–2194.

Kern, R. and Egelhaaf, M. (2000). Optomotor course control in flies with largely asymmetric visual input. *J. Comp. Physiol. A* 186, 45–55.

Krapp, H. G., Hengstenberg, R. and Egelhaaf, M. (2001). Binocular contributions to optic flow processing in the fly visual system. *J. Neurophysiol.* 85, 724–734.

Land, M. (1993). Chasing and pursuit in the dolichopodid fly *Poecilobothrus nobilitatus*. *J. Comp. Physiol. A* 173, 605–613.

Laughlin, S. B., Howard, J. and Blakeslee, B. (1987). Synaptic limitations to contrast coding in the retina of the blowfly *Calliphora*. *Proc. R. Soc. Lond. B* 231, 437–467.

Liang, P., Heitwerth, J., Kern, R., Kurtz, R. and Egelhaaf, M. (2012). Object representation and distance encoding in three-dimensional environments by a neural circuit in the visual system of the blowfly. *J. Neurophysiol.* *107*, 3446–3457.

Maimon, G., Straw, A. D. and Dickinson, M. H. (2010). Active flight increases the gain of visual motion processing in *Drosophila*. *Nat. Neurosci.* *13*, 393–399.

Maisak, M. S., Haag, J., Ammer, G., Serbe, E., Meier, M., Leonhardt, A., Schilling, T., Bahl, A., Rubin, G. M., Nern, A., Dickson, B. J., Reiff, D. F., Hopp, E. and Borst, A. (2013). A directional tuning map of *Drosophila* elementary motion detectors. *Nature* *500*, 212216.

Matyas, F., Sreenivasan, V., Marbach, F., Wacogne, C., Barsy, B., Mateo, C., Aronoff, R. and Petersen, C. C. (2010). Motor control by sensory cortex. *Science* *330*, 1240–1243.

McCann, G. D. and MacGinitie, G. F. (1965). Optomotor response studies of insect vision. *Proc. R. Soc. Lond. B* *163*, 369–401.

Menne, D. and Spatz, H.-C. (1977). Colour vision in *Drosophila melanogaster*. *J. of Comp. Physiol.* *114*, 301–312.

Millard, S. S., Flanagan, J. J., Pappu, K. S., Wu, W. and Zipursky, S. L. (2007). Dscam2 mediates axonal tiling in the *Drosophila* visual system. *Nature* *447*, 720–724.

Millard, S. S., Lu, Z., Zipursky, S. L. and Meinertzhagen, I. A. (2010). *Drosophila* dscam proteins regulate postsynaptic specificity at multiple-contact synapses. *Neuron* *67*, 761–768.

Mronz, M. and Lehmann, F. O. (2008). The free-flight response of *Drosophila* to motion of the visual environment. *J. Exp. Biol.* *211*, 2026–2045.

Nagel, G., Brauner, M., Liewald, J. F., Adeishvili, N., Bamberg, E. and Gottschalk, A. (2005). Light activation of channelrhodopsin-2 in excitable cells of *Caenorhabditis elegans* triggers rapid behavioral responses. *Curr. Biol.* *15*, 2279–2284.

Raghu, S. V., Joesch, M., Borst, A. and Reiff, D. F. (2007). Synaptic organization of lobula plate tangential cells in *Drosophila*: gamma-aminobutyric acid receptors and chemical release sites. *J. Comp. Neurol.* 502, 598–610.

Raghu, S. V., Joesch, M., Sigrist, S. J., Borst, A. and Reiff, D. F. (2009). Synaptic organization of lobula plate tangential cells in *Drosophila*: D α 7 cholinergic receptors. *J. Neurogenet.* 23, 200–209.

Reichardt, W. and Wenking, H. (1969). Optical detection and fixation of objects by fixed flying flies. *Naturwissenschaften* 56, 424–425.

Reiser, M. B. and Dickinson, M. H. (2008). A modular display system for insect behavioral neuroscience. *J. Neurosci. Methods* 167, 127–139.

Reiser, M. B. and Dickinson, M. H. (2010). *Drosophila* fly straight by fixating objects in the face of expanding optic flow. *J. Exp. Biol.* 213, 1771–1781.

Rister, J., Pauls, D., Schnell, B., Ting, C. Y., Lee, C. H., Sinakevitch, I., Morante, J., Strausfeld, N. J., Ito, K. and Heisenberg, M. (2007). Dissection of the peripheral motion channel in the visual system of *Drosophila melanogaster*. *Neuron* 56, 155–170.

Schmucker, D. and Chen, B. (2009). Dscam and DSCAM: complex genes in simple animals, complex animals yet simple genes. *Genes Dev.* 23, 147–156.

Schnell, B., Joesch, M., Forstner, F., Raghu, S. V., Otsuna, H., Ito, K., Borst, A. and Reiff, D. F. (2010). Processing of horizontal optic flow in three visual interneurons of the *Drosophila* brain. *J. Neurophysiol.* 103, 1646–1657.

Schnell, B., Raghu, S. V., Nern, A. and Borst, A. (2012). Columnar cells necessary for motion responses of wide-field visual interneurons in *Drosophila*. *J. Comp. Physiol. A* 198, 389–395.

Schoenenberger, P., Gerosa, D. and Oertner, T. G. (2009). Temporal control of immediate early gene induction by light. *PLoS ONE* 4, e8185.

Schoonheim, P. J., Arrenberg, A. B., Bene, F. D. and Baier, H. (2010). Optogenetic localization and genetic perturbation of saccade-generating neurons in zebrafish. *J. Neurosci.* *30*, 7111–7120.

Schümperli, R. A. (1973). Evidence for Colour Vision in *Drosophila melanogaster* through Spontaneous Phototactic Choice Behaviour. *J. comp. Physiol.* *86*, 77–94.

Single, S., Haag, J. and Borst, A. (1997). Dendritic computation of direction selectivity and gain control in visual interneurons. *J. Neurosci.* *17*, 6023–6030.

Spradling, A. C. and Rubin, G. M. (1982). Transposition of cloned P-elements into *Drosophila* germ-line chromosomes. *Science* *218*, 341–347+.

Takemura, S. Y., Bharioke, A., Lu, Z., Nern, A., Vitaladevuni, S., Rivlin, P. K., Katz, W. T., Olbris, D. J., Plaza, S. M., Winston, P., Zhao, T., Horne, J. A., Fetter, R. D., Takemura, S., Blazek, K., Chang, L.-A., Ogundeyi, O., Saunders, M. A., Shapiro, V., Sigmund, C., Rubin, G. M., Scheffer, L. K., Meinertzhagen, I. A. and Chklovskii, D. B. (2013). A visual motion detection circuit suggested by *Drosophila* connectomics. *Nature* *500*, 175181.

Tammero, L. F. and Dickinson, M. H. (2002). Collision-avoidance and landing responses are mediated by separate pathways in the fruit fly, *Drosophila melanogaster*. *J. Exp. Biol.* *205*, 2785–2798.

Tammero, L. F., Frye, M. A. and Dickinson, M. H. (2004). Spatial organization of visuomotor reflexes in *Drosophila*. *J. Exp. Biol.* *207*, 113–122.

Tessier-Lavigne, M. and Goodman, C. S. (1996). The Molecular Biology of Axon Guidance. *Science* *274*, 1123–1133.

Theobald, J. C., Ringach, D. L. and Frye, M. A. (2010). Dynamics of optomotor responses in *Drosophila* to perturbations in optic flow. *J. Exp. Biol.* *213*, 1366–1375.

VanderWerf, F., Brassinga, P., Reits, D., Aramideh, M. and Ongerboer de Visser, B. (2003). Eyelid movements: behavioral studies of blinking in humans under different stimulus conditions. *J. Neurophysiol.* *89*, 2784–2796.

Wang, T. and Montell, C. (2007). Phototransduction and retinal degeneration in *Drosophila*. *Pflugers Arch.* 454, 821–847.

Wardill, T. J., List, O., Li, X., Dongre, S., McCulloch, M., Ting, C. Y., O’Kane, C. J., Tang, S., Lee, C. H., Hardie, R. C. and Juusola, M. (2012). Multiple spectral inputs improve motion discrimination in the *Drosophila* visual system. *Science* 336, 925–931.

Wehner, R. (1972). Spontaneous pattern preferences of *Drosophila melanogaster* to black areas in various parts of the visual field. *J. Insect Physiol.* 18, 1531–1543.

Wertz, A., Haag, J. and Borst, A. (2009). Local and global motion preferences in descending neurons of the fly. *J. Comp. Physiol. A* 195, 1107–1120.

Yaksi, E. and Wilson, R. I. (2010). Electrical coupling between olfactory glomeruli. *Neuron* 67, 1034–1047.

Yamaguchi, S., Wolf, R., Desplan, C. and Heisenberg, M. (2008). Motion vision is independent of color in *Drosophila*. *Proc. Natl. Acad. Sci. U.S.A.* 105, 4910–4915.

Zbikowski, R. (2005). Fly like a fly. *Spectrum, IEEE* 42, 46–51.

Zimmermann, G., Wang, L. P., Vaughan, A. G., Manoli, D. S., Zhang, F., Deisseroth, K., Baker, B. S. and Scott, M. P. (2009). Manipulation of an innate escape response in *Drosophila*: photoexcitation of acj6 neurons induces the escape response. *PLoS ONE* 4, e5100.

Acknowledgements

First I would like to thank my supervisor and “Doktorvater” Axel Borst for his advice and discussions during my PhD work. I especially want to thank him for giving me the opportunity to take my first steps as a biologist. Without his trust I would not have had the courage to follow this – for me – unknown path.

I would like to thank Maximilian Jösch and his passion for biology for showing and convincing me that biology is interesting and fun. Thank you Max, I have not regretted my decision.

I want to thank Alex Mauss and Maximilian Jösch for their help and discussions during the Channelrhodopsin Project and Bettina Schnell, Friedrich Förstner, Jing Shi and Dierk Reiff for inviting me to participate in the Dscam Project.

Furthermore, I would like to thank Johannes Plett for advice on the LED arena and electronics in general and for our discussions about scientific and non-scientific things. Thanks to Armin Bahl with whom I had several discussions regarding behavioural experiments and how to improve our setups. Also thanks to Jürgen Haag for sharing his knowledge of flies.

Thanks to Wolfgang Essbauer and Christian Theile for helping me with fly care. Also, without the excellent work of the MPI workshop I would not have been able to build my setup. Thanks to the whole Borst Department and Griesbeck group working never felt like work. Every member was always keen to help with any difficulties, thank you all for being there.

I would also like to thank Dierk Reiff and Johannes Plett for carefully reading this thesis and making helpful comments.

Last but not least, I would like to thank my family, Vero, Alina and Amanda who have accompanied me on my scientific journey and always find a way to brighten up each day regardless of how dark it sometimes appears to be.

VÄINÖ VILHELM KRISTIAN HAIKALA

Current Address

Hauptstrasse 1
Albert-Ludwigs-Universität Freiburg
Biologie 1
79104 Freiburg
Germany

Email: vaeinoe.haikala@biologie.uni-freiburg.de

Personal Details

Gender: Male

Marital status: Married

Date of birth: 03-07-1980

Place of birth: Helsinki, Finland

Citizenship: Finnish

Languages: Finnish, German, Spanish and English

Education

2008 – PhD Thesis: “The Role of Horizontal System Cells in Optomotor Responses in *Drosophila melanogaster*”
 Max-Planck-Institute of Neurobiology, Department of Systems and Computational Neuroscience.
 Adviser: Prof. Alexander Borst

- 2005 – 2007 Master of Science, Physics Thesis: “Speed Of Pulled Fronts With A Cutoff And Growth Enhancement”
Pontificia Universidad Católica, Chile
Advisers: Rafael Benguria Ph.D. and Cristina Depassier Ph.D.
- 2000 – 2007 Civil Electrical Engineering Title, Pontificia Universidad Católica, Chile

Research Experience

- 2012 – Research Fellow (Wissenschaftlicher Mitarbeiter), Department of Neurobiology (Prof. Dierk Reiff), Albert-Ludwigs-Universität Freiburg

Teaching Experience

Teaching Assistant at Pontificia Universidad Católica de Chile

- 03/2007 – 07/2007 “Thermodynamics and kinetic theory”
- 03/2006 – 07/2006 “Electromagnetism”
- 03/2005 – 07/2005 “Electrical Machines Laboratory”
- 08/2004 – 12/2004 “Electrical Machines Laboratory”

Publications

- [1] Haikala, V., Joesch, M., Borst, A. and Mauss, A. S. (2013). Optogenetic control of fly optomotor responses. *J. Neurosci.* 33, 13927 - 13934.
- [2] Depassier, M. C. and Haikala, V. (2009). Analytic upper and lower bounds for the period of nonlinear oscillators. *J. Sound Vibr.* 328, 338 -344.
- [3] Benguria, R. D., Depassier, M. C. and Haikala, V. (2007). Effect of a cutoff on pushed and bistable fronts of the reaction-diffusion equation. *Phys. Rev. E* 76, 051101.